

University of New Mexico

## UNM Digital Repository

---

Economics ETDs

Electronic Theses and Dissertations

---

Summer 7-17-2019

# Dynamic and Integrated Models of the Energy-Water-Land Nexus: Economic and Environmental Evaluation of Policy Decisions

Elmira Kalhor

*University of New Mexico - Main Campus*

Follow this and additional works at: [https://digitalrepository.unm.edu/econ\\_etds](https://digitalrepository.unm.edu/econ_etds)



Part of the [Agricultural and Resource Economics Commons](#), and the [Econometrics Commons](#)

---

### Recommended Citation

Kalhor, Elmira. "Dynamic and Integrated Models of the Energy-Water-Land Nexus: Economic and Environmental Evaluation of Policy Decisions." (2019). [https://digitalrepository.unm.edu/econ\\_etds/112](https://digitalrepository.unm.edu/econ_etds/112)

This Dissertation is brought to you for free and open access by the Electronic Theses and Dissertations at UNM Digital Repository. It has been accepted for inclusion in Economics ETDs by an authorized administrator of UNM Digital Repository. For more information, please contact [amywinter@unm.edu](mailto:amywinter@unm.edu), [lsloane@salud.unm.edu](mailto:lsloane@salud.unm.edu), [sarahrk@unm.edu](mailto:sarahrk@unm.edu).

Elmira Kalhor

*Candidate*

Economics

*Department*

This dissertation is approved, and it is acceptable in quality and form for publication:

*Approved by the Dissertation Committee:*

Dr. Janie M. Chermak , Chairperson

Dr. Robert P. Berrens

Dr. Alok Bohara

Dr. Gregory Rowangould

**Dynamic and Integrated Models of the Energy-Water-Land Nexus:  
Economic and Environmental Evaluation of Policy Decisions**

by

Elmira Kalhor

B.Sc., Civil Engineering, Iran University of Science and Technology, 2007

M. Sc., Civil Engineering, Iran University of Science and Technology, 2010

Ph.D., Civil Engineering, University of New Mexico, 2017

M.A. Economics, University of New Mexico, 2017

Dissertation

Submitted in Partial Fulfillment of the  
Requirements for the Degree of

**Doctor of Philosophy**

**Economics**

The University of New Mexico

Albuquerque, New Mexico

**December, 2019**

## **Dedication**

To the loving memory of my grandparents, Akbar and Khadija.

To Simin and Nasrollah, I could not ask for better parents.

To my best friend, Ali.

## **Acknowledgments**

I am tremendously proud to have worked under the guidance of Dr. Janie Chermak in writing this dissertation and conducting the underlying research. You are the best teacher and mentor a student could ask for, a true professional, and an excellent role model. You generously supported me throughout the trials and tribulations of the past few years, and I am forever indebted to you.

My sincere thanks to Dr. Robert Berrens, Dr. Alok Bohara and Dr. Gregory Rowangould. Your valuable comments, recommendations and feedback have strengthened this work substantially.

I'd also like to thank the New Mexico Experimental Program to Stimulate Competitive Research (NM EPSCoR), NSF Award # IIA1301346 for partial funding of this work, as well as Dr. Enid Graham Sullivan and the Oil Conservation Division at Mexico Energy Mining and Minerals Department. I also sincerely appreciate the support I received from Dr. Gregory Rowangould under the Environmental Protection Agency's Assistance Agreement No. R835885.

**Dynamic and Integrated Models of the Energy-Water-Land Nexus:  
Economic and Environmental Evaluation of Policy Decisions**

by

Elmira Kalhor

B.Sc., Civil Engineering, Iran University of Science and Technology, 2007

M. Sc., Civil Engineering, Iran University of Science and Technology, 2010

Ph.D. Civil Engineering, Univeristy of New Mexico, 2017

M.A. Economics, University of New Mexico, 2017

Ph.D., Economics, University of New Mexico, 2019

**Abstract**

This dissertation contributes to the field of environmental and natural resource economics by employing data and hybrid simulation models to assess the economic and environmental outcomes of policy instruments applied to the complex systems of humans and the physical environment. Three integrated and dynamic models are developed to measure short- and long-term outcomes of price scenarios and resource capacity constraints.

The first chapter examines the balancing problem faced by a state-level policymaker. The Permian Basin is a source of a significant revenue to the state of New Mexico; however, unconventional oil and gas production in this highly productive field require large amounts of freshwater and generates billions of barrels of wastewater. By integrating economic and reservoir engineering models, we measure the impacts of freshwater consumption constraints, early shutdown of wells, and a combination of increased treatment capacity and freshwater constraint on the balance between revenue generation and resource exhaustion. We show that improving treatment capacity along with a freshwater capacity constraint (5,000 acre-feet per

month) results in relatively better outcomes in both economic and environmental terms.

The second chapter presents a vector error correction model to test the impact of price shocks on drilling activity in the New Mexico and Texas portions of the Permian Basin. We are interested in understanding how operators choose from two different regulatory systems that share the same basin. We show that an increase in prices has both short- and long-term positive impacts on drilling activity in the New Mexico and Texas portions. However, under the same price shock, Texas drilling shows a larger response. Furthermore, we show that Texas drilling drives a small part of the drilling activity in the New Mexico portion of the Permian Basin, but this relationship is not bi-directional. Although in the short run drilling activity in the Permian Basin does not influence U.S. oil prices, in the long run, as drilling activity increases in the Permian Basin (either side), oil prices experience a very small decline. In other words, U.S. oil prices are not fully driven by exogenous variables, at least not in the long run.

The third chapter is focused on two objectives: (1) to provide a simulation tool to test the economic and environmental impacts of an urban policy instrument, and (2) to test the need for adopting a high temporal resolution in the evaluation of the outcomes of a long-range regional transportation plan. We investigate evidence of the congestion rebound effect in Albuquerque using an annually integrated land-use travel model. Although we do not find evidence of congestion reappearance over a 2012-2040 period, our proposed approach could capture short-term changes in travel behavior and long-term land-use changes resulting from a capacity expansion policy. Furthermore, we show that integrating the land-use and travel demand modules only in the beginning and at the end of a long-range plan results in biased evaluations

of the plan, but more so in evaluating environmental outcomes.



## Contents

Chapter 1. Introduction .....	1
The energy-water nexus in the New Mexico portion of the Permian Basin .....	2
A cointegrated system of supply in the Permian Basin .....	5
Integrated and dynamic land-use travel demand modeling .....	7
Research Methods and chapter summary.....	8
References .....	11
Chapter 2. Sustainability of Energy, Water, and the Environment in the Permian Basin, New Mexico: A Dynamic System Approach .....	13
1. Introduction .....	13
2. Background .....	16
2.1. Hydrocarbon production from unconventional resources .....	16
2.2. Production decline curve .....	17
2.3. Drilling .....	19
2.4. Shutdown condition .....	20
2.5. Hydraulic fracturing water demand .....	21
2.6. Produced water .....	23
2.7. Produced water management .....	24
3. Theoretical model .....	26
4. The study area.....	29
5. Model architecture and data .....	32
5.1. Causal loop diagram .....	33
5.2. Stocks and flows .....	37
5.3. Computer simulation .....	37
6. Data and model inputs.....	41
6.1. Historical data (2000-2018).....	41
6.2. Future values (2018-2050) .....	47
6.3. Scenarios .....	51
7. Simulation results and discussion .....	57
7.1. Price scenarios.....	57
Impacts on drilling.....	57

Impacts on oil production .....	58
Impacts on revenue .....	59
Impact on freshwater consumption .....	60
Impact on PW generation .....	62
7.2. Water consumption capacity scenarios .....	62
Impacts on drilling.....	64
Impacts on oil production .....	65
Impact on revenue .....	66
Impact on freshwater consumption .....	67
Impacts on PW generation .....	67
7.3. Treatment capacity scenario.....	68
Impact on drilling .....	69
Impacts on oil production .....	69
Impact on revenue .....	70
Impact on freshwater consumption .....	70
Impact on PW generation .....	71
7.4. Shutdown conditions .....	73
Impacts on drilling.....	73
Impacts on oil production .....	74
Impacts on the economic revenue .....	74
Impact on freshwater consumption .....	75
Impact on PW generation .....	75
7.5. Summary of the results .....	75
8. Conclusions and policy implications .....	77
9. Limitations and future work .....	81
References .....	83
Chapter 3. Drilling activity in the Permian Basin: A Vector Error Correction Model.....	88
1. Introduction .....	88
2. Background .....	90
2.1. U.S. oil prices .....	90
2.2. The relationship between oil price and drilling activity in the United States.....	92

3.	Study area and data .....	95
3.1.	Study area.....	95
3.2.	Data .....	98
4.	Econometric modeling .....	99
4.1.	Vector autoregressive models and Granger causality .....	100
4.2.	Impulse-response functions.....	101
4.3.	Stationarity and unit root test.....	102
4.4.	Cointegration.....	104
4.5.	Vector error correction models .....	105
5.	Estimation results .....	105
5.1.	Descriptive statistics.....	105
5.2.	Stationarity test results .....	106
5.3.	Cointegration test results.....	107
5.4.	VECM model, lag selection and estimated coefficients.....	107
5.5.	Granger causality.....	110
5.6.	Impulse response functions .....	111
6.	Conclusion.....	114
	References .....	116
	Chapter 4. A Dynamic and Integrated Simulation for Measuring Economic and Environmental Outcomes of a Long-Range Regional Transportation Plan with a Congestion Reduction Goal .	120
1.	Introduction .....	120
2.	Background .....	122
2.1.	Long Range Regional Transportation plan (LRTP).....	122
2.2.	Congestion relief and induced demand .....	123
2.3.	Interactive land-use and travel demand modeling.....	126
3.	Theoretical model .....	127
3.1.	Travel demand model .....	128
	Trip generation.....	128
	Trip distribution .....	129
	Mode choice.....	129
	Time of day model .....	130

Highway and public transport assignment .....	130
3.2. Land-use model .....	130
Accessibility .....	131
Economic transition .....	131
Mobility .....	131
Location choice .....	132
Real estate development .....	132
Land price .....	132
4. The study area .....	133
5. Model architecture and data .....	136
6. Simulation results and discussion .....	138
6.1. Road expansion outcomes .....	138
6.2. Comparison between the results of the ALT and endpoint approaches .....	149
7. Conclusions .....	152
References .....	155
Chapter 5. Conclusion and Summary .....	158

## List of Figures

Figure 1.1: Percentage of horizontal wells in the stock of new wells in the New Mexico portion of the Permian Basin (Source: Rystad Energy ShaleWellCube Browser) .....	3
Figure 1.2: Cointegration between drilling activity in New Mexico and Texas portions of the Permian Basin .....	6
Figure 1.3: Cointegration between oil price and drilling activity in the Permian Basin (both New Mexico and Texas) .....	7
Figure 2.1: The U.S. onshore proved reserves stocks (Source Energy Information Administration [EIA] 2018a).....	17
Figure 2.2: Time series of oil production its relationship to oil prices .....	19
Figure 2.3: Time series of oil production (above) and drilled wells count (below) and their relationship to prices .....	20
Figure 2.4: Shut down criteria.....	21
Figure 2.5: Count of horizontal wells drilled (and completed) with certain lateral length in the Delaware sub-basin of the Permian Basin (New Mexico portion). (Source: Rystad Energy ShaleWellCube Browser) .....	23
Figure 2.6: HF fluid used per lateral length, by year of completion .....	23
Figure 2.7: Volumes produced and injected for disposal in New Mexico Permian (Source: Goetze 2018) .....	25
Figure 2.8: Location map of the study area (Map source: Bureau of Economic Geology, The University of Texas at Austin) .....	30
Figure 2.9: Count of horizontal, vertical, and all wells in New Mexico Permian.....	31
Figure 2.10: Selected oil-producing formations in the Permian Basin (Source: Budzik & Perrin 2014) .....	32
Figure 2.11: Causal loop diagram for economic and environmental analysis of the Permian Basin's energy-water nexus .....	34
Figure 2.12: New wells module snapshot.....	38
Figure 2.13: Hydraulic fracturing water demand .....	39
Figure 2.14: Produced water .....	39
Figure 2.15: Oil production module.....	40
Figure 2.16: Historical PW-to-oil ratio for Bone Spring formation .....	45
Figure 2.17: Historical PW-to-oil ratio for Delaware formation .....	45
Figure 2.18: Historical PW-to-oil ratio for Glorieta & Yeso formations.....	46

Figure 2.19 Historical PW-to-oil ratio for Wolfcamp formation .....	46
Figure 2.20: Average PW-to-oil ration, Bone Spring.....	48
Figure 2.21: Average PW-to-oil ration, Delaware.....	49
Figure 2.22: Average PW-to-oil ration, Glorieta & Yeso .....	49
Figure 2.23: Average PW-to-oil ration, Wolfcamp .....	49
Figure 2.24: Actual and estimated logarithmic time series for average HF water per well in Bone Spring .....	50
Figure 2.25: Actual and estimated logarithmic time series for average HF water per well in Delaware .....	50
Figure 2.26: Actual and estimated logarithmic time series for average HF water per well in Glorieta & Yeso .....	51
Figure 2.27: Actual and estimated logarithmic time series for average HF water per well in Wolfcamp.....	51
Figure 2.28: Oil price scenarios.....	53
Figure 2.29: Well drilling activity under different price regimes.....	58
Figure 2.30: Oil production volumes under different price regimes.....	59
Figure 2.31: NM state revenue under different price regimes .....	59
Figure 2.32: Annual freshwater consumption under different price regime scenarios .....	61
Figure 2.33: PW generation under different price regimes.....	62
Figure 2.34: Well drilling activity under different freshwater consumption constraint scenarios .....	64
Figure 2.35: Change in the number of wells by formation as a result of posing a 5,000 acre-feet per month freshwater consumption constraint .....	65
Figure 2.36: Oil production volumes under different freshwater consumption constraint scenarios .....	66
Figure 2.37: Annual freshwater consumption under different freshwater consumption constraint scenarios .....	67
Figure 2.38: PW generation under freshwater withdrawal limit scenarios .....	68
Figure 2.39: Well drilling activity under different treatment capacity scenarios.....	69
Figure 2.40: Oil production volumes under different treatment capacity scenarios.....	70
Figure 2.41: Annual freshwater consumption under different treatment capacity scenarios ....	71
Figure 2.42: PW generation under different treatment capacity scenarios .....	71
Figure 2.43: Generated and disposed PW volumes (acre-feet) under BASE scenario .....	72

Figure 2.44: Generated and disposed PW volumes (acre-feet) under W5K scenario.....	72
Figure 2.45: Generated and disposed PW volumes (acre-feet) under TREAT scenario .....	72
Figure 2.46: Oil production volumes under different shutdown condition scenarios .....	74
Figure 2.47: PW generation under shutdown condition scenarios .....	75
Figure 2.48: Net present value of revenue and freshwater consumption tradeoff results .....	79
Figure 2.49: Revenue and PW generation tradeoff results .....	81
Figure 3.1: The U.S. West Texas Intermediate crude oil price .....	91
Figure 3.2: Changes in oil prices and U.S. oil production .....	92
Figure 3.3: Relationship between oil price and drilling activity in the U.S. ....	93
Figure 3.4: The U.S. onshore proved reserves stocks (Source Energy Information Administration [EIA] 2017).....	94
Figure 3.5: Location map for the study area.....	96
Figure 3.6:Percentage of oil production by land ownership in NM .....	97
Figure 3.7: Percentage of oil production by land ownership in TX .....	98
Figure 3.8: AIC for lag selection; an order of 3 results in the minimum AIC and is selected as the optimal order .....	108
Figure 3.9: Response of TX and NM drilling to one SD unit shock to oil price .....	112
Figure 3.10: Response of oil price and NM drilling to one SD unit shock to TX drilling .....	113
Figure 3.11: Response of oil price and TX drilling to one SD unit shock to NM drilling .....	113
Figure 4.1: Market for vehicle miles traveled (VMT).....	124
Figure 4.2: Location map of the capacity expansion project.....	135
Figure 4.3: Proposed model architecture .....	136
Figure 4.4: Percentage change in morning peak-hour traffic load between the original and derived LRTPs for year 2015 .....	141
Figure 4.5: Percentage change in morning peak-hour traffic load between the original and derived LRTPs for year 2020 .....	141
Figure 4.6: Percentage change in morning peak-hour traffic load between the original and derived LRTPs for year 2025 .....	141
Figure 4.7: Percentage change in morning peak-hour traffic load between the original and derived LRTPs for year 2030 .....	142
Figure 4.8: Percentage change in morning peak-hour traffic load between the original and derived LRTPs for year 2035 .....	142
Figure 4.9: Percentage change in morning peak-hour traffic load between the original and derived	

L RTPs for year 2040 .....	142
Figure 4.10: Percentage change in morning peak-hour traffic speed between the original and derived L RTPs for year 2015 .....	143
Figure 4.11: Percentage change in morning peak-hour traffic speed between the original and derived L RTPs for year 2020 .....	143
Figure 4.12: Percentage change in morning peak-hour traffic speed between the original and derived L RTPs for year 2025 .....	143
Figure 4.13: Percentage change in morning peak-hour traffic speed between the original and derived L RTPs for year 2030 .....	144
Figure 4.14: Percentage change in morning peak-hour traffic speed between the original and derived L RTPs for year 2035 .....	144
Figure 4.15: Percentage change in morning peak-hour traffic speed between the original and derived L RTPs for year 2040 .....	144
Figure 4.16: Absolute change in population between the original and derived L RTPs for year 2015 .....	145
Figure 4.17: Absolute change in population between the original and derived L RTPs for year 2020 .....	145
Figure 4.18: Absolute change in population between the original and derived L RTPs for year 2025 .....	145
Figure 4.19: Absolute change in population between the original and derived L RTPs for year 2030 .....	146
Figure 4.20: Absolute change in population between the original and derived L RTPs for year 2035 .....	146
Figure 4.21: Absolute change in population between the original and derived L RTPs for year 2040 .....	146
Figure 4.22: Percentage of congested links during the morning and afternoon peak hours for the original and new L RTPs .....	147
Figure 4.23: Annual energy consumption on the original and derived networks .....	148
Figure 4.24: Annual CO <sub>2</sub> emission on the original and derived networks .....	149
Figure 4.25: Vehicle miles traveled per household .....	150
Figure 4.26: Average traffic speed on the network .....	150
Figure 4.27: Fuel energy consumption on modified network .....	152
Figure 4.28: CO <sub>2</sub> accumulation on the modified network .....	152



## List of Tables

Table 1.1: Summary of estimated drilling elasticities in the literature .....	6
Table 2.1: Description of the links in the causal loop diagram (Figure 2.11) .....	35
Table 2.2: Description and sources of the historical data .....	41
Table 2.3: Type curve parameter estimates for four top producing formations in the New Mexico Permian .....	43
Table 2.4: Average HF water consumption volumes per well in acre-feet .....	47
Table 2.5: Average PW-to-oil ratio and the pertaining mean-reversing interval .....	48
Table 2.6: Scenario variables and their values .....	56
Table 2.7: Price scenarios .....	57
Table 2.8: Net present value (NPV) of the gross revenue and state revenue generated from oil production.....	60
Table 2.9: Withdrawal volumes for mining practices in acre-feet (Source: OSE 2019) .....	60
Table 2.10: Freshwater consumption scenarios .....	63
Table 2.11: Net present value (NPV) of the gross revenue and state revenue generated from oil production.....	66
Table 2.12: PW generation volumes (2050) .....	68
Table 2.13: Treatment capacity scenarios .....	69
Table 2.14: Net present value (NPV) of the gross revenue and state revenue generated from oil production under treatment capacity scenarios .....	70
Table 2.15: Shutdown condition scenarios.....	73
Table 2.16: Net present value (NPV) of the gross revenue and state revenue generated from oil production under shutdown condition scenarios .....	74
Table 2.17: Summary of policy scenario outcomes .....	76
Table 3.1: Time series variables' description.....	99
Table 3.2: Descriptive statistics .....	105
Table 3.3: Unit-root test results.....	106
Table 3.4: VECM coefficient estimates .....	109
Table 3.5: Coefficients of the error correction term .....	109
Table 3.6: Model measures.....	109
Table 3.7: Granger causality results.....	110
Table 3.8: LM test results for testing VECM residuals' white noise characteristics .....	111

## Chapter 1. Introduction

The late Stephen Hawking predicted that as we approach unprecedented *extreme conditions*, we will face complex problems that cannot be addressed by basic theories meant for normal conditions; to solve such problems, we will need to compile and unify those basic theories and to build complex means for addressing 21st-century problems. (Chui 2000)

Managing limited resources for growing populations exemplifies a 21st-century complex problem. The command-and-control approach towards resource management, together with unprecedented world population, has resulted in the depletion and exhaustion of some of the resources under critical levels (Vitousek et al. 1997; Foley et al. 2005; Boumans et al. 2015). To develop policies that ensure the sustainable use of depleting resources, the dynamics of the socioeconomic system, the physical systems, and the interaction between the two should be accounted for.

The socioeconomic system consists of profit or utility maximizing economic agents who do not

account for the aggregate impacts of their choices. It is for the policymaker to undertake sustainability accounting and to ensure that correct policies are in place so that the resources are utilized efficiently and sustainably. The underlying objective of this work is to use data and simulation techniques to examine the collective, multifaceted and dynamic impacts of price or quantity instruments designed for resource utilization. The impact of policies on three systems is investigated, namely the energy-water nexus, new wells supply in a shared basin, and the land-use transportation system. The dynamic and integrated properties of these systems are explained in the following.

#### *The energy-water nexus in the New Mexico portion of the Permian Basin*

New Mexico's economy relies strongly on oil and Gas (O&G) production. In 2018, the state revenue from O&G production was \$2.2 billion (New Mexico Oil and Gas Association 2019), which accounts for roughly 37 percent<sup>1</sup> of the state income in fiscal year 2018. The economic agents in this system are the O&G producers who would decide the production intensity by observing oil prices and choosing the number of new wells to be drilled and completed for production. However, the social planner—the state regulator, in this case—faces a balancing decision between maximizing the revenue generated from O&G production and minimizing the burden on two other resources: freshwater resources and the disposal-receiving geologic layer.

The majority of production in the Permian Basin is by unconventional technology, namely by

---

<sup>1</sup> New Mexico's largest source of revenue is from general and selective taxes. During fiscal year 2018, general and selective taxes accounted for \$2.978 billion, or 50.1 percent of the state's revenue. The \$2.2 billion income generated from O&G production and sales in the state is 37 percent of the total state revenue tax (State of New Mexico 2018).

hydraulic fracturing of the impervious layers that are accessed via horizontal drilling technology. Since the shale revolution in 2009, the number of horizontal wells drilled in the Permian Basin has risen constantly; during the past five years, about 90% of the new wells in the New Mexico portion of the Permian Basin are horizontal wells (as shown in **Error! Reference source not found.**).

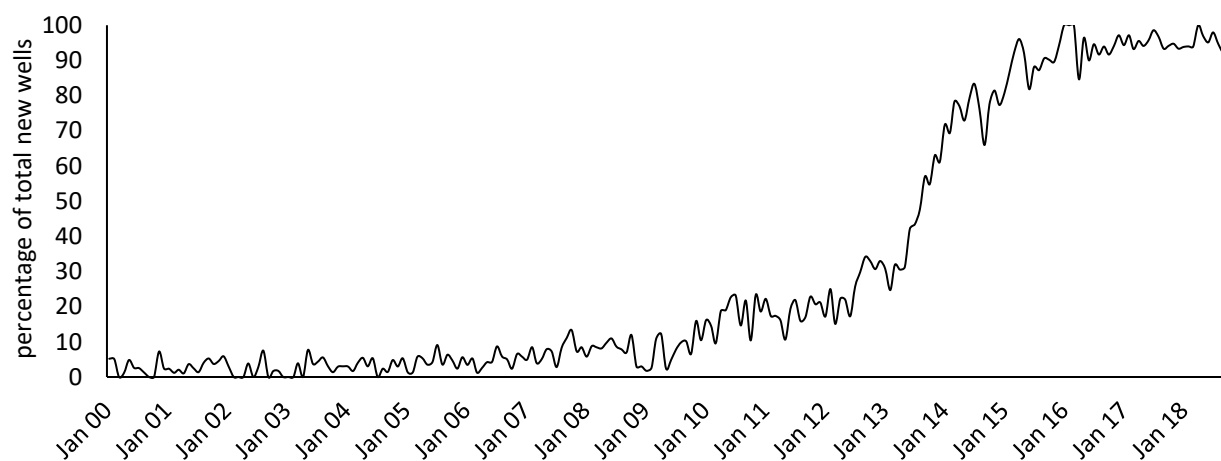


Figure 1.1: Percentage of horizontal wells in the stock of new wells in the New Mexico portion of the Permian Basin  
(Source: Rystad Energy ShaleWellCube Browser)

Hydraulic fracturing is a water-intensive process. In the Permian Basin, 34.5 acre-feet of water was used for hydraulic fracturing of an average well in 2016; furthermore, the amount of water used for hydraulic fracturing has increased over time (Kondash, Lauer and Vengosh 2018). Since most of the water used in the hydraulic fracturing process comes from freshwater sources, intense O&G production translates into severe stress on freshwater resources. High levels of withdrawals are especially damaging to groundwater resources of the Permian Basin with low recharge rates.

In addition, O&G production generates a large stream of wastewater (also called produced water.) In 2017, about 108,000 acre-feet of produced water was generated in the New Mexico portion

of the Permian Basin (Goetze 2018). From the operator's perspective, the cheapest way of handling this wastewater is to dispose of it in deep injection wells. However, the receiving geologic layer has limited capacity and drowning the underground formation with large volumes of wastewater could cause seismic activity, as was evident in the case of Oklahoma (Keranen et al. 2013).

The dynamics of the interplay between oil production, water consumption, and produced-water disposal is an important element of sustainability accounting in the energy-water nexus. When the price of oil goes up, producers have incentive to drill more wells and to produce more O&G, but this could result in alarming rates of freshwater withdrawal as well as generation of large volumes of produced water. A case in point is the account of water usage that the New Mexico Office of the State Engineer (OSE) publishes. The report on water use by category is published every five years, with the accounting pertaining to 2015 published in 2019 (New Mexico Office of the State Engineer 2019). The account shows that in 2015, withdrawal volumes associated with mining practices added up to 20,388 acre-feet. However, there was a collapse in oil prices during 2014-2016, which was attributed to global economic events (McNally 2017; Baumeister and Kilian 2014). Hence, the groundwater withdrawal levels in 2015, when the oil prices were low, may not represent the severity of water consumption in the area.

The policymaker can benefit from price and/or quantity policy instruments to achieve a sustainable balance between revenue generated from oil production, water consumption, and produced-water disposal. The policymaker is a price taker in the oil market and cannot control oil prices but can impose capacity constraint on freshwater consumption, induce shorter production life for wells (by raising disposal costs), or motivate treatment of produced water.

### *A cointegrated system of supply in the Permian Basin*

Drilling and completion of a well is the largest investment in the process of producing O&G, which is also a sunk cost immediately after the well is completed. Kellogg (2014) asserts that such characteristics make the drilling investment decision a real option problem; the operator chooses the time of investment based on its observation of the oil prices and price volatility. For large operators with the capacity to invest in different states or basins, there is also the option of the location of the new well; in other words, not only do they choose when to drill a new well but also where to place it.

Arguably, the Permian Basin presents a natural assignment of drilling location options. Producers who are active in the Permian Basin observe the same commodity price, price volatility, and the same productivity,<sup>2</sup> but two different regulatory environments, namely New Mexico and Texas. The existence of cointegration, a common trend, between drilling activity in the Texas and New Mexico portions of the Permian Basin is empirical evidence that the interaction between the two supply models exists. Figure 1.2 shows that New Mexico and Texas drilling could be cointegrated as they move together.

---

<sup>2</sup> Ratio of expected production to the drilling cost (Kellogg 2014).

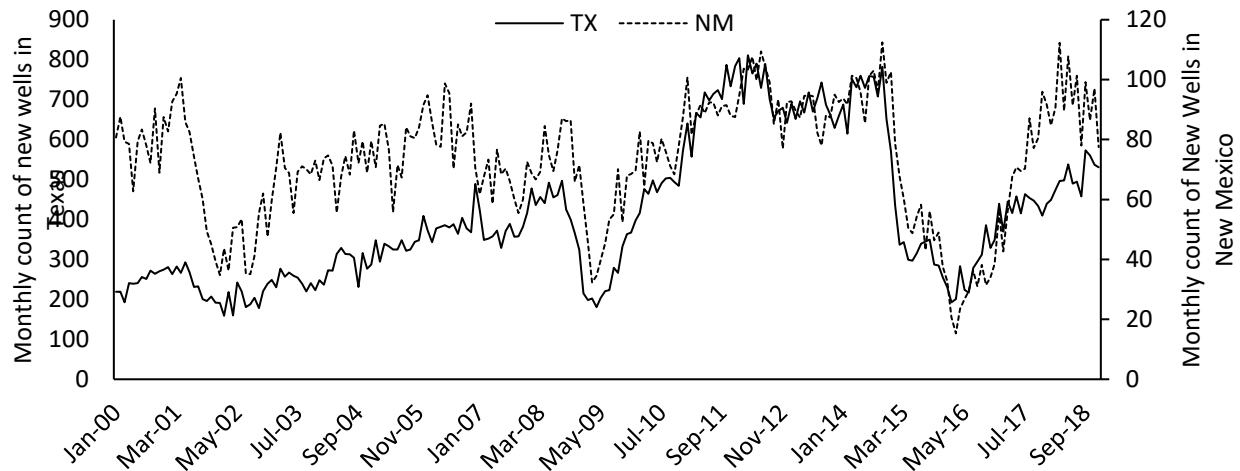


Figure 1.2: Cointegration between drilling activity in New Mexico and Texas portions of the Permian Basin

The relationship between oil price and drilling activity has been previously studied by empirical analysis of the price elasticity of new well supply (Table 1.1).

Table 1.1: Summary of estimated drilling elasticities in the literature

Author(s)	Study area (study period)	Drilling type	Price type	Long-run elasticity
Newell, Prest & Vissing (2016)	Texas (2000-2015)	Unconventional gas	Smoothed natural gas futures price	0.65
		Conventional gas		0.64
		All gas wells		0.66
		Unconventional gas	Smoothed crude oil futures price	0.56
		Conventional gas		0.58
		All gas wells		0.56
Hausman & Kellogg (2015)	Multiple States (2007-2013)	Unconventional gas	Average monthly natural gas price	0.81
Ringlund, Rosendahl & Skjerpen (2008)	United States (1987-2006)	Conventional and unconventional oil rigs	Crude oil spot prices	1.28

That drilling activity has a significant long-run elasticity proves that cointegration between prices

and drilling activity exists. Empirical data can also suggest the existence of a common trend, or cointegration, between oil price and drilling activity in the Permian Basin (Figure 1.3).

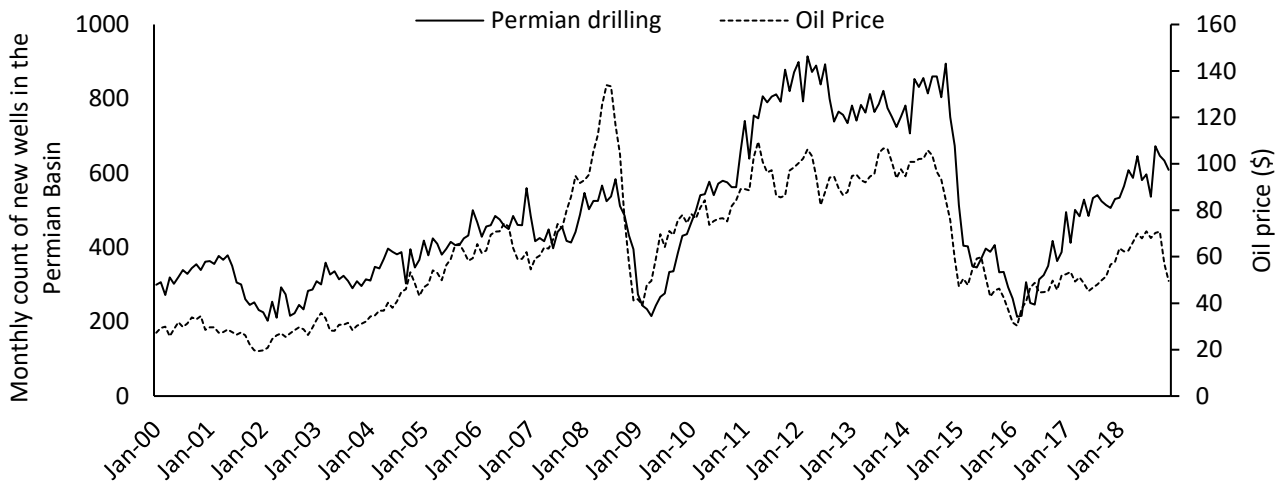


Figure 1.3: Cointegration between oil price and drilling activity in the Permian Basin (both New Mexico and Texas)

All in all, a system of cointegrated economic variables explains the dynamic and cointegrated characteristics of the supply of new wells in the Permian Basin.

### Integrated and dynamic land-use travel demand modeling

Transportation and land-use systems are interconnected (Coppola et al. 2013). Accessibility is a normal good in the location choices made by households and firms (Waddell et al. 2003). On the other hand, utilization of the links in the transportation network depends on the land-use characteristics, namely population and the level of economic activity. To assess the performance of an urban policy, especially in the long run, the interaction between land-use and travel demand models should be accounted for.

A classic urban policy instrument is to increase in the number of lanes on the transportation network to alleviate congestion (Hansen 1995). However, it is empirically shown that additional



lanes attract more traffic and the congestion problems resurface after a few years. The underlying causes of the congestion rebound are the short-run changes in travel behavior, mainly route diversion, and the long-run land-use changes (Cervero 2003). Hence, in order to evaluate the outcome of a lane addition in the long run, the dynamic interaction between land-use and travel demand models should be accounted for. The optimal frequency of the interaction between land-use and travel demand models is an open question. The common practice of policy evaluation by metropolitan planning organizations (MPOs) is to assume that during a long-range (>20 years) planning interval, land use and travel demand change in isolation from one another (Tayarani et al. 2018). They use the travel demand and land-use scheme of the final year of the long-range planning interval to calculate travel times, vehicle miles traveled, etc. This can result in biased estimations of the policy outcomes.

#### Research Methods and chapter summary

This study uses data and simulation models in order to test the performance of price or quantity policy instruments on complex systems that involve economic agents and the physical and natural resources.

Chapter 2 integrates economic and reservoir engineering models to assess the economic and environmental outcomes of three policy instruments, namely freshwater consumption constraint, shutdown conditions, and produced water treatment scenarios, and compares the resulting tradeoffs between economic and environmental outcomes. The New Mexico portion of the Permian Basin is selected as the study area; the Permian Basin is a highly productive oil field and unconventional operation is the main method of oil production in the study area. This system

dynamics model integrates four modules including well drilling, oil production, water consumption, and produced water generation and estimates performance outcomes under different policy scenarios. The nexus between energy and natural resources is modeled in a system dynamics platform, the planning horizon is 2000-2050, and a monthly time-step is selected.

Chapter 3 presents a simultaneous timeseries analysis of three variables, namely oil price, drilling activity in the New Mexico portion of the Permian Basin, and drilling activity in the Texas portion of the Permian Basin. By presenting the cointegration between the three timeseries, we verify that the relationship between the three variables is not just a correlation but that a change in one variable derives changes in other two variables. Using a vector error correction model on monthly data for the 2000-2018 period (228 observations), we test the hypotheses of Granger causality between the three variables of interest. Furthermore, we present the impulse-response functions and map the response of each variable to a shock in another variable.

Chapter 4 develops an annually integrated land-use travel demand model to measure the short and long-term outcomes of a capacity expansion policy instrument. In addition to testing the fundamental law of road congestion,<sup>3</sup> we explore the possibility that models with lower frequencies of integration between the land-use and travel demand models can produced biased performance measures. The study area is the Albuquerque metropolitan area, and the policy instrument of interest is to double the lanes on the Paseo del Norte river overpass. The planning

---

<sup>3</sup> that is, lane additions will become inefficient over time as a result of the induced and latent demand.

horizon is 2012-2040 and an annual time step is selected.

## References

- Baumeister, C. and Kilian, L. (2014). Real-time analysis of oil price risks using forecast scenarios. *IMF Economic Review*, 62(1), pp. 119-145.
- Boumans, R., Roman, J., Altman, I. and Kaufman, L. (2015). The Multiscale Integrated Model of Ecosystem Services (MIMES): Simulating the interactions of coupled human and natural systems. *Ecosystem Services*, 12, pp. 30-41.
- Cervero, R. (2003). Road expansion, urban growth, and induced travel: A path analysis. *Journal of the American Planning Association*, 69(2), pp. 145-163.
- Coppola, P., Ibeas, A., dell'Olio, L. and Cordera, R. (2013). LUTI model for the metropolitan area of Santander. *Journal of Urban Planning and Development*, 130(3), pp. 153-165.
- Chui, G. (2000). "Unified Theory" is getting closer, Hawking predicts. *San Jose Mercury News*, January 23. Accessed June 23, 2019. [https://nl.newsbank.com/nl-search/we/Archives?p\\_action=doc&p\\_docid=0EB71461A598B45F&p\\_docnum=2&s\\_orderid=NB0119062403453606354&s\\_dlid=DL0119062403461606401&s\\_ecproduct=DOC&s\\_ecprodttype=NORENEW&s\\_trackval=&s\\_sitelog=SJ&s\\_referrer=&s\\_username=ekal2019&s\\_accountid=AC0119062403435306229&s\\_upgradeable=no](https://nl.newsbank.com/nl-search/we/Archives?p_action=doc&p_docid=0EB71461A598B45F&p_docnum=2&s_orderid=NB0119062403453606354&s_dlid=DL0119062403461606401&s_ecproduct=DOC&s_ecprodttype=NORENEW&s_trackval=&s_sitelog=SJ&s_referrer=&s_username=ekal2019&s_accountid=AC0119062403435306229&s_upgradeable=no).
- Foley, J.A., DeFries, R., Asner, G.P., Barford, C., Bonan, G., Carpenter, S.R., Chapin, F.S. et al. (2005). Global consequences of land use. *Science* 309(5734), pp. 570-574.
- Goetze, P. (2018). Current status of the New Mexico Underground Injection Control. Paper presented at the New Mexico Produced Water Conference: Policy, Regulations and Economics to Support Total Resource Recovery, Nov. 15-16. Santa Fe, NM.
- Hansen, M. (1995). Do new highways generate traffic? *ACCESS Magazine*, 1(7), pp. 16-23.
- Hausman, C. and Kellogg, R. (2015). *Welfare and distributional implications of shale gas* (NBER Working Paper 21115). Cambridge, MA: National Bureau of Economic Research.
- Kellogg, R. (2014). The effect of uncertainty on investment: Evidence from Texas oil drilling. *American Economic Review* 104(6), pp. 1698-1734.
- Keranen, K.M., Savage H.M., Abers, G.A. and Cochran, E.S. (2013). Potentially induced earthquakes in Oklahoma, USA: Links between wastewater injection and the 2011 Mw5.7 earthquake sequence. *Geology* 41 (6), pp. 699-702. <https://doi.org/10.1130/G34045.1>.
- Kondash, A.J., Lauer, N.E. and Vengosh, A. (2018). The intensification of the water footprint of hydraulic fracturing. *Science Advances*, 4(8). DOI: 10.1126/sciadv. aar5982.
- McNally, R. (2017). *Crude volatility*. New York, NY: Columbia University Press. Kindle Edition.

- New Mexico Office of the State Engineer (OSE). (2019). *New Mexico water use by categories 2015* (Technical Report 55). Santa Fe: New Mexico Office of the State Engineer. [http://www.ose.state.nm.us/Pub/wucTechReports/2015/2015%20WUR%20final\\_05142019.pdf](http://www.ose.state.nm.us/Pub/wucTechReports/2015/2015%20WUR%20final_05142019.pdf).
- New Mexico Oil and Gas Association (NMOGA). (2019). New Mexico Tax Research Institute: State and local revenue impacts of the oil and gas industry. Accessed May 2019. [https://www.nmoga.org/new\\_mexico\\_tax\\_research\\_institute\\_state\\_and\\_local\\_revenue\\_impacts\\_of\\_the\\_oil\\_and\\_gas\\_industry](https://www.nmoga.org/new_mexico_tax_research_institute_state_and_local_revenue_impacts_of_the_oil_and_gas_industry).
- Newell, R.G., Prest, B.C. and Vissing, A. (2016). *Trophy hunting vs. manufacturing energy: The price-responsiveness of shale gas* (NBER Working Paper 22532). Cambridge, MA: National Bureau of Economic Research.
- Vitousek, P.M., Mooney, H.A., Lubchenco, J. and Melillo, J.M. (1997). Human domination of Earth's ecosystems. *Science*, 277(5325), pp. 494–499.
- Ringlund, G.B., Rosendahl, K.E. and Skjerpen, T. (2008). Does oilrig activity react to oil price changes? An empirical investigation. *Energy Economics*, 30(2), pp. 371-396.
- State of New Mexico. (2018). *Component appropriation funds annual financial report, June 30, 2018*. Accessed June 10, 2019. [http://nmdfa.state.nm.us/uploads/files/306\\_Component\\_Appropriations\\_Fund\\_State\\_General\\_FundFY2018\\_Final\\_reissued\(2\).pdf](http://nmdfa.state.nm.us/uploads/files/306_Component_Appropriations_Fund_State_General_FundFY2018_Final_reissued(2).pdf)
- Tayarani, M., Nadafianshahamabadi, R., Poorfakhraei, A. and Rowangould, G. (2018). Evaluating the cumulative impacts of a long-range regional transportation plan: Particulate matter exposure, greenhouse gas emissions, and transportation system performance. *Transportation Research Part D: Transport and Environment*, 63, pp. 261-275.
- Waddell, P., Borning, A., Noth, M., Freier, N., Becke, M. and Ulfarsson, G. (2003). Microsimulation of urban development and location choices: Design and implementation of UrbanSim. *Networks and Spatial Economics*, 3(1), pp. 43-67.

## **Chapter 2. Sustainability of Energy, Water, and the Environment in the Permian Basin, New Mexico: A Dynamic System Approach**

### **1. Introduction**

Oil and Gas (O&G) production in the Permian Basin is the source of substantial state income for both Texas and New Mexico. In a recent comparative analysis among nine western onshore O&G producing states (including New Mexico, Wyoming, Texas, Montana, North Dakota, Colorado, Oklahoma, Utah, and Kansas), it was shown that New Mexico collects an equivalent of 20% of the O&G production revenue in the state in terms of taxes (severance, conservation, and school tax) as well as land income (federal and state leases), the largest state revenue, in terms of percentage of the O&G revenue, among studied states (Tysseling, Bjarke & Anklam 2019). In 2018, O&G production in New Mexico contributed \$2.2 billion to the state's general fund (New Mexico Oil and Gas Association 2019), making up 37% of state tax revenue (State of New Mexico 2018).

Although O&G production in the Permian Basin provides substantial revenue to New Mexico's economy, there are associated negative environmental outcomes: (1) Large volumes of freshwater are consumed for the recovery of O&G from unconventional resources. Production of O&G from unconventional (shale and tight sand) formations depends on hydraulic fracturing, a water-intensive technology used for stimulating the impermeable and impervious geologic layers. The Permian Basin region is arid, and water is a scarce resource. Due to its scarcity, mining, agriculture, and municipal sectors are continually competing over water, increasing the scarcity value of water. For example, a study by James et al. (2014) showed that a 10% decline in water availability in the Colorado River could translate into a \$143.4 billion decline in Arizona's Gross State Product. Due to water scarcity, large withdrawals of freshwater for hydraulic fracturing (HF) operations are becoming a concern to the southwestern states (Scanlon, Reedy & Nicot 2014a; Scanlon et al. 2017; Nicot & Scanlon 2012).

(2) A substantial stream of wastewater is generated along with O&G liquids (Veil et al. 2004). The common practice for handling produced water is disposal in deep injection wells, also known as class II disposal wells (State of New Mexico & U.S. Environmental Agency 2018). The disposal capacity depends on the stock of disposal wells as well as the capacity of the receiving geologic formation. Even when there are enough disposal wells, the reservoir engineering wisdom suggests that the geologic capacity of disposal is limited and that drowning an underground geologic layer could result in adverse system shocks as well as the loss of hydrocarbon. Besides, injecting high volumes of wastewater in underground geologic formations has been associated

with induced seismicity (Keranen et al. 2013). In 2015, about 900  $M_w \geq 3$ <sup>4</sup> earthquakes were reported in Oklahoma, whereas only one  $M_w \geq 3$  earthquake took place before 2009 (Johann, Shapiro & Dinske 2018). In the same year (2015), to curtail seismic activity, the Oklahoma Corporation Commission (OCC) restricted the wastewater injection for disposal volumes in northern Oklahoma County and southern Logan County.<sup>5</sup> According to this restriction, O&G producers in those areas had to decrease their disposal volumes by 38 percent or 3.4 million barrels below their 2014 injection volumes. The New Mexico Oil Conservation Division (NM-OCD) is New Mexico's agency in charge of the management of O&G production operations as well as waste disposal operations. Conversations with the engineers of the Engineering Bureau at the NM-OCD have indicated that New Mexico is moving towards controlling disposal volumes in order to protect the underground layers and reduce the risk of induced seismicity.

Overall, New Mexico faces a problem of balancing between maximizing tax revenue and minimizing negative environmental outcomes. The motivation of this study is to use data and simulation models to inform policy decisions at the state level. In addition, we are interested in estimating the monetary impacts of hypothetical capacity constraints on freshwater withdrawal and/or wastewater disposal volumes in the Permian Basin. This study adopts an integrated modeling approach to match the complex nature of the problem. In this study, we investigate policy scenarios and instruments that could lead to sustainable economic and environmental

---

<sup>4</sup>  $M_w$  is the moment magnitude scale to measure the intensity of an earthquake, the largest recorded earthquake in the world was 9.5  $M_w$  in Chile in 1960. Earthquakes with  $M_w \geq 3$  can be felt by humans,  $M_w = 5$  is considered a light earthquake and magnitude  $M_w \geq 7$  is associated with \$ billions loss to the human communities. (USGS Earthquake Facts). <https://earthquake.usgs.gov/learn/facts.php>

<sup>5</sup> Oklahoma Oil and Gas Disposal Well Volume Reduction Plan, <https://www.occeweb.com/News/08-03-15VOLUME%20ADVISORY%20RELEASE.pdf>



outcomes. What makes this study unique is that it combines economic and physical processes to arrive at a realistic and multifaceted assessment of potential policy outcomes. Focusing solely on maximum economic revenue could result in alarming exhaustion to the freshwater resources. On the other hand, posing overly strict constraints on disposal of produced water (PW) or the use of freshwater could limit the state income and ultimately social welfare.

## **2. Background**

### **2.1. Hydrocarbon production from unconventional resources**

Conventional resources refer to hydrocarbon accumulations in permeable geologic layers. The common practice for extracting O&G from conventional resources is to drill a well into pools of hydrocarbon and to let the pressure difference between the geologic layer and the wellbore along with pumping operations to drive hydrocarbon to the surface. On the other hand, unconventional geologic layers<sup>6</sup> are characterized by the geologic layer's pressure abnormalities and low to very low permeability and/or porosity (Johnson, Crawford & Bunger 2004). In the 1990s, a combination of horizontal drilling and hydraulic fracturing (HF) technologies contributed to the successful recovery of O&G from an unconventional resource in Texas (Ridley 2011). However, due to complex technological requirements, unconventional resources were deemed economically unyielding until the early 2010s (Bartis et al. 2005; Mohr & Evans 2010). A rapid rise in oil prices between early 2007 and mid-2008 and speculations about a continued decline in the United States' conventional oil production led U.S. O&G producers to reevaluate the economic

---

<sup>6</sup> There are three types of unconventional layers, namely shale, tight sand, and coalbed methane. Shale and tight sands are the two forms of unconventional resources that are discussed in these paragraphs.

profitability of unconventional resources (Biglarbigi et al. 2009). The mass adoption of unconventional technologies to recover O&G from unconventional resources is marked as the shale revolution that took place around 2009-2011. Subsequently, large estimates of unconventional resources were added into the U.S. O&G proved reserves<sup>7</sup> (Figure 2.1).

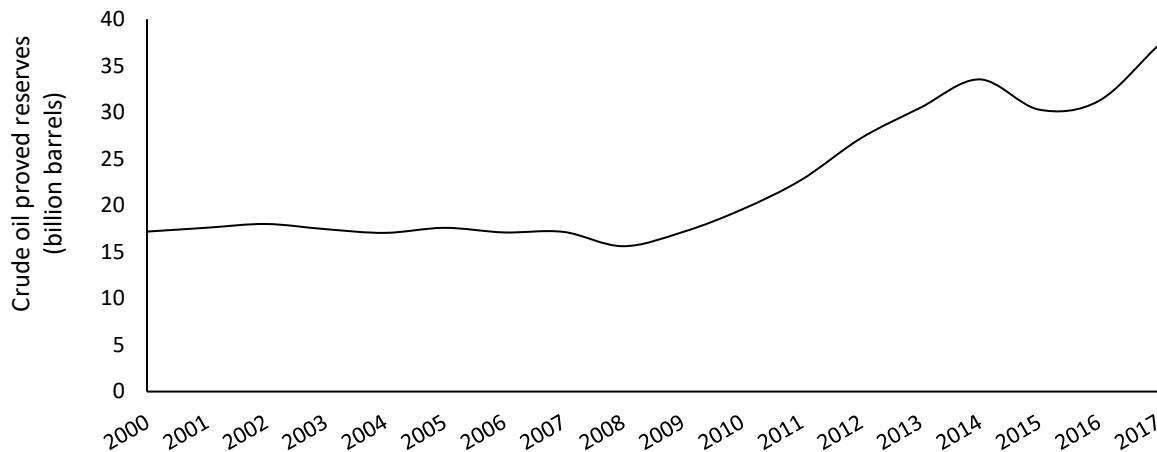


Figure 2.1: The U.S. onshore proved reserves stocks (Source Energy Information Administration [EIA] 2018a)

## 2.2. Production decline curve

Once a well is drilled, the petrophysical characteristics, such as permeability, pressure, density, etc., of the well's targeted formation govern the hydrocarbon volumes that flow to the surface at the wellhead (Mason & van't Veld 2013). Since the pressure of the formation decays as more hydrocarbon liquids are extracted, the amount of production at the wellhead declines over the production life of a well, regardless of the type of resource (i.e. conventional or unconventional).

Johnson and Bollens (1927), observing well production data, showed that the decline in

---

<sup>7</sup> High confidence estimations of available crude oil (and natural gas) liquids which is recoverable in an economically feasible manner. <https://www.eia.gov/tools/glossary/index.php?id=P>

production over equal time periods could be graphed mathematically. Arps (1945) classified decline curves based on the dynamic behavior of the decline loss ratio (constant, arithmetic series, and geometric series). Arps' decline curve method is widely used to this date. For example, Wachtmeister et al. (2017) estimated decline curve parameters for individual wells as well as an aggregated decline curves for tight oil production from the Eagle Ford Basin. Similarly, Guo et al. (2016) estimated the shale gas decline curve from the Eagle Ford Basin. Paryani et al. (2016) proposed an approximate Bayesian computation framework to derive the distribution of the type curve parameters. Using a hindcasting methodology, Male (2019) measured uncertainties in the decline curve parameter estimation for the Marcellus, Fayetteville, Haynesville, and Barnett plays. Arp's decline curve has a generic hyperbolic functional form, as shown in equation (1):

$$Q = \frac{Q_0}{(1 + bDt)^{\frac{1}{b}}}, \quad (1)$$

where  $Q_0$  is the peak production volume,  $b$  is the curvature,  $D$  is the initial decline rate ( $D = \left(\frac{Q}{\Delta Q}\right)_{Q=Q_0}$ ), and  $t$  is the time index.

Since different formations have different initial pressures and structures, the parameters in equation (1), *i. e.*  $Q_0$ ,  $b$ , and  $D$ , should be estimated for each formation separately. A distinctive characteristic of the unconventional production decline curve is high peak production ( $Q_0$ ) and large initial decline rate ( $D$ ) (McNally 2017). The difference between production decline from conventional and unconventional formations is described by McNally as follows:

If conventional oil production is like sticking a straw in the ground and letting natural pressure push oil out steadily for a long period of time, shale oil production is like wringing

a wet sponge: You get a lot of liquid right away, but it dries up fast.

### 2.3. Drilling

Previous studies have shown that drilling activity in the United States is more price responsive than are oil production rates. Mason and Roberts (2018) showed that after a well is drilled, oil prices have little to no impact on the volume of production. This is also evident in the empirical data. As shown in Figure 2.2, throughout the 2000-2018 period, irrespective of the West Texas Intermediate (WTI<sup>8</sup>) oil price boom and bust cycles, oil production has increased. The increase in production was reasonably slow until 2011 and intensified during 2011 and 2015. Following a slight decrease in production after 2015, production increased sharply around August 2017 and continued to increase until the end of 2018.

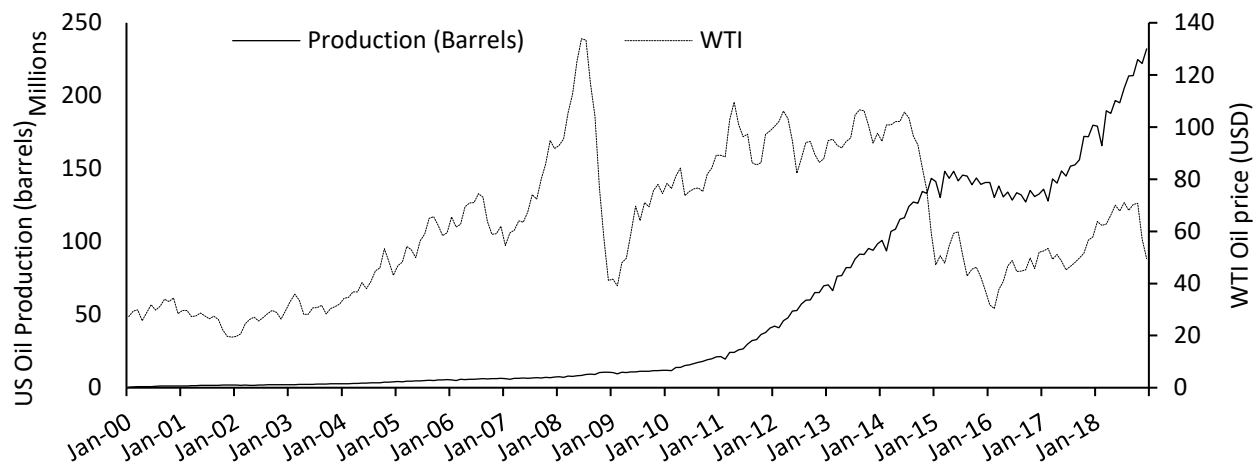


Figure 2.2: Time series of oil production its relationship to oil prices

For comparison, the relationship between oil prices and drilling activity is shown in Figure 2.3.

---

<sup>8</sup> WTI price is a grade of crude oil that is produced in Texas and southern Oklahoma, and is the reference grade for pricing at Cushing, Oklahoma. All these prices pertain to U.S. onshore oil productions.

Unlike production, U.S. drilling activity does follow price cycles, although with some delay. The responsiveness of drilling activity to oil prices is visibly higher after 2011.

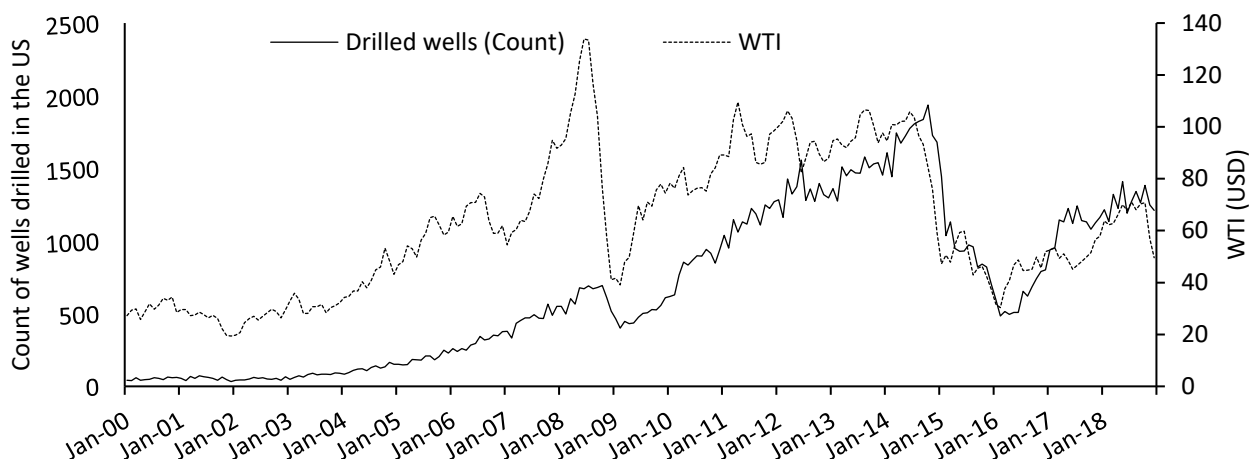


Figure 2.3: Time series of oil production (above) and drilled wells count (below) and their relationship to prices

It is expected that drilling activity in unconventional formations is yet more price responsive than in conventional formations; in the 2013 *World Energy Outlook* report by the International Energy Agency, high responsiveness of shale oil drilling to oil prices is linked to the unconventional production profile: high initial production rate and steep and early decline.

The relationship between drilling activity and prices has been investigated based on the law of supply and by estimating the price elasticity of the supply of new wells. The general assumption in these studies is that the United States is a price taker in the oil market (Kellogg 2014; McNally 2017).

#### 2.4. Shutdown condition

Compared to the literature focusing on estimating drilling activity as an economic activity, the decision to stop production from a well is less studied. If the revenue generated from a well

covers the maintenance and product handling costs, operations will continue production (Energy Information Administration 2016)<sup>9</sup>. The shutdown time of a well can be estimated based on the well's decline curve, as is shown in Figure 2.4, for a representative decline curve.

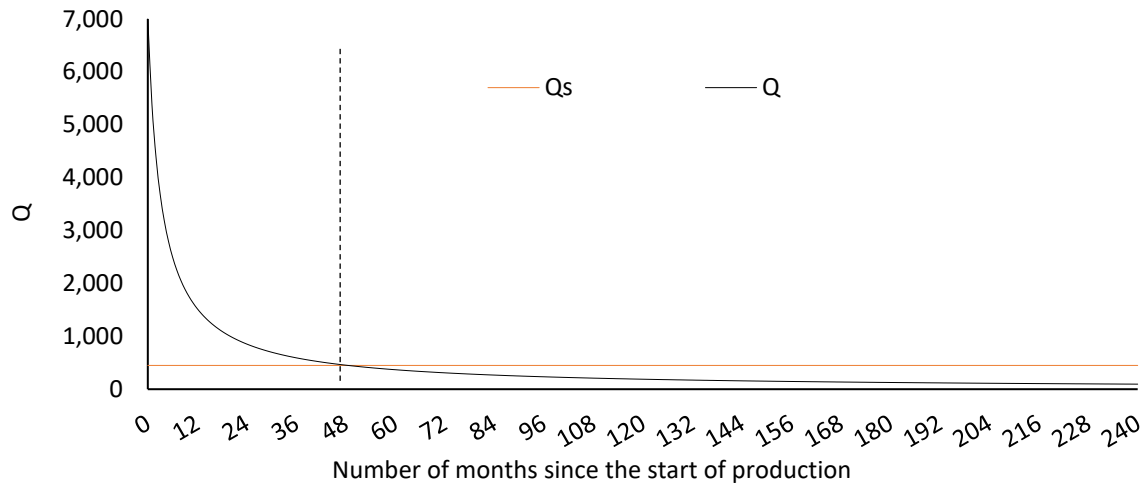


Figure 2.4: Shut down criteria

For the representative production decline curve shown in Figure 2.4 ( $Q_0 = 7,000 \frac{\text{BBL}}{\text{month}}$ ,  $b = 1$ , and  $D = 0.3$ ) the well reaches shutdown condition ( $Q_s = 450 \frac{\text{BBL}}{\text{month}}$ ) in month 48.

## 2.5. Hydraulic fracturing water demand

Unconventional hydrocarbon-bearing layers have low permeability and pressure abnormalities. In addition, hydrocarbon accumulations in these formations occur in disperse locations. Due to such difficult characteristics, stimulation is required to facilitate the production of hydrocarbon from unconventional resources. Stimulating an unconventional formation is done at the well

---

<sup>9</sup> Stripper wells accounted for 10% of U.S. oil production in 2015.

location and through hydraulic fracturing (HF).

The HF process uses water, water additives, and proppants (Energy Information Administration 2016). Water acts as the main carrier in HF and makes up a large portion of the fluid used in HF (Scanlon, Reedy & Nicot 2014b). Designing the HF fluid mix is a complex process involving a variety of variables related to the design of the well as well as the characteristics of the target formation. In a recent study, Kondash, Lauer and Vengosh (2018) showed that the amount of water used for HF per well has generally increased in the United States. According to Kondash, Lauer and Vengosh (2018), the growth in water consumption for HF was highest in the Permian Basin, where water used for HF, per well, increased 770% from 4 acre-feet in 2011 to 34.5 acre-feet in 2016. The authors argued that the increase in water consumption correlated with an increase in the lateral length of wells and the hydrocarbon yield.

Figure 2.5 illustrates changes in the lateral lengths of wells drilled in the New Mexico portion of the Permian Basin since 2011. According to Figure 2.5, the number of wells with short laterals (3,000 ft) had been reduced to almost none in 2018, whereas the number of wells with ultra-long laterals ( $\geq$  9,000 ft) had significantly increased.

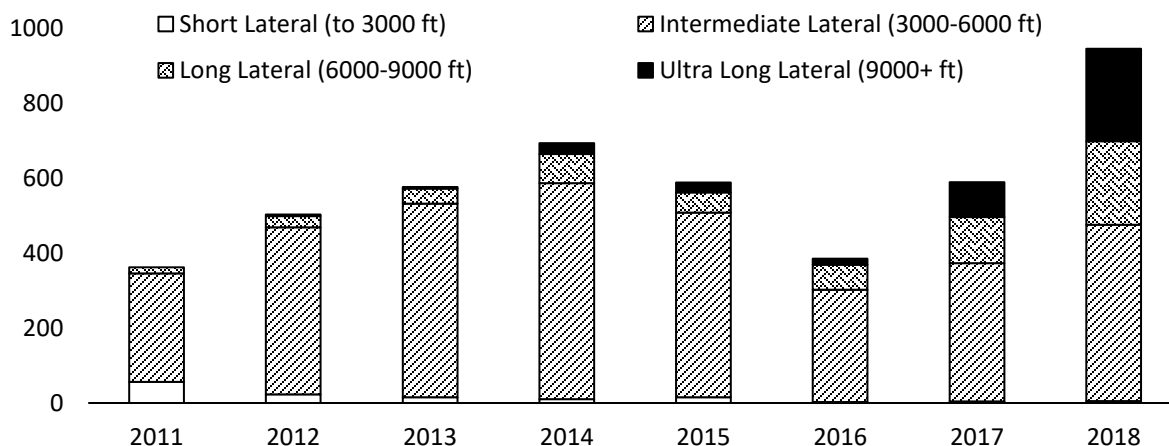


Figure 2.5: Count of horizontal wells drilled (and completed) with certain lateral length in the Delaware sub-basin of the Permian Basin (New Mexico portion). (Source: Rystad Energy ShaleWellCube Browser)

Similar to the findings of Kondash, Lauer and Vengosh (2018), when water consumption is normalized per lateral length, the increase in water use is still significant (Figure 2.6).

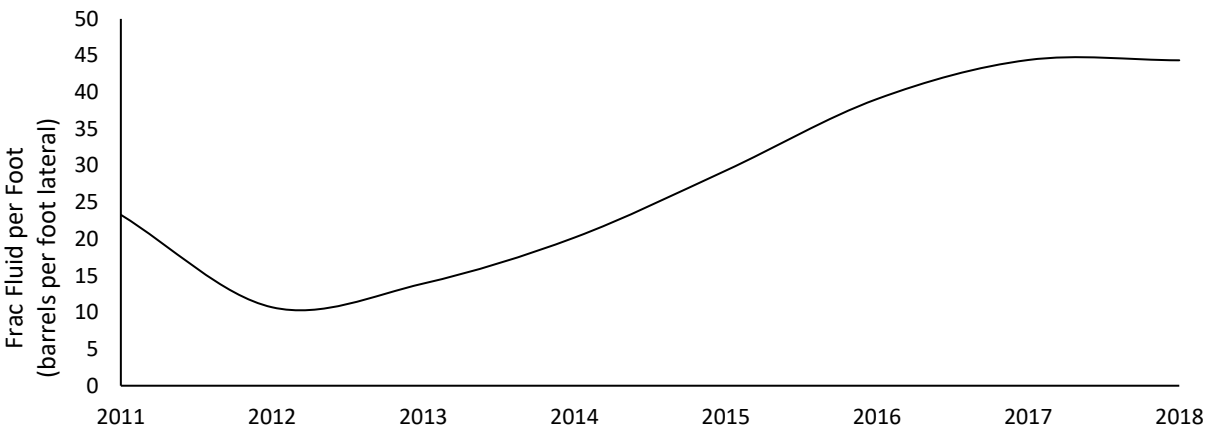


Figure 2.6: HF fluid used per lateral length, by year of completion

It is unclear how much of the increase in the amount of water used per lateral length is due to the aging of the formation and/or to increase the yield, or both. Through experimental analysis, Fitzgerald (2015) showed that by increasing water content, there could be gains in terms of hydrocarbon yield, but the relationship is not empirically confirmed. To forecast future (after 2016) water consumption rates, (water use per well), Kondash, Lauer and Vengosh (2018) assumed that the water use would increase at the highest increase rate recorded between 2011 and 2016.

## 2.6. Produced water

Concurrent with the production of O&G, low-quality water, referred to as produced water (PW), is also brought to the surface at the wellhead. PW contains a variety of contaminants, including



total dissolved solids (TDS), some amounts of hydrocarbon, bacteria, and naturally occurring radioactive materials (Chermak & Patrick 2016; Veil et al. 2004). The PW-to-oil ratio is used to study the patterns of PW production. Scanlon et al. (2017) showed that in the Permian Basin, the ratio of PW-to-oil has increased from 1.4 in 2008 to 1.7 in 2015. In the Delaware sub-basin of the Permian Basin, 6 acre-feet of produced water was generated per well in 2008 which increased to 16 acre-feet per well in 2015 (Scanlon et al. 2017). On average, 51.8 acre-feet of PW was generated per year throughout the Permian Basin, between 2005 and 2016; most of this volume (40,633 acre-feet) was produced by vertical wells (Zemlick et al. 2018).

## 2.7. Produced water management

Produced water is the largest waste stream in the O&G industry (Veil et al. 2004). Handling PW is becoming increasingly problematic in O&G operations and adds to the operational costs of oil production (Chermak & Patrick 2016), reducing the economic profitability of the industry. PW is handled either through disposal or salvaging. Three modes of salvaging PW include reuse, recycling, and renewal. A white paper prepared by the State of New Mexico and U.S. Environmental Protection Agency (2018), explains the terms as follows:

- Reuse: to minimally treat the produced water and use it in O&G production operations
- Recycle: to significantly treat the produced water and use it in O&G production operations
- Renew: to significantly treat the produced water and use it in non-O&G related operations

Depending on the characteristics of the water and the regulatory environment in different O&G basins, the industry might prefer one or more approaches. However, while both EPA and New Mexico environmental and mineral agencies advocate for reuse and recycling of produced water,

data shows that disposal of PW is still the most attractive handling option in the New Mexico portion of the Permian Basin.

In New Mexico, the Oil Conservation Division (NM-OCD) regulates the disposal of PW in injection wells. Since 1982, NM-OCD has issued permits for disposal applications and determined injection pressure and injection rates. As for now, the agency issues injection permits based on engineering discretion and knowledge of the geologic layers. The permitting process sometimes results in a backlog in disposal that results in additional storage costs to the operators. In order to promote recycling and reusing of the produced water, to protect the underground strata from overloading with wastewater, and to reduce the seismic risk of disposal, NM-OCD could seek disposal capacity constraints, similar to Oklahoma. However, the economic impact of such capacity constraints is unknown.

Disposal of PW is by injection in Class II injection wells. In New Mexico Permian, 729 active injection wells were recorded in November 2018. Figure 2.7 summarizes the total volumes of PW generated and injected for disposal between 2002 and 2017.

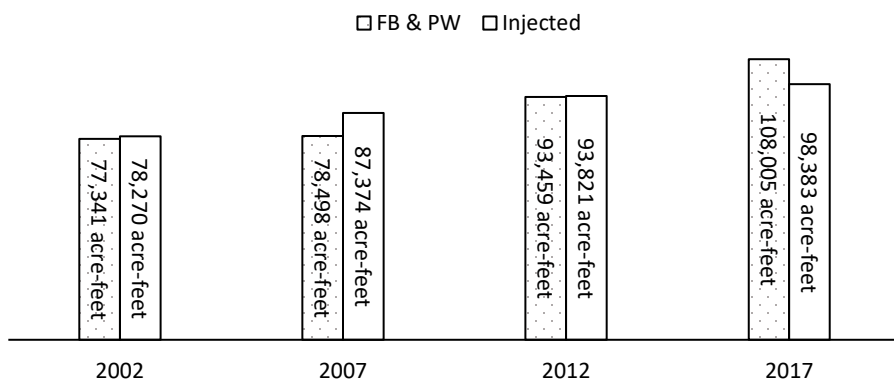


Figure 2.7: Volumes produced and injected for disposal in New Mexico Permian (Source: Goetze 2018)

Due to the capacity constraints of the PW-receiving geologic formations and the induced

seismicity hazard associated with the disposal of PW, economically viable policy scenarios to limit disposal are called for. However, to the best of our knowledge, there is no existing framework to assess the impact of a potential disposal capacity constraint on O&G revenue generation.

### 3. Theoretical model

The decision maker of in this study is the state-level policymaker who has multiple objectives including maximizing tax revenue, minimizing freshwater consumption and minimizing produced water disposal:

$$\max_{\alpha_t} \{R(\alpha_t), -W(\alpha_t), -PW(\alpha_t)\}, \quad (2)$$

where  $\alpha_t$  is an array of policy instruments that the policymaker can choose from,  $R(\alpha_t)$  is the net present value of the tax revenue generated for the state during the planning horizon,  $W(\alpha_t)$  is the maximum monthly freshwater consumption volume and  $PW(\alpha_t)$  is the maximum monthly PW disposal volume. A no-action or business-as-usual policy is shown by  $\emptyset$  symbol. Under business-as-usual scenario, the tax revenue to the state is as follows:

as follows:

$$R(\emptyset) = \sum_{i=1}^{X_t(\emptyset)} \eta_t \times P_t \times Q_t, \quad (3)$$

where  $X_t(\emptyset)$  is the number of producing wells;  $\eta_t$ <sup>10</sup> is the percentage of the O&G production revenue that the state collects as tax income;  $P_t$  is the average monthly oil price in month  $t$  and

---

<sup>10</sup> The policymaker does not observe or accrue drilling, completion and operation costs, but  $\eta(t)$  accounts for the deducted tax that, to some degree, reflects the costs accrued to the producers.

$Q_t$  is the total volume of oil produced during month  $t$ .

$X_t(\emptyset)$  is the sum of wells that are drilled and completed for production on or before month  $t$  and have not reached the end of their production life:

$$X_t(\emptyset) = \left( \sum_{m=0}^t N_m(\emptyset) \right) - \left( \sum_{m=0}^t \sum_{i=1}^{X_m(\emptyset)} s_{im}(\emptyset) \right), \quad (4)$$

where  $N_m$  is the number of new wells drilled in month  $m \leq t$  and  $s_{im}$  is a dummy variable determining whether well  $i$  is shutdown on or before month  $m$ . The number of new wells,  $N_t(\emptyset)$ , drilled during month  $t$  is determined by the price elasticity of the supply of new wells,  $\varepsilon$ .

$$N_t(\emptyset) \leq N_{t-1} + \varepsilon \cdot \% \Delta P_t \cdot N_{t-1}(\emptyset), \quad (5)$$

where  $\% \Delta P_m = \frac{\Delta P_m}{P_{m-1}}$  is the percentage change in oil prices. The shutdown indicator for well  $i$  is defined as follows:

$$s_{im}(\emptyset) = \begin{cases} 1 & \text{if } Q_{it} \leq Q_s(\emptyset) \\ 0 & \text{otherwise} \end{cases}. \quad (6)$$

Under no-action policy,  $Q_s(\emptyset)$  is the production rate below which the operational cost of production is not covered by the revenue generate from production:

$$P_t Q_s(\emptyset) \leq C(Q_s(\emptyset)) \quad (7)$$

Production volume from well  $i$  drilled in month  $t_i^0$  declines exponentially based on the production rate and the production schedule has a hyperbolic functional form (Arps 1945):

$$Q_i(m) = \frac{Q_i^0}{\left(1 + b_i \cdot D_i(m - t_i^0)\right)^{\frac{1}{b_i}}}, \quad (8)$$

where  $Q_i^0$  is the initial production rate for well  $i$ ,  $b_i$  is the well's decline curvature,  $D_i$  is the well's

initial decline rate, and  $m - t_i^0 \geq 0$  is the production age of the well in months .

Based on the number of wells drilled during month  $m$ , demand for freshwater for HF,  $W(t)$ , can be calculated as follows:

$$W_t(\emptyset) = \varphi_t(\emptyset) \cdot \omega_t \cdot N_t(\emptyset), \quad (9)$$

where  $\omega_t$  is the HF water required for the completion of an average well in month  $t$  and  $\varphi_t$  is the percentage HF water that is from freshwater resources, and not reused or recycled PW. The amount of water generated during each month,  $PWG_t$ , is estimated based on the oil production volumes as well as the PW-to-oil ratio,  $\Omega_t$ , which is assumed to be constant for simplicity:

$$PWG_t(\emptyset) = Q_t(\emptyset) \times \Omega_t(\emptyset). \quad (10)$$

We assume that all the formation water produced and not treated for reuse in HF operations is disposed of during the same month of its production:

$$PW_t(\emptyset) = PWG_t(\emptyset) - (1 - \varphi_t(\emptyset))W_{t+1}(\emptyset), \quad (11)$$

where  $PW_t$  is the PW disposal volume in month  $t$ . By imposing  $\alpha_t$  the revenue, water consumption volume and PW generation volume or  $R(\alpha_t) \neq R(\emptyset)$ ,  $PW_t(\alpha_t) \neq PW_t(\emptyset)$ , and  $W_t(\alpha_t) \neq W_t(\emptyset)$ . We can rewrite (2) as follows:

$$\begin{aligned} \max_{\alpha_t} \{ \Delta R(\alpha_t) = R(\alpha_t) - R(\emptyset), \Delta W(\alpha_t) = W_t(\emptyset) - W_t(\alpha_t), \Delta PW(\alpha_t) \\ = PW_t(\emptyset) - PW_t(\alpha_t) \}. \end{aligned} \quad (12)$$

Equation (12) doesn't yield a closed form solution. And we use a numerical approach to find  $\alpha_t$  that satisfies multiple objectives. There are various policy fscenarios available to the policymaker. We select three instruments to analyze and discuss in this chapter. The three policy instruments are freshwater consumption constraint  $W(\alpha_w)$ , shutdown condition  $Q_s(\alpha_s)$  and treatment

requirement  $\varphi_t(\alpha_\varphi)$ . The freshwater consumption constraint together with the treatment requirement limits the amount of water used for HF processes, by limiting the number of new wells:

$$N_t(\alpha) = \frac{W(\alpha_W)}{c\varphi_t(\alpha_\varphi) \cdot \omega_t}. \quad (13)$$

The shutdown condition controls the shutdown production rate ( $Q_s(\alpha_s)$ ):

$$s_{im}(\alpha) = \begin{cases} 1 & \text{if } Q_{it} \leq Q_s(\alpha_s) \\ 0 & \text{otherwise} \end{cases}. \quad (14)$$

#### 4. The study area

Located in western Texas and southeastern New Mexico (Figure 2.8), the Permian Basin is one of the most active and productive basins in the United States. During 2017 and 2018, about 50% of the total active rigs in the United States were in the Permian Basin (Energy Information Administration 2019, May). During the same period, the Permian Basin produced 45% of the oil and 15% of the natural gas in the United States (Energy Information Administration 2019, May). This study focuses on the New Mexico portion of the Permian Basin between 2000 and 2018. New Mexico owns roughly 26% of the oil resources and 37% of the gas resources of the Delaware Basin,<sup>11</sup> one of the most productive sub-basins of the Permian Basin. Throughout the 2000-2018 period, on average, about one-fifth of the rig activity in the Delaware Basin has been in the New Mexico part.

---

<sup>11</sup> Based on the EIA's proved reserves of the eastern New Mexico and Texas Railroad Commission (District 08).

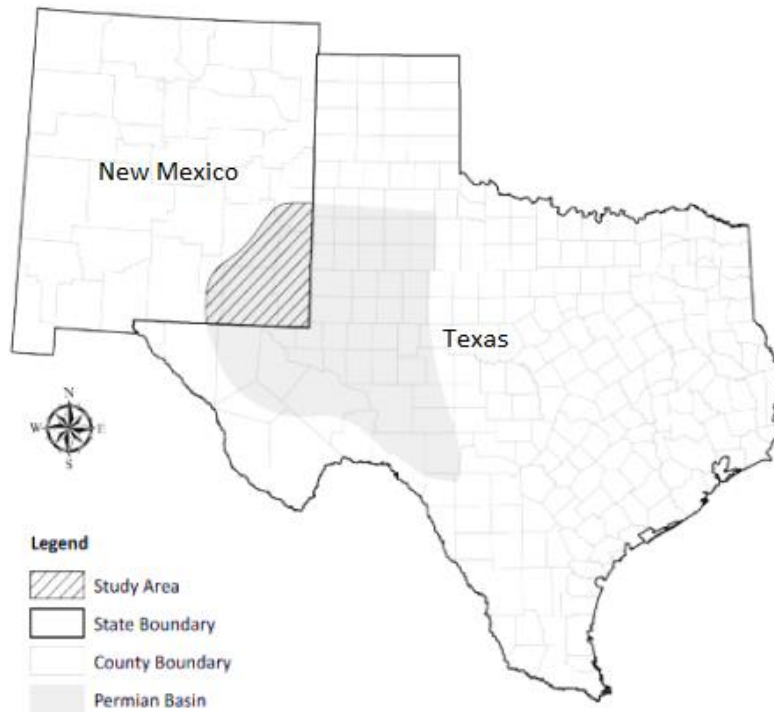


Figure 2.8: Location map of the study area (Map source: Bureau of Economic Geology, The University of Texas at Austin)<sup>12</sup>

This study mainly focuses on unconventional resources of New Mexico Permian for the following reasons:

1. An important characteristic of producing from unconventional reserves is the high initial production rate along with an early and sharp decline in the production rate. As a result, the production of O&G from unconventional reserves depends significantly on the number of new wells drilled. Consequently, the responsiveness of unconventional drilling activity to prices is higher than it would be for conventional drilling. (International Energy

---

<sup>12</sup> Permian Basin Geologic Synthesis Project: Project GIS Data  
<http://www.beg.utexas.edu/resprog/permianbasin/gis.htm>.

Agency 2013)

2. The number of vertical wells, associated with conventional formations, in the Permian has decreased substantially over the past 10 years (Figure 2.9).

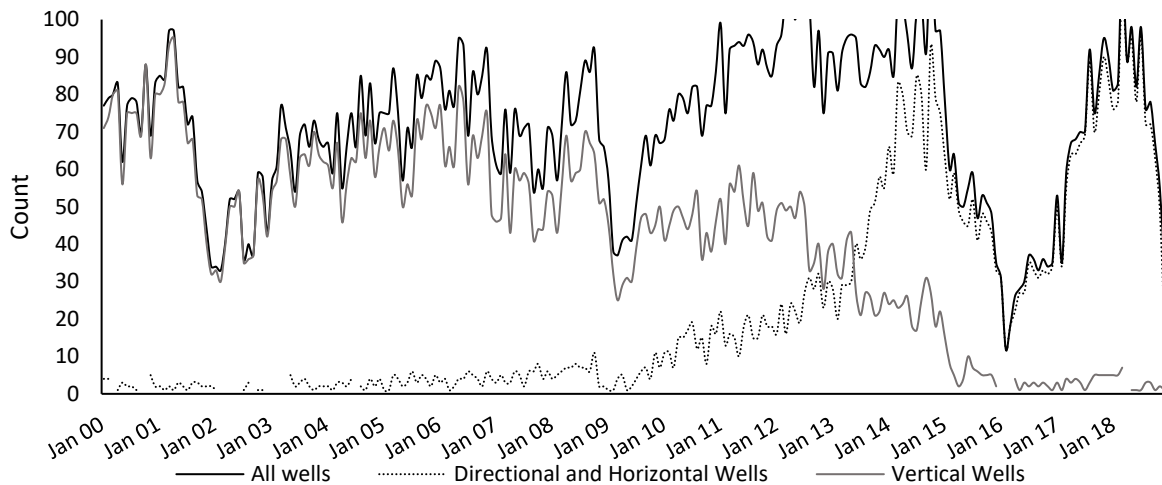


Figure 2.9: Count of horizontal, vertical, and all wells in New Mexico Permian

3. In the study period, most of the production in the Permian Basin comes from unconventional resources, especially in the Delaware sub-basin (Energy Information Administration 2014). The recent discovery of the largest unconventional reserve in the Delaware sub-basin adds to the unconventional production prospect of the basin, and conventional drilling and production are expected to decrease even more in the future.

Among unconventional resources of the New Mexico Permian, this study focuses especially on four formations, namely Bone Spring, Delaware, Glorieta & Yeso, and Wolfcamp (see Figure 2.10). These formations, along with the Spraberry formation, which is mainly on the Texas side of the Permian Basin, were responsible for 60% of the significant production growth in the Permian Basin since 2007 (Budzik & Perrin 2014). The Permian Basin has shown a high drilling success rate.



Over 92% of the wells drilled in the New Mexico portion of the Permian Basin and during 2000-2018 were completed at least once within 6 months from the drilling date, and 96% of the wells were completed within a year from the drilling date. Wells that are not productive are normally shut-in prior to completion. Here it is safe to assume that the number of shut-ins are insignificant in the study area.

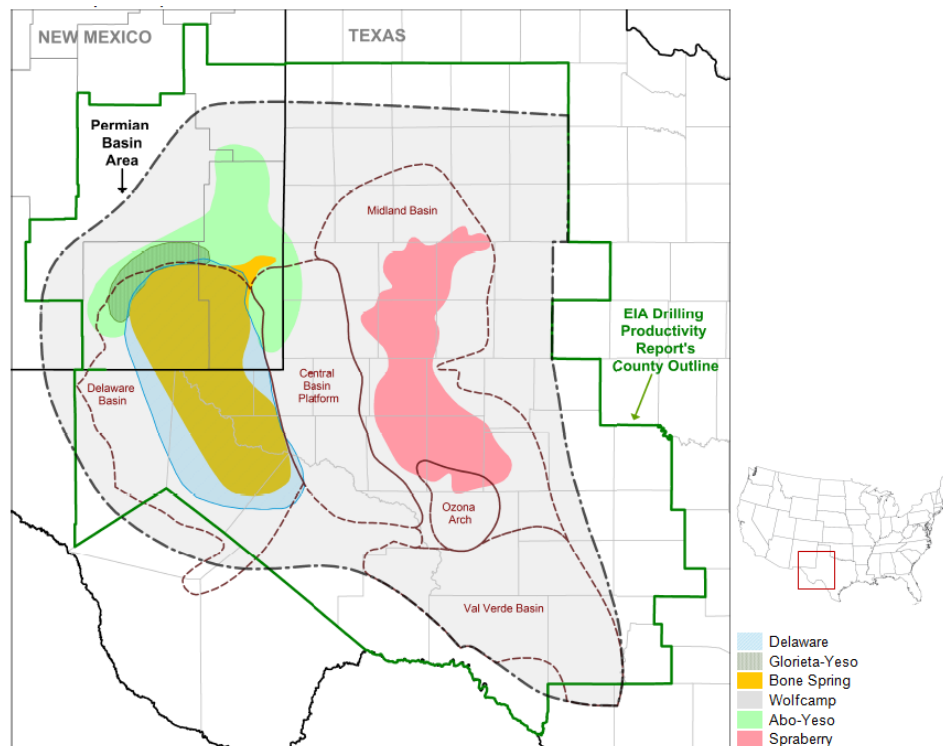


Figure 2.10: Selected oil-producing formations in the Permian Basin (Source: Budzik & Perrin 2014)

## 5. Model architecture and data

System dynamics is a simulation perspective first proposed by J.W. Forrester in 1958 and is celebrated for its ability to represent the complexities, nonlinearities, and feedback relationships that make up the social and physical systems of the real world (Forrester 1961). System dynamics provides an appropriate environment for integrating disparate models of socioeconomic and

physical systems regarding complex resource management issues while welcoming policy and planning interaction with the regulatory and governmental entities as well as the public (Tidwell et al. 2004). The selection of system dynamics for this study is based on two criteria. First, we are interested in showing the integrated nature (systems view) of the coupled human-natural system under investigation. Second, we are interested in the trajectory of outcomes over a planning period, hence we need a dynamic modeling environment.

The system dynamics modeling environment is based on a network of stock and flow variables that are connected to each other through known relationships (Tidwell et al. 2004; Sterman 2001). The first step in a system dynamics modeling technique is to identify variables, their type (stock or flow), and their conceptualized relationships. A causal loop diagram is a tool to present the cause and effect relationship between variables. The causal loop diagram of this study is described in the first part of this section. Variables, relationships among variables, and relationships between variables and time are explained in the following part. Next, data sources and treatments are described, and this section is completed by a presentation of the modeling environment in Powersim Studio software.

### 5.1. Causal loop diagram

The causal loop of the proposed system dynamics model is shown in Figure 2.11. Links in the causal loop diagram are charged by positive or negative polarity (Sterman 2000). A positive link from variable  $x$  to variable  $y$  means that all else equal, an increase in  $x$  causes an increase in  $y$  and vice versa.



Table 2.1: Description of the links in the causal loop diagram (Figure 2.11)

Link			Description
Source	End	Polarity	
OIL PRICES	DRILLING ACTIVITY	+	The relationship between the oil prices and drilling activity is through price elasticity of supply of new wells.
DRILLING ACTIVITY	STOCK OF ACTIVE WELLS	+	All else equal, an increase in the number of new wells extends the stock of active wells.
DRILLING ACTIVITY	FRESHWATER CONSUMPTION	+	In an unconventional production setting, for each new well drilled, water is required for hydraulic fracturing.
DRILLING ACTIVITY	PRODUCED WATER GENERATION	+	As explained in section 2.5, during the flowback period, HF water is recovered at the wellhead. Flowback water recovery occurs for 1-3 months following the drilling of the new well.
STOCK OF ACTIVE WELLS	OIL PRODUCTION	+	More active wells simply mean more oil production, as is shown in equation 1.
OIL PRODUCTION	STATE REVENUE	+	The state's revenue from O&G production is expressed in terms of the percentage of O&G production revenue (price × quantity).
OIL PRODUCTION	PRODUCED WATER GENERATION	+	Produced water is the by-product of oil production; through PW-to-oil ratio estimates, there is a direct relationship between the production of oil and produced water generation.
TREATMENT FOR REUSE	FRESHWATER CONSUMPTION	-	Treated produced water could be a substitute for fresh water; in other words, reusing or recycling more PW in HF operations, reduces the demand for freshwater.

PRODUCED WATER GENERATION	DISPOSAL VOLUME	+	Larger volumes of produced water, beyond the producer's capacity for storage and treatment, will result in higher demand for injection for disposal.
PRODUCED WATER GENERATION	TREATMENT FOR REUSE	+	With higher volumes of produced water generated, there is a higher potential for treatment.
DISPOSAL CAPACITY CONSTRAINT	DISPOSAL VOLUME	-	Imposing a capacity constraint below the business-as-usual volumes results in lower disposal volumes.
DISPOSAL CAPACITY CONSTRAINT	TREATMENT FOR REUSE	+	For an individual firm, a disposal capacity constraint could play as an incentive for treatment.
DISPOSAL CAPACITY CONSTRAINT	PRODUCED WATER GENERATION	-	Another possible outcome of imposing a capacity constraint could be the reduction of produced water generation, which ultimately means lowering hydrocarbon production volumes.
FRESHWATER WITHDRAWAL CAPACITY	TREATMENT FOR REUSE	+	Since freshwater and treated water are substitutes, a constraint on one could motivate the use of the other one.
FRESHWATER WITHDRAWAL CAPACITY	FRESHWATER CONSUMPTION	-	Imposing a capacity constraint below the business-as-usual withdrawal volumes results in lower withdrawals.

## 5.2. Stocks and flows

“Flow” and “stock” variables represent the dynamics of a system by identifying how variables’ values change with time. Whereas a flow variable passes value during each time step, without retaining it, a stock variable accumulates value (Sterman 2001). Among all the variables shown in Figure 2.11, only the STOCK OF ACTIVE WELLS is considered a stock. However, OIL PRODUCTION, PRODUCED WATER GENERATION, DISPOSAL VOLUME, TREATMENT FOR REUSE, and FRESHWATER CONSUMPTION act as stocks in the geospatial dimension. In other words, they present aggregate values of flow variables over groups of wells.

## 5.3. Computer simulation

The system dynamics model developed for this study was simulated in Powersim Studio 10, a product of Powersim Software AS. The simulation was run from January 2000 to January 2050 on a monthly basis. Figures 2.12 to 2.15 illustrate snapshots of four modules, namely new well drilling, hydraulic fracturing HF water demand, oil production, and produced water generation. These modules were repeated for each formation (Bone Spring, Delaware, Glorieta & Yeso, and Wolfcamp), and the aggregate results were used for calibration and analyses. The names of variables that appear in more than one module, and as such, provide the link between modules, are in bold font. Powersim Studio uses icons to present stocks, flows, constant, and auxiliary variables. A description of these icons is provided by Malczynski (2011).

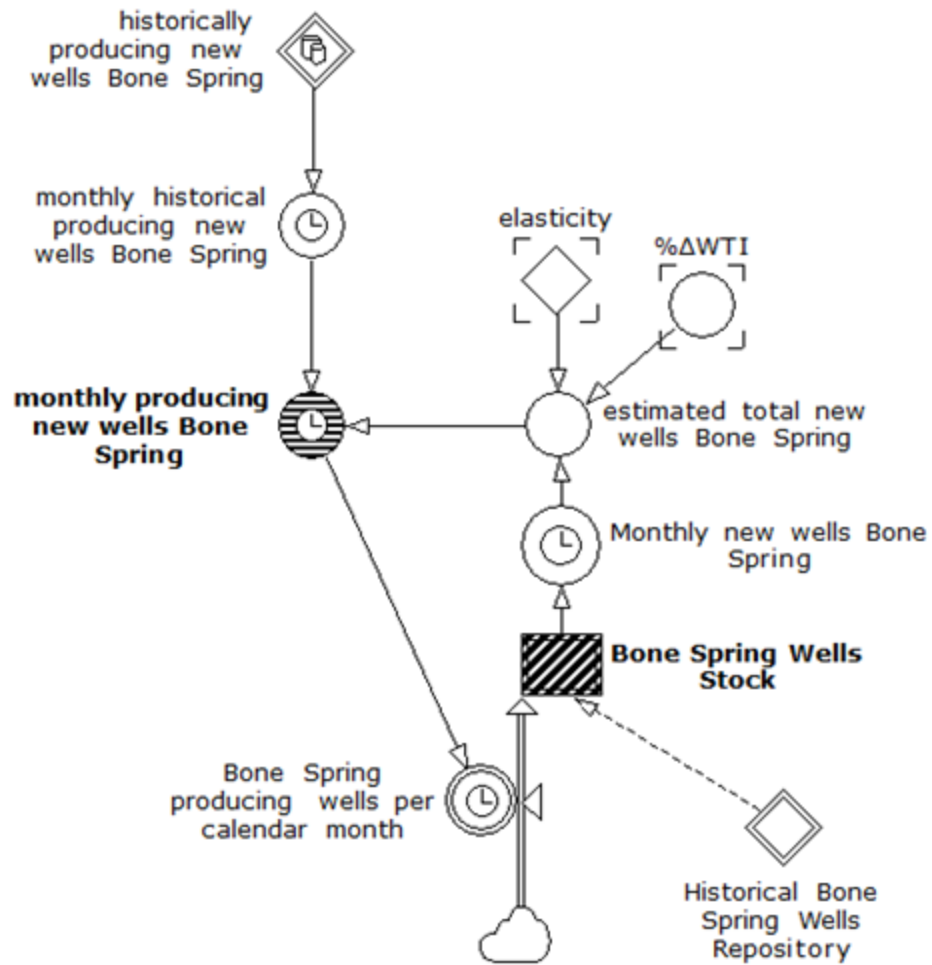


Figure 2.12: New wells module snapshot

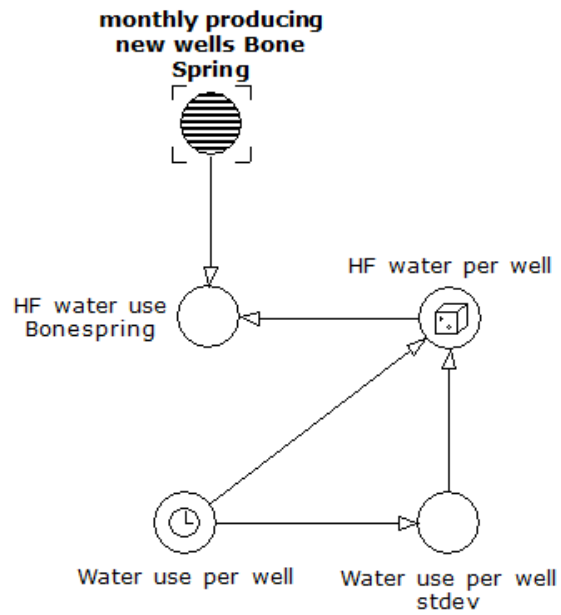


Figure 2.13: Hydraulic fracturing water demand

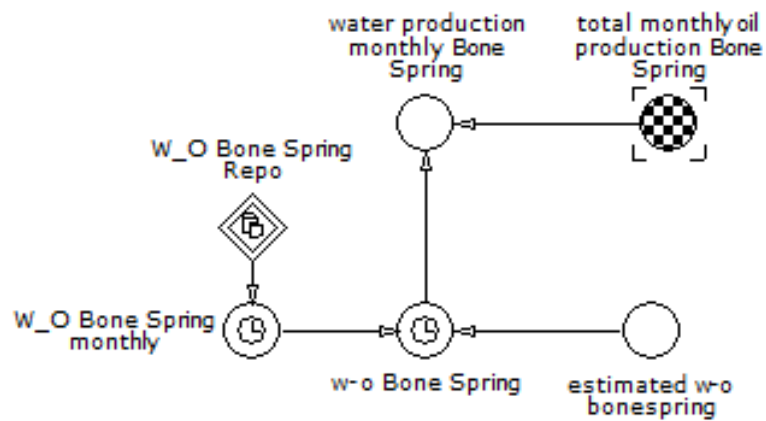


Figure 2.14: Produced water



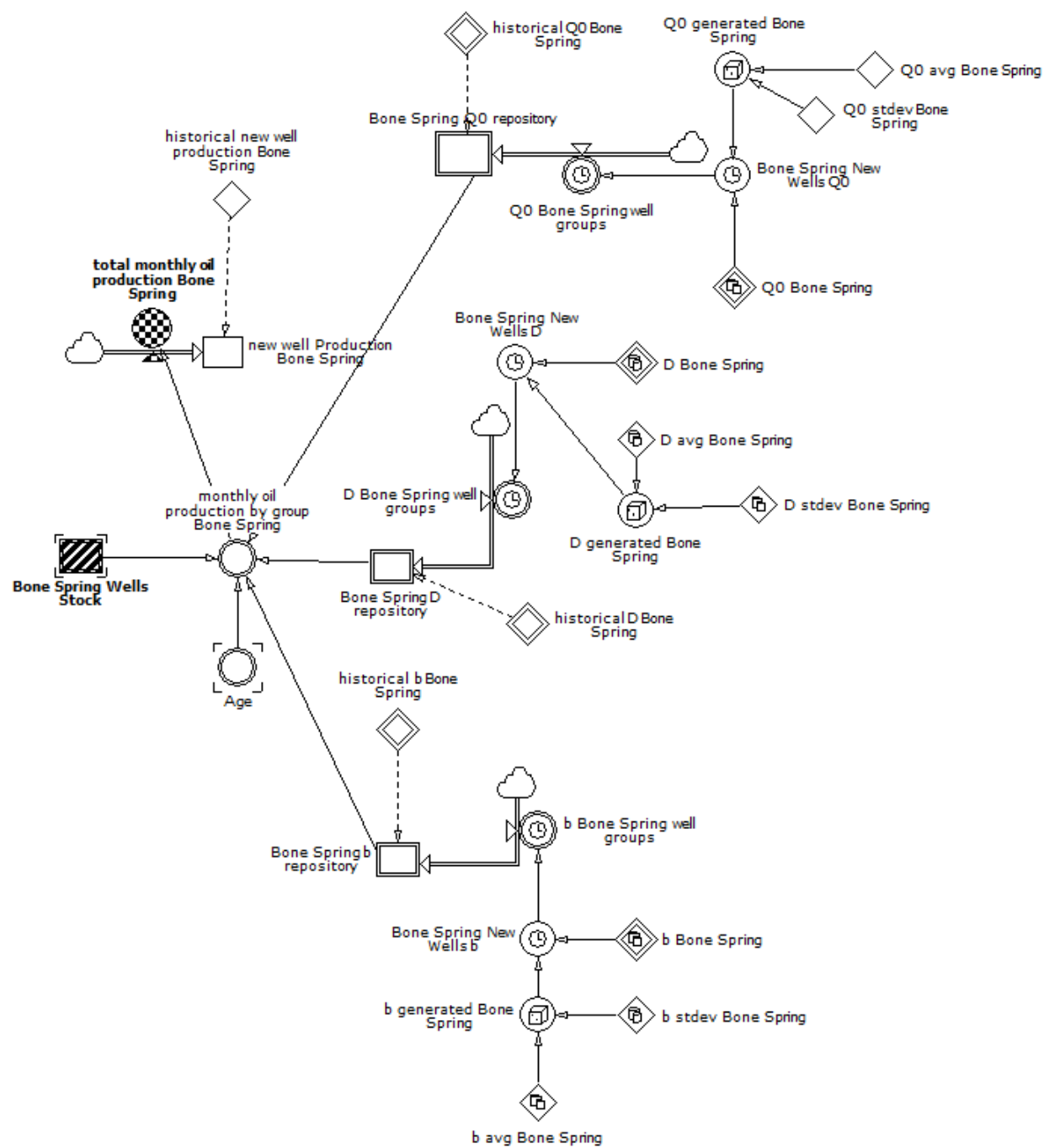


Figure 2.15: Oil production module

## 6. Data and model inputs

### 6.1. Historical data (2000-2018)

The historical part of the system dynamics model included January 2000 to January 2018. Historical data came from disparate sources. Table 2.2 summarizes the historical data used in this study.

Table 2.2: Description and sources of the historical data

Data item	Description	Source
Oil prices	Spot and futures contracts associated with the West Texas Intermediate grade crude oil	EIA <sup>a</sup>
Well counts	Number of wells drilled in a single month	NM-OCD <sup>b</sup>
Water consumption volumes	Volumes of water used for hydraulic fracturing of wells	Rystad Energy <sup>c</sup>
Oil volumes	Barrels of oil produced from each well	NM-OCD
Produced water volumes	Barrels of water produced from each well during oil production	NM-OCD

Notes:

U.S. Energy Information Administration. Petroleum & other liquids: Data: Cushing, OK WTI spot price FOB. Accessed January 2019. <https://www.eia.gov/dnav/pet/hist/RWTCD.htm>  
New Mexico Oil Conservation Division. T\_WC\_VOL, OCD Data and Statistics (Energy, Mining, and Natural Resources Department) Accessed January 2019

<ftp://164.64.106.6/Public/OCD/OCD%20Data>

Rystad Energy. *ShaleWellCube* (Shale Well Database).

In both the NM-OCD database and the ShaleWellCube database, wells are identified using a standard numerical identification system defined by the American Petroleum Institute. This identification system, called an API number, consists of a two-digit state code, a two-digit county code, and up to five digits for an individual well. NM-OCD records well information in a separate database from well production data. The well information dataset includes information about

each well that was obtained from the operators for issuing the drilling permit. The year and month of drilling is specified for each well; that information is used for counting the number of active wells during each month. Using the active wells count data as well as oil prices, drilling costs, and drought information, an econometric model was developed by Kalhor (2019) to model the supply of new wells. The immediate supply elasticity of wells was estimated as 0.729 with respect to spot prices.

The well information dataset also includes wells' target formations. This attribute was used to render the wells and production data pertaining to the formations of interest (Bone Spring, Delaware, Glorieta & Yeso, and Wolfcamp). Instead of using individual wells' production data directly, we grouped wells based on their target formations and their drilling year and estimated decline curve parameters for each group of wells. Decline curve parameters were estimated using a simple non-linear least square curve fitting method based on Arps' type curve model. The estimation model is shown in the following equation:

$$\begin{aligned} & \min_{b,D,Q_0} \sum_{t=0}^T e_t^2 \\ \text{s. t.} \quad & e_t = Q_t - \frac{Q_0}{(1 + bDt)^{\frac{1}{b}}}, \end{aligned} \quad (10)$$

where  $Q_t$  is the aggregated  $t^{th}$  month production of a group of wells;  $b$ ,  $D$  and  $Q_0$  are curvature, initial decline, and initial production rate of the group of wells, respectively; and  $e_t$  is the estimation error.

Table 2.3: Type curve parameter estimates for four top producing formations in the New Mexico Permian

(blank rows indicate lack of sufficient data for decline curve estimation)

Year drilled	Bone Spring			Delaware			Glorieta & Yeso			Wolfcamp		
	$\bar{Q}_0$	$b$	$D$	$\bar{Q}_0$	$b$	$D$	$\bar{Q}_0$	$b$	$D$	$\bar{Q}_0$	$b$	$D$
2000	7,990	2.42	0.14	4,828	0.95	0.19	2,095	3.33	4.55			
2001	3,660	2.35	0.04	6,078	1.87	0.41	7,986	0.45	0.08	535	10.0	10.0
2002	6,802	3.20	0.50									
2003	5,000	10.0	10.0	1,200	20.0	0.02	1,400	4.57	1.00	3,145	1.0	0.80
2004	2,379	6.00	0.50	1,305	1.04	0.07	2,555	3.47	0.40	4,496	1.0	0.50
2005	9,594	1.80	1.30									
2006	4,085	1.50	0.50	2,708	0.56	0.04	868	0.39	0.06	1,012	1.20	0.20
2007	983	4.50	2.00	2,107	1.12	0.15	881	1.61	0.23	970	2.65	0.76
2008	3,237	1.80	0.60	3,332	0.98	0.13	732	1.37	0.30	1,441	1.18	0.10
2009	4,244	3.00	0.75	931	1.09	0.10	1,857	0.77	0.07	6,147	1.10	0.21
2010	5,907	1.90	0.65	6,912	1.02	0.19	2,246	0.91	0.11	6,905	1.32	0.31
2011	8,181	2.00	0.70	6,624	0.80	0.18	2,193	1.00	0.28	5,707	1.10	0.22
2012	10,921	2.00	1.00	6,225	1.15	0.28	2,635	0.74	0.11	6,662	1.47	0.46
2013	9,861	1.50	0.40	8,218	0.73	0.15	3,721	0.61	0.11	7,624	1.45	0.29
2014	1,969	1.30	0.30	11,401	0.66	0.13	4,714	0.94	0.17	12,174	0.72	0.13
2015	7,456	1.20	0.30	14,806	0.80	0.29	8,500	0.46	0.12	23,779	1.00	1.00
2016	5,829	1.00	0.25	8,696	0.29	0.14	10,370	0.81	0.27	30,692	0.78	0.30
2017	8,259	0.05	0.20	18,932	0.20	0.2	8,676	0.01	0.10	28,738	0.14	0.24
2018	7,680	0.01	0.40				10,332	0.05	0.40	23,625	0.01	0.50

The calendar month of initial production varies among wells within a group. To remove skewness of the aggregate production volumes, the production schedules of all wells in a group were moved to the January of their drilling year, similar to the approach used in the Oil and Gas Supply Module of the National Energy Modeling System (Energy Information Administration 2014). To simulate the type curve parameters of an individual well, it was assumed that the curvature,  $b$ , and the initial decline rate,  $D$ , of an individual well were identical to those values for the group of wells; the initial production of all the wells in the same group was assumed to be the same and so the individual well's initial production,  $Q_i(t)$ , was calculated as follows:

$$Q_i^0 = \bar{Q}_{G_i}^0 = \frac{Q_{G_i}^0}{N_{G_i}}, \quad (11)$$

where  $G_i$  is the group of wells that well  $i$  belongs to, which includes wells that are drilled during the same year and share the same target formation. The estimated decline curve parameters' values are shown in Table 2.3.

The amounts of produced water generated from each well is also recorded in the NM-OCD's production dataset. To model the dynamics of PW generation, the PW-to-oil ratio was used. Historical monthly aggregate production of oil and water pertaining to each formation was used to calculate the PW-to-oil ratio. Figures 2.16 to 2.19 illustrate the time series of PW-to-oil ratios for the formations of interest.

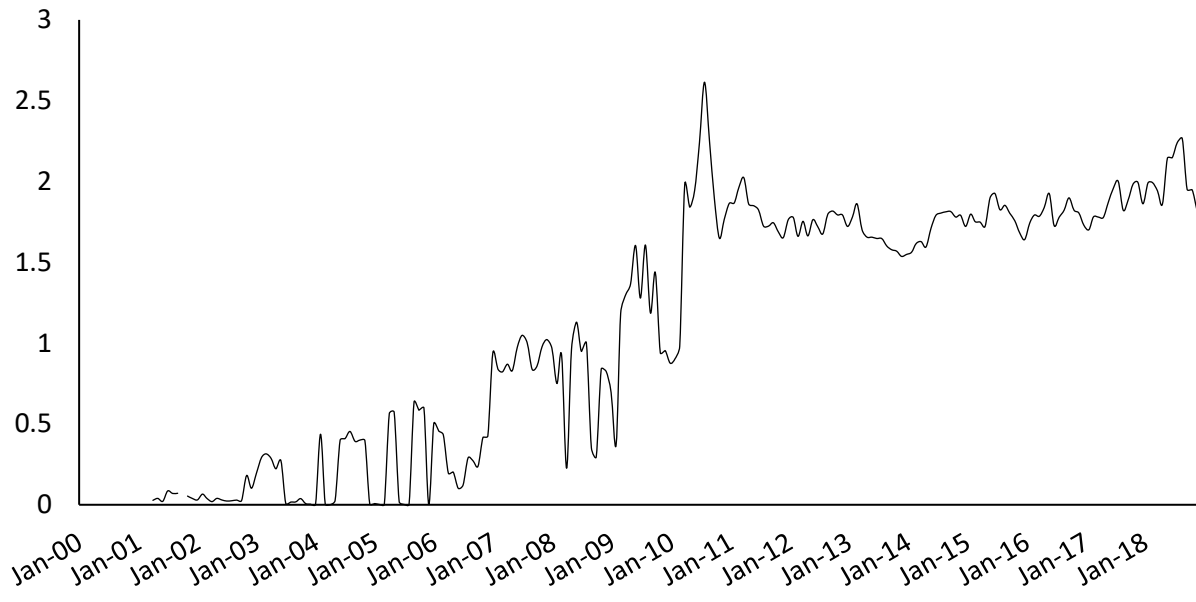


Figure 2.16: Historical PW-to-oil ratio for Bone Spring formation

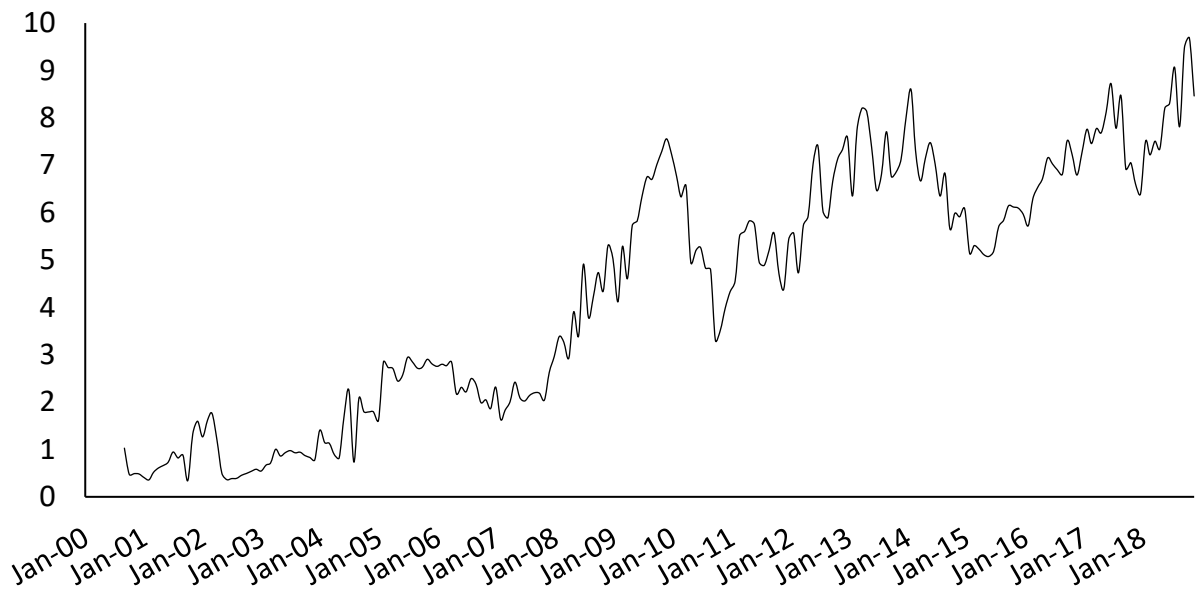


Figure 2.17: Historical PW-to-oil ratio for Delaware formation

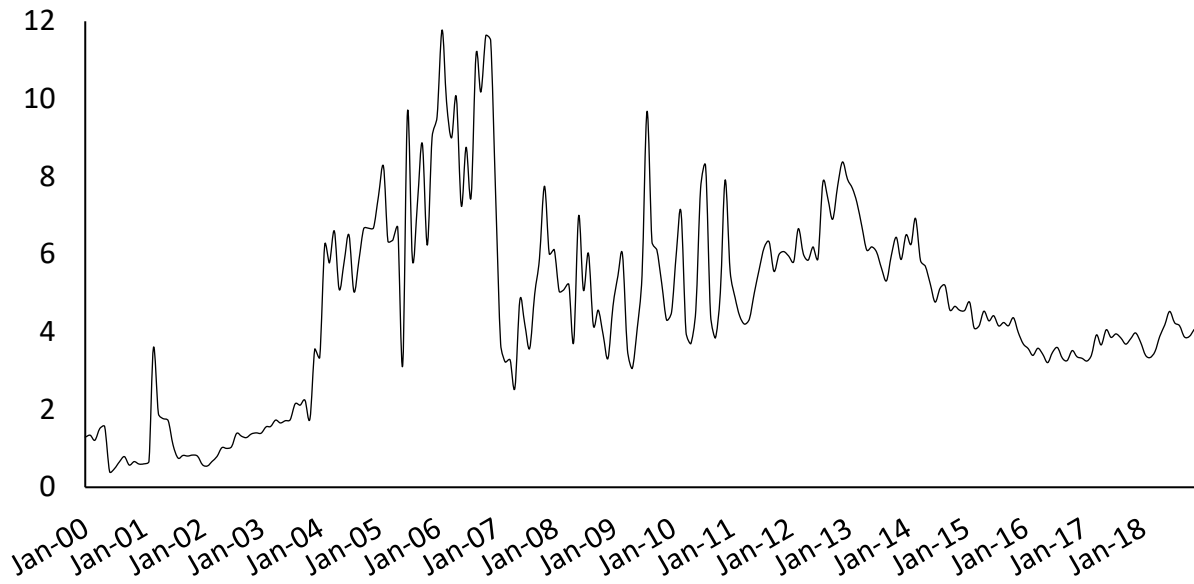


Figure 2.18: Historical PW-to-oil ratio for Glorieta & Yeso formations

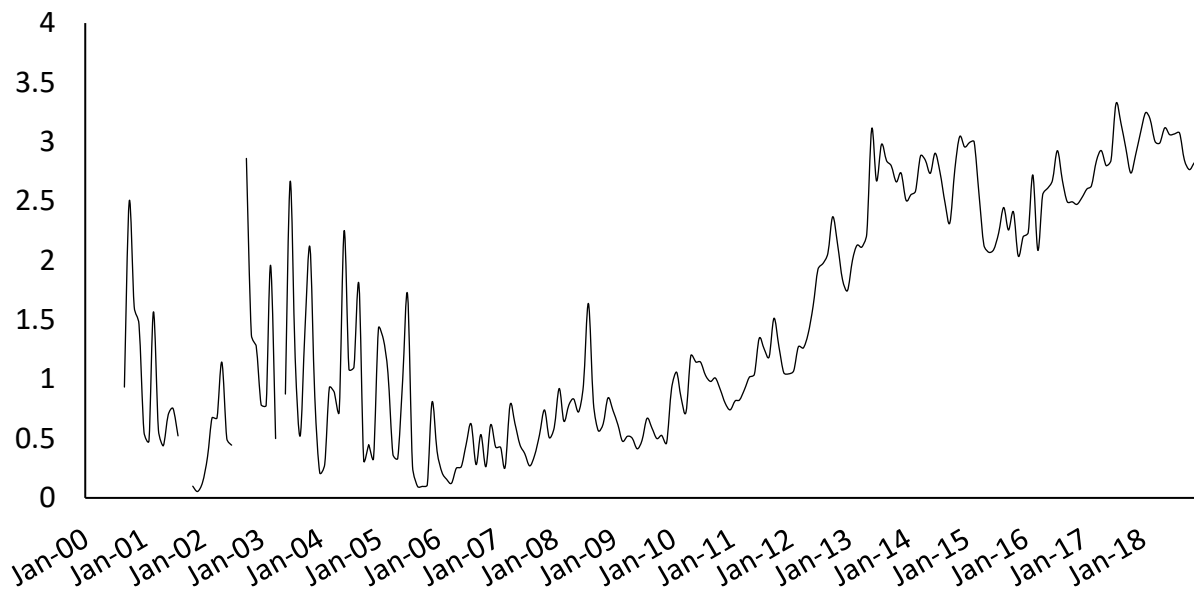


Figure 2.19 Historical PW-to-oil ratio for Wolfcamp formation

From 2011 until recently, hydraulic fracturing water use was reported to the NM-OCD and to FracFocus.org voluntarily. FracFocus.org is a chemical disclosure registry that provides well-level data on chemicals used for completion (Dundon, Abkowitz & Camp 2015). In addition to the chemical data, FracFocus.org collects data on HF water consumption volumes. Since August 2017, NM-OCD has mandated operators to report their HF fluid volumes and chemical composition to

FracFocus.org. Rystad Energy Inc., an independent energy research and business intelligence company headquartered in Norway, retrieves data from the FracFocus database frequently and provides that data in a format useful for research and business analytics. The HF water consumption data used in this study was from Rystad Energy’s ShaleWellCube database. The HF water consumption volumes for each well were matched based on the wells’ API numbers. The HF volumes are also aggregated for each formation and HF year and are listed in Table 2.4.

Table 2.4: Average HF water consumption volumes per well in acre-feet

Year	Bone Spring	Delaware	Wolfcamp	Glorieta & Yeso
2012	8.61	3.37	6.71	6.41
2013	8.80	4.89	8.92	2.59
2014	16.20	8.81	19.82	2.77
2015	18.84	10.19	27.39	6.91
2016	30.74	9.37	35.20	4.74
2017	35.86	50.59	39.45	14.67
2018	38.72	70.73	38.56	21.81

## 6.2. Future values (2018-2050)

Future oil prices were retrieved from the 2018 *Annual Energy Outlook* (AEO) by the EIA (2018). Annual WTI prices in the EIA’s AEO come from the national energy modeling system (NEMS<sup>13</sup>) and are calculated for the various market, technology, and resource scenarios. Future values of other variables were retrieved based on statistics, econometrics, and time series analyses, as will be discussed in the following paragraphs.

Future oil production rates from wells drilled prior to 2018 were retrieved from the decline curve parameters listed in Table 2.3. For wells that will be drilled in the future, the decline curve

---

<sup>13</sup> NEMS is a large-scale energy-economic equilibrium model, disaggregated at the county level and encompassing the entire United States (Gabriel, Kydes & Whitman 1999).



parameters ( $Q_0$ ,  $b$ , and  $D$ ) are unknown and need to be generated. Random values for decline curve parameters were generated from a normal distribution with the mean and standard deviation calculated from the historical values. Future PW-to-oil ratios were estimated based on the simple mean of historical data during an interval where the data exhibit mean reversion behavior<sup>14</sup>. The average water-to-oil ratio and the mean-reversing interval for the data is shown in Figures 2.20 to 2.23 and are summarized in Table 2.5.

Table 2.5: Average PW-to-oil ratio and the pertaining mean-reversing interval

Formation	Average PW-to-oil ratio	Mean-reversing interval
Bone Spring	1.80	January 2011 - December 2018
Delaware	6.69	January 2011 - December 2018
Glorieta & Yeso	4.17	January 2014 - December 2018
Wolfcamp	2.53	January 2012 - December 2018

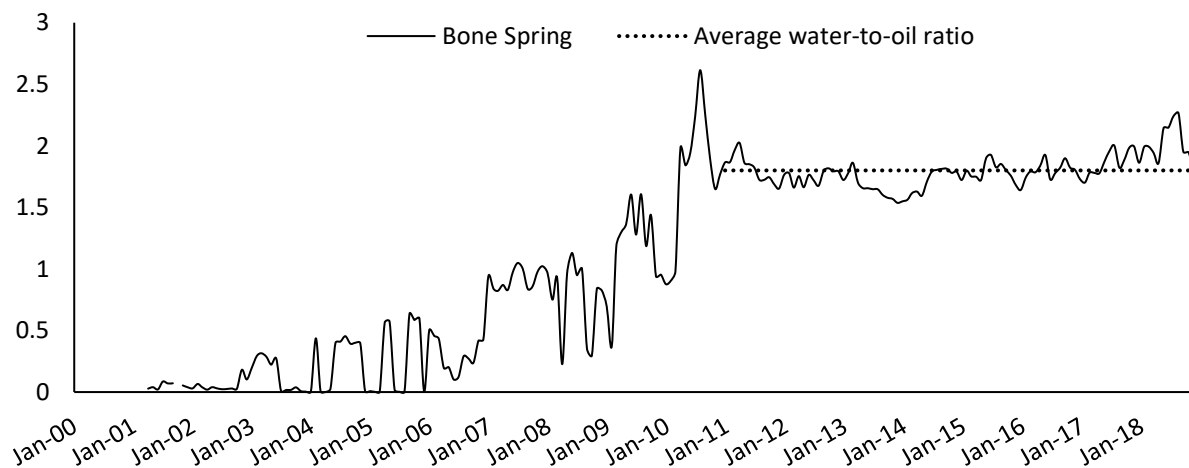


Figure 2.20: Average PW-to-oil ratio, Bone Spring

<sup>14</sup> Mean reversion is the characteristics of a timeseries that deviations from the average can be expected to be reverted to the average. Mean reversion could indicate that the value of the variable of interest can be expected to be stabilized.

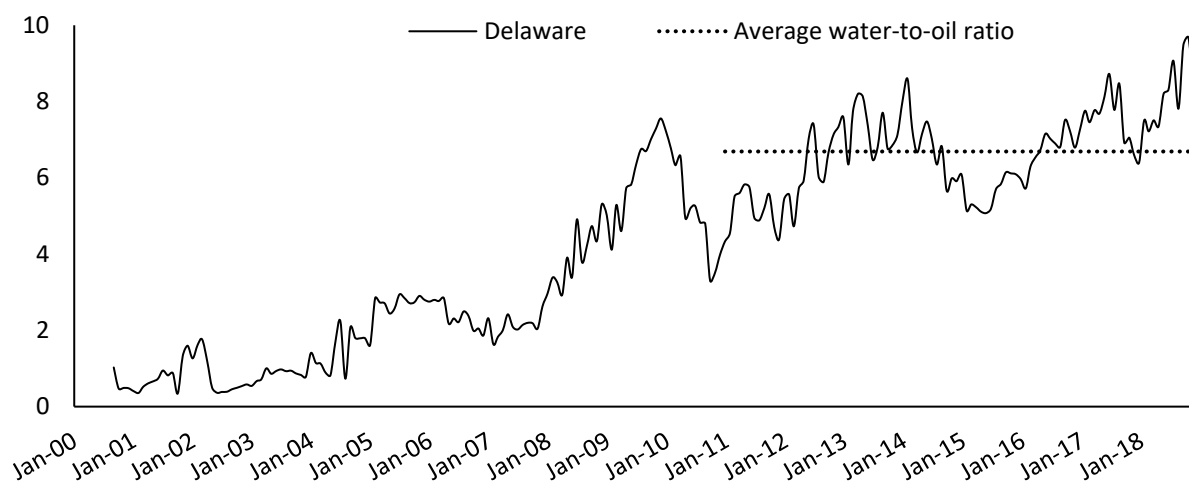


Figure 2.21: Average PW-to-oil ratio, Delaware

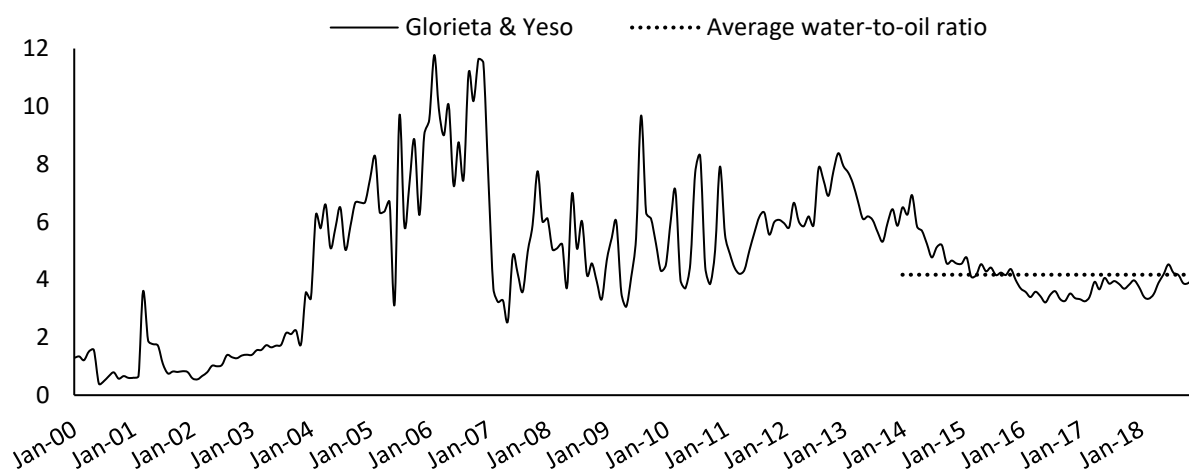


Figure 2.22: Average PW-to-oil ratio, Glorieta & Yeso

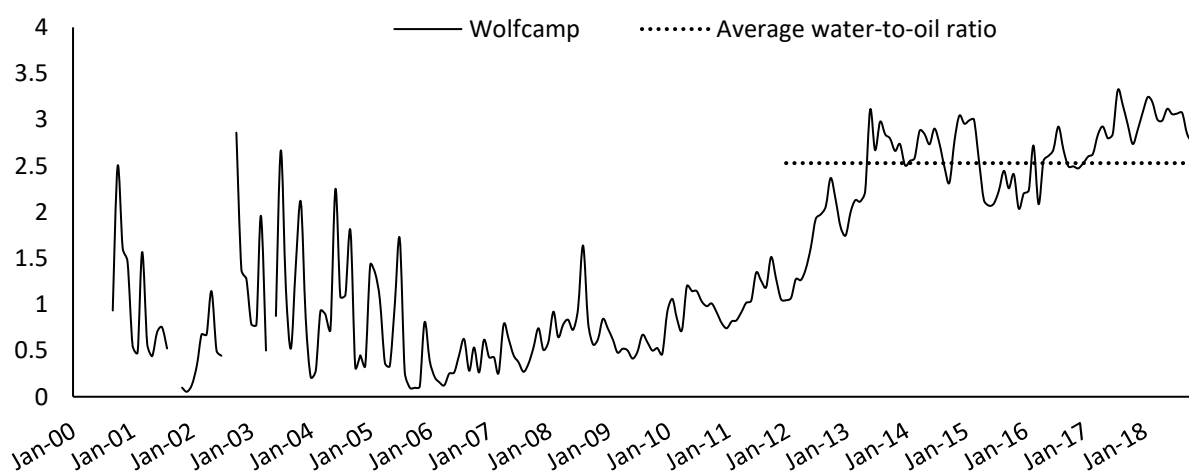


Figure 2.23: Average PW-to-oil ratio, Wolfcamp

HF water demand for the future was estimated using a simple curve fitting methodology. In the lack of a well-established principle for the dynamic behavior of freshwater consumption rates, it was assumed that HF water demand increases at a decreasing rate over time. Hence, the logarithmic functional form was selected for curve fitting. The estimated curves for the HF water consumption rates of each formation are shown in Figures 2.24 to 2.27.

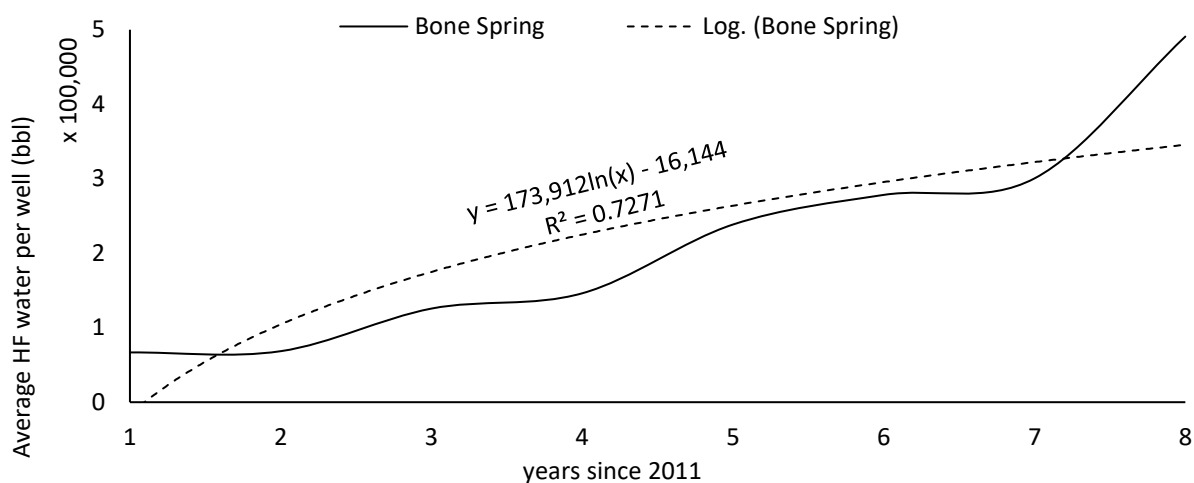


Figure 2.24: Actual and estimated logarithmic time series for average HF water per well in Bone Spring

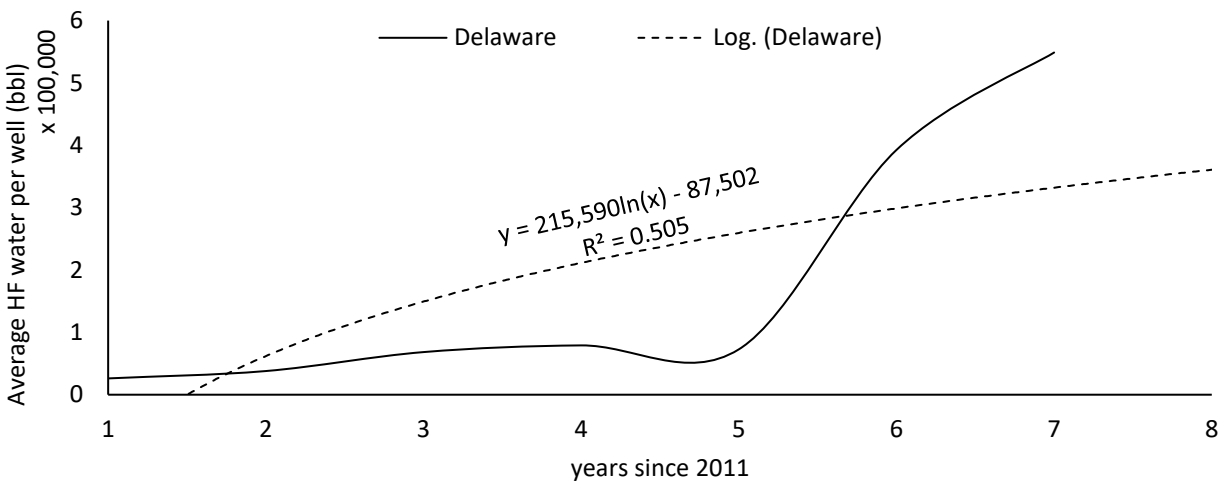


Figure 2.25: Actual and estimated logarithmic time series for average HF water per well in Delaware

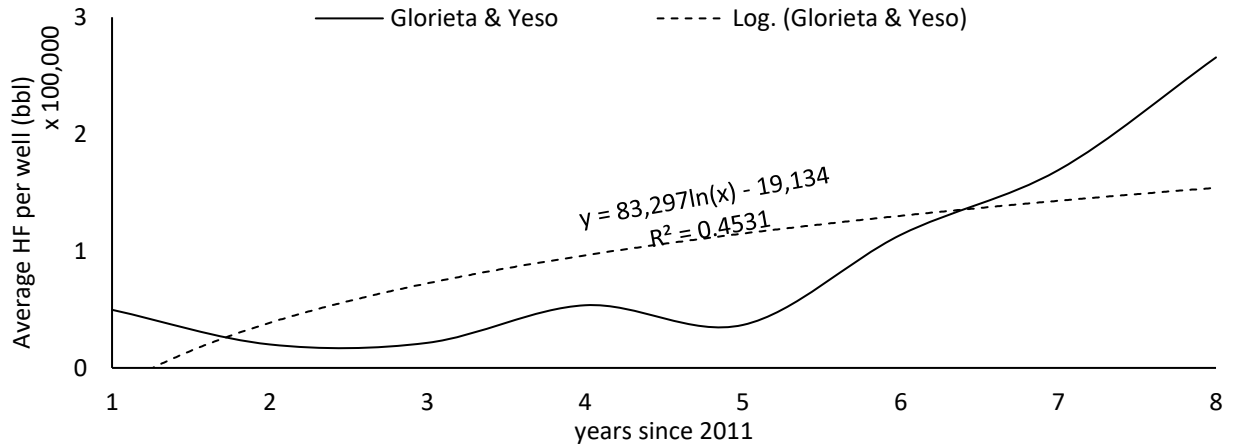


Figure 2.26: Actual and estimated logarithmic time series for average HF water per well in Glorieta & Yeso

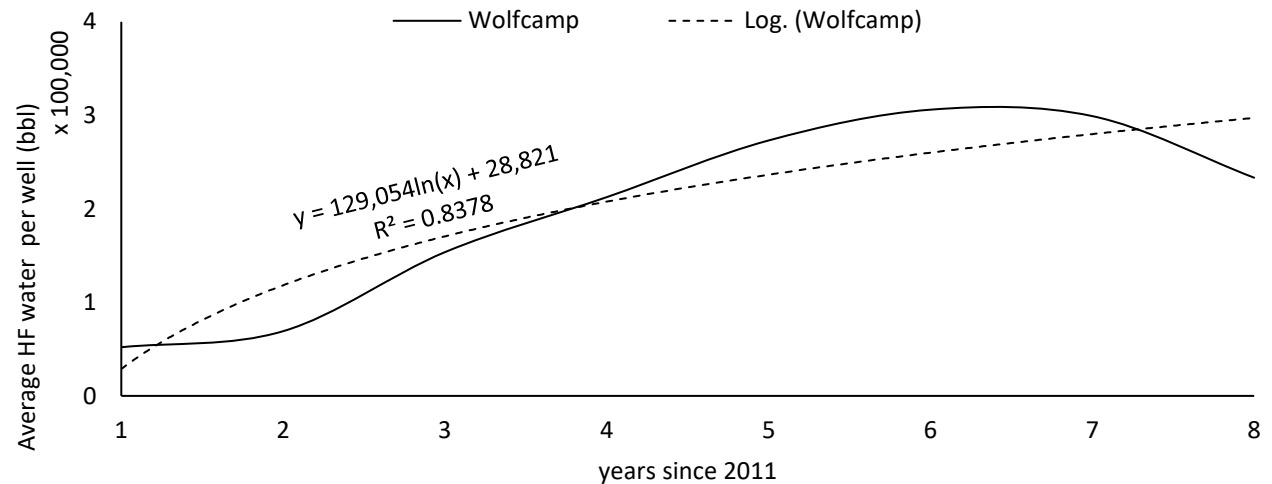


Figure 2.27: Actual and estimated logarithmic time series for average HF water per well in Wolfcamp

### 6.3. Scenarios

This study used three economic scenarios constructed by the U.S. Energy Information Administration (EIA) as price scenarios. The price scenarios are drawn from NEMS and are based on different assumptions. These scenarios are projected until 2050 and pertain to the average annual WTI spot prices. There are eight price scenarios defined in NEMS, however the reference case, high oil price, and low oil price scenarios are the scenarios used in this study. Assumptions made for estimating each scenario are as follows:

The reference case price scenario:

For the reference case price scenario, it is assumed that current laws and regulations remain unchanged; the annual growth rate for the real gross domestic product is 1.9%; improvements to energy production technology are expected; current views in economic and demographic trends will hold in the future; and the Brent<sup>15</sup> crude oil price will be \$108 (2018 dollars) per barrel by 2050. The reference case price is the baseline price projection in the US energy outlook provided by the EIA (Energy Information Agency 2018b).

High and low oil price scenarios:

Assumptions made for the high and low oil price scenarios are like the reference case scenario, except for the Brent crude oil price of 2050. For the high oil price scenario, the 2050 Brent crude oil price is forecast at \$211 per barrel; whereas, for the low oil price, the 2050 Brent crude oil price is forecast to be as low as \$50 per barrel in 2050 (Energy Information Agency 2018b).

The WTI price trajectories for the given scenarios are presented in Figure 2.28.

---

<sup>15</sup> A grade of crude oil produced and traded in the North Sea Region.

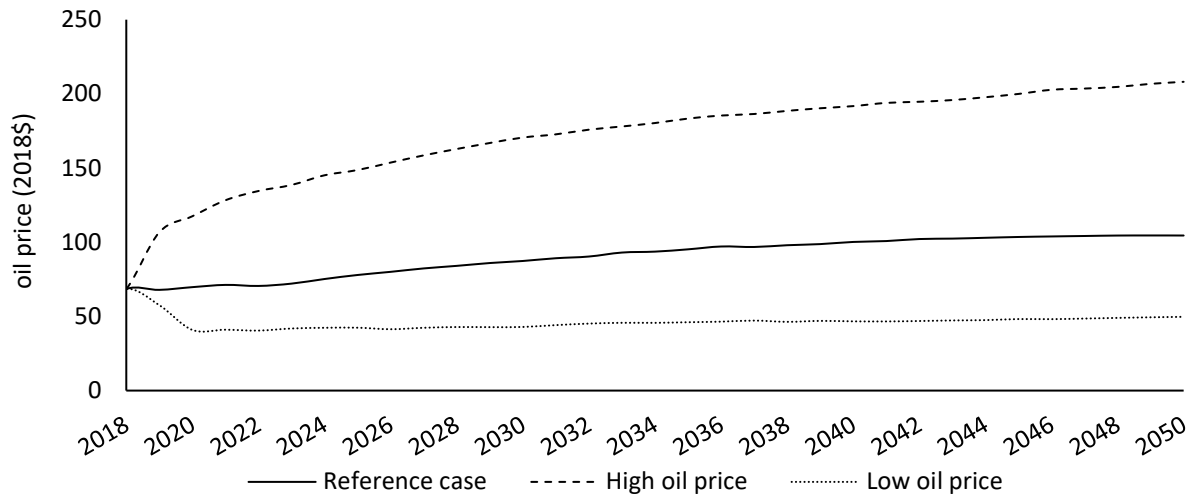


Figure 2.28: Oil price scenarios

In addition to the price scenarios, three policy instruments are investigated, namely freshwater consumption constraint, shutdown condition, and treatment capacity. Based on different combinations of the price scenarios and policy instruments, nine scenarios are constructed and tested in the next section. The scenarios are as follow:

*a.* Base case scenario (BASE)

The BASE scenario assumes the reference case for oil price and no constraint on the freshwater consumption rates or the shutdown condition. It also assumes that 20% of the HF water is provided by PW treatment.

*b.* High oil price scenario (HI)

Like the base case scenario, the high oil price scenario does not assume any constraints on freshwater consumption, or the shutdown condition; it also assumes that 20% of HF water comes from treated PW. The only difference is that the high oil price projections (as shown in Figure 2.28) are used.

c. Low oil price scenario (LO)

The low oil price scenario is like the previous two scenarios, except that the low oil price regime is used.

d. 10,000 acre-feet per month freshwater consumption constraint (W10K)

The W10K scenario assumes that a 10,000 acre-feet per month constraint is imposed on freshwater consumption, or that  $W(\alpha_w) = 10,000$ . The oil price regime here is the reference case scenario and no shutdown condition is assumed (i.e.,  $Q_s = 0$ ). Furthermore, the treatment capacity is similar to the BASE scenario (20%).

e. 5,000 acre-feet per month freshwater consumption constraint (W5K)

The W5K scenario assumes that monthly freshwater consumption cannot exceed 5,000 acre-feet, or that  $W(\alpha_w) = 5,000$ . The price regime is the reference case oil price, there is no shutdown condition in place, and the treated PW makes up 20% of the HF water.

f. 1,000 acre-feet per month freshwater consumption constraint (W1K)

In the W1K scenario, monthly water consumption should not exceed 1,000 acre-feet, or that  $W(\alpha_w) = 1,000$ . As with W5K, the price regime is the reference case oil price, there is no shutdown condition in place, and the treated PW makes up 20% treatment level.

g. 10%Q<sup>0</sup> shutdown scenario (S10)

S10 assumes the reference case oil price regime, 20% treatment level, and no freshwater consumption constraint, but adds a shutdown condition. The S10at shutdown scenario assumes that wells reaching 10% of their initial production rate ( $Q_i^0$ ) will be shut down. In other words,

$$Q_{is}(\alpha_s) = 0.1Q_i^0.$$

*h.* 25%  $Q^0$  shutdown scenario (S25)

This scenario results in a rather early shutdown of wells. S25 assumes the reference case oil price regime, 20% treatment level, and no freshwater consumption constraint, as above. However, this scenario assumes wells will be shut down when they reach 25% of their initial production,

$$Q_{is}(\alpha_s) = 0.25Q_i^0.$$

*a.* 50% treatment level scenario (TREAT)

The TREAT scenario is identical to the W5K scenario except for the level of treatment. Treat assumes that 50% of the HF water comes from PW treatment ( $\varphi(\alpha_\varphi)=0.5$ ), there is a 5,000 acre-feet per month constraint on the freshwater consumption ( $W(\alpha_w) = 5,000$ ), no shut down condition, and the reference case price regime prevails. A summary of scenarios and their description is listed in Table 2.6.



Table 2.6: Scenario variables and their values

Scenario ID	BASE	HI	LO	W10K	W5K	W1K	S10	S25	TREAT
Policy Instrument	Price <sup>a</sup>			Freshwater consumption constraint			Shutdown condition		Treatment level
Oil price regime	Reference case	High oil price	Low oil price	Reference case	Reference case	Reference case	Reference case	Reference case	Reference case
Freshwater capacity constraint (acre-foot per month)	10 <sup>6</sup> <sup>b</sup>	10 <sup>6</sup>	10 <sup>6</sup>	10,000	5,000	1,000	10 <sup>6</sup>	10 <sup>6</sup>	5,000
Shutdown condition (percentage of the initial production rate)	0	0	0	0	0	0	10	25	0
Treatment level (percentage of HF water provided by treating PW)	20	20	20	20	20	20	20	20	20

## Notes:

<sup>a</sup> It is beyond the regulatory power of this study's policymaker to determine which price regime prevails in the market.

<sup>b</sup> 10<sup>6</sup> is a very large value for water capacity constraint which resembles no capacity constraint at all.

## 7. Simulation results and discussion

Simulation results for scenarios HI, BASE, and LO (see Table 2.6) are presented in the following sections. Five outcomes are discussed for each group of scenarios; changes in drilling activity, oil production volumes, economic revenue, freshwater consumption volumes, and PW generation volumes. The results rendered for each group of scenarios are discussed in the following paragraphs.

### 7.1. Price scenarios

Scenarios HI, BASE, and LO are identical in all policy variables except for oil price regime. Scenario HI presents AEO's high oil price regime, scenario BASE demonstrates the reference case price regime, and scenario LO is associated with a low oil price regime. In all of these scenarios, other variables are fixed at the baseline levels; that is, 20% of HF water demand is provided by treated PW, wells are shut down when their oil production rates approach zero, and there is no freshwater consumption constraint. Table 2.7 summarizes the characteristics of scenarios HI, BASE, and LO.

Table 2.7: Price scenarios

Scenario ID	Price scenarios	Freshwater consumption	Treatment	Shutdown condition
HI	High oil price	No limit	20%	0
BASE	Reference case	No limit	20%	0
LO	Low oil price	No limit	20%	0

#### Impacts on drilling

Drilling activity responds to oil prices through price elasticity of supply, which is the same for all scenarios (0.729). In the high oil price scenario, over 300 wells will be drilled on a monthly basis

towards 2050, whereas in the low oil price scenario the number of wells will not exceed 100 in the following years, falling below the current (2018) levels of drilling activity. With the reference case price regime, the number of wells drilled each month will be slightly higher than the present count, reaching 183 wells per month towards the end of the planning horizon (2050).

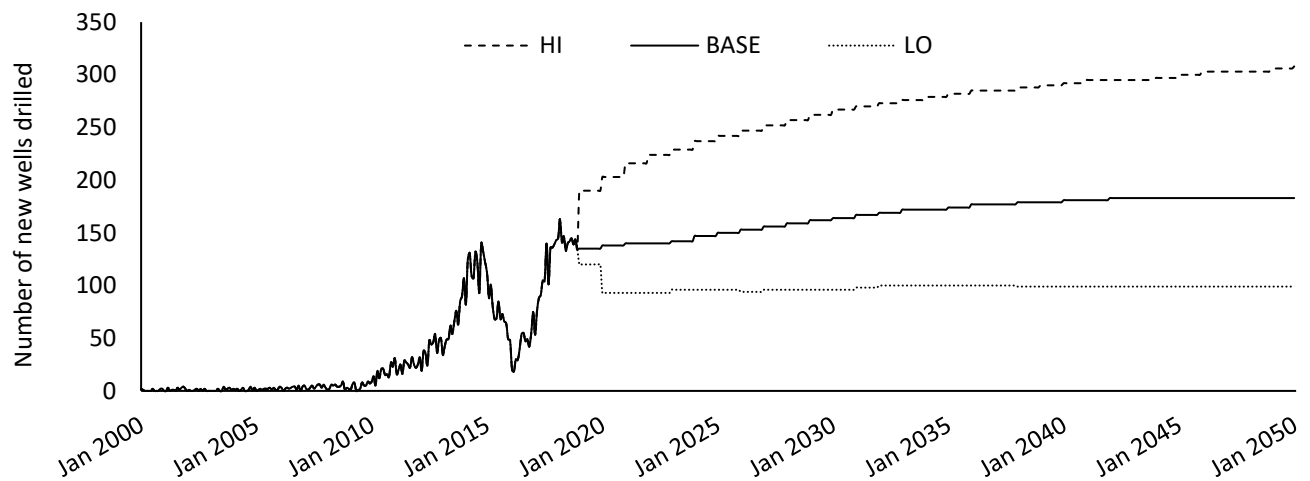


Figure 2.29: Well drilling activity under different price regimes

### Impacts on oil production

Oil production depends on the number of wells, both existing and newly drilled wells, in addition to the decline curve parameters. The total monthly production of oil for different price regimes is mapped in Figure 2.30. Oil production increases over time, even in the case of low oil price regimes. New wells, even at small numbers, will be added to the stock of existing wells, adding to total oil production levels. At the end of the planning period (2050), the oil production rate under the high oil price regime is 263 million barrels per month, which is roughly 2.55 times more than the oil production rate under the low oil price regime.

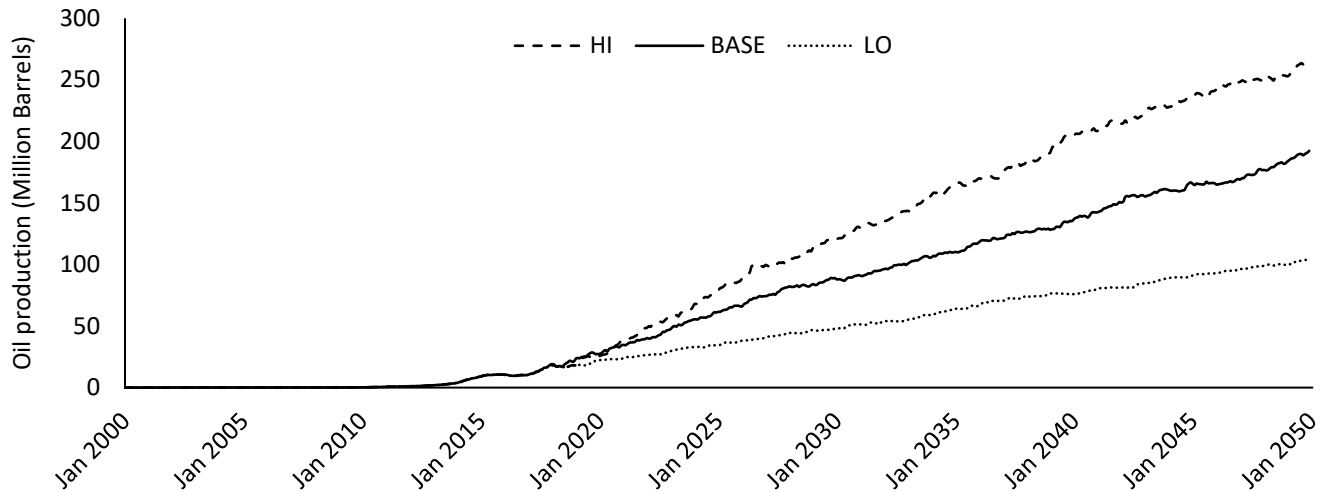


Figure 2.30: Oil production volumes under different price regimes

### Impacts on revenue

Gross annual revenue generated from oil production from the selected unconventional formations in the Permian Basin is calculated as the product of oil production volumes and WTI price per barrel, and the results for scenarios HI, BASE, and LO are presented in Figure 2.31.

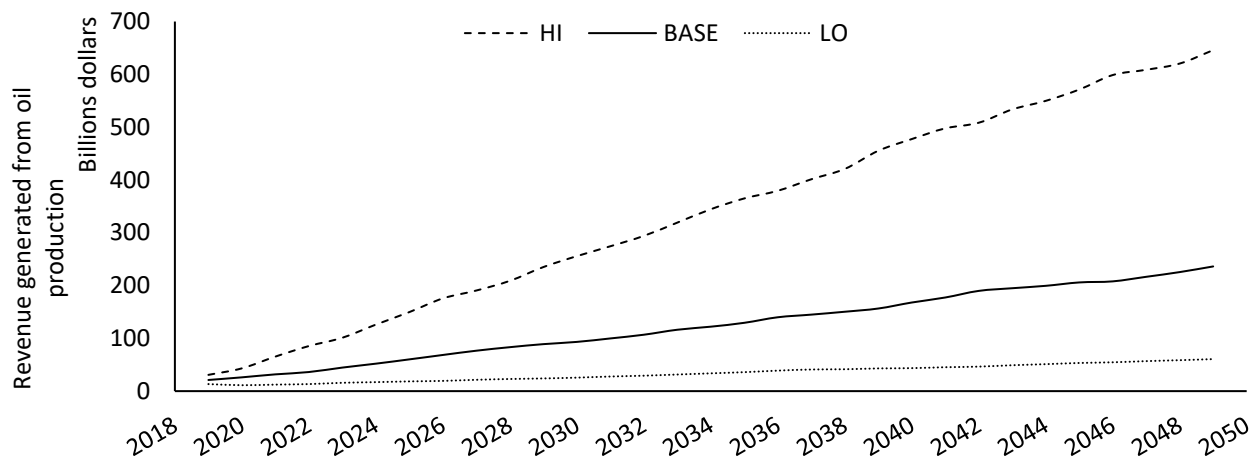


Figure 2.31: NM state revenue under different price regimes

Net present values of the total oil production revenue are calculated under the three price

regimes and presented in Table 2.8. The state revenue is calculated as 20.7%<sup>16</sup> gross oil production revenue following the findings of Tysseling, Bjarke, and Anklam (2019).

Table 2.8: Net present value (NPV) of the gross revenue and state revenue generated from oil production

Scenario ID	Description	NPV revenue (billion dollars)	NPV state revenue (billion dollars)
HI	High oil prices	5,810	1200
BASE	Reference case	2,160	445
LO	Low oil prices	0.602	125

Prices are assumed to be exogenous to the policymaker. The price regime does not pose a constraint to the revenue maximization problem. The values in Table 2.8 only provide reference point for comparison.

#### Impact on freshwater consumption

New Mexico's Office of the State Engineer (OSE) reported the following groundwater withdrawal volumes for mining purposes (mainly O&G production) for 2015 (New Mexico Office of the State Engineer [OSE] 2019). Table 2.9 summarizes the reported volumes for Chaves, Eddy, Lea, and Roosevelt counties, which are counties located within the study area.

Table 2.9: Withdrawal volumes for mining practices in acre-feet (Source: OSE 2019)

County	2015
Chaves	293
Eddy	18,490
Lea	1,603
Roosevelt	2
Sum	20,388

---

<sup>16</sup>  $\eta(t) = 0.207$ . It is assumed that the tax revenue share of production revenue is constant through time, including historical and future intervals.

The annual freshwater consumption computed by this simulation for 2015<sup>17</sup> is 12,000 acre-feet (equivalent to 92.30 million barrels). Since this study is focused on only four formations in the New Mexico portion of the Permian Basin, the finding of this study is within reasonable amounts when compared with the actual data. Annual freshwater consumption volumes for hydraulic fracturing for the years following 2015 are represented in Figure 2.32.

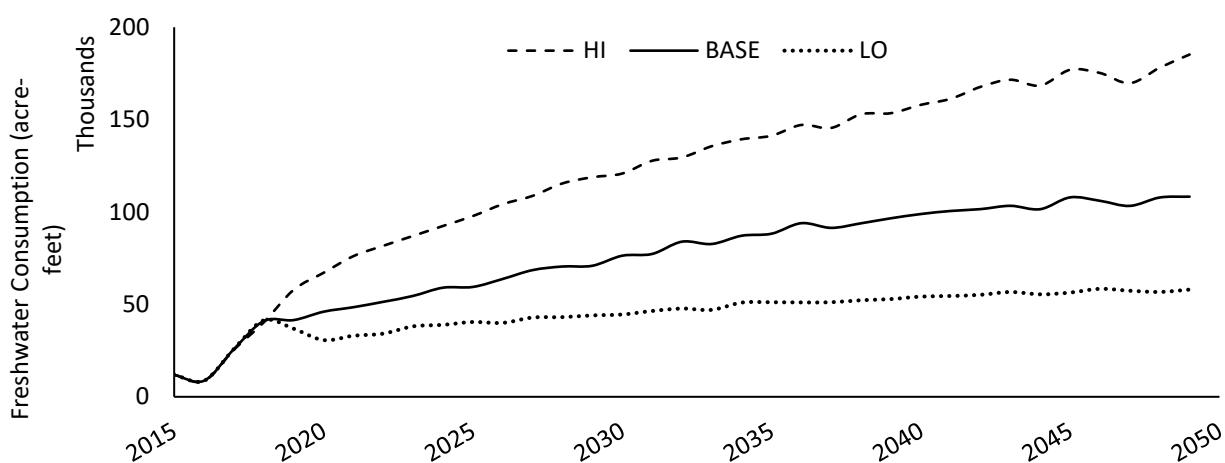


Figure 2.32: Annual freshwater consumption under different price regime scenarios

According to the simulation projections, the annual water consumption levels will increase as high as 14 times the 2015 volumes by 2050 in the high oil price scenario. With the low oil price scenario, however, freshwater consumption will reach 60,000 acre-feet, which is 4.5 times the 2015 volumes.

It is important to notice how freshwater consumption levels change with prices. The OSE collects freshwater consumption data by category (commercial, industrial, mining and power) every five years. The 2015 water report was issued in May 2019. Oil prices have increased sharply since

---

<sup>17</sup> Since year 2015 falls within the historical period, it does not relate to a future price regime.

2015, resulting in a much higher demand for water for mining. Hence, the 2015 water consumption for mining should not be used as an input for water management practices in 2018.

### Impact on PW generation

Monthly PW volumes generated under different price regimes are presented in Figure 2.33.

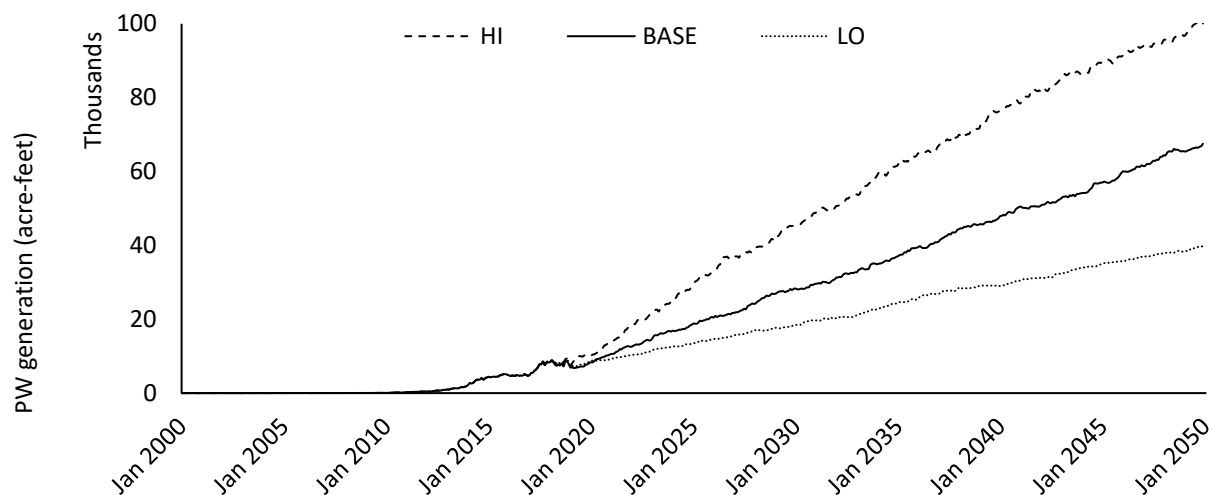


Figure 2.33: PW generation under different price regimes

Higher volumes of PW will be generated under the high oil price scenario, reaching approximately 100,000 acre-feet of PW in 2050; under the low oil price scenario, 39,000 acre-feet of PW will be generated by 2050.

## 7.2. Water consumption capacity scenarios

Lower levels of freshwater consumption could be achieved through either drilling fewer wells or by increasing the use of treated PW. This section focuses on limiting the number of wells drilled to lower groundwater withdrawal volumes. The number of wells drilled during each month is governed by the freshwater constraint  $\bar{W}$  as shown below:

$$N(t) \leq \frac{\bar{W}}{\phi(t) \times \omega(t)}, \quad (15)$$

where  $N(t)$  is the number of new wells drilled in the month  $t$ ,  $\omega(t)$  is the water consumption for hydraulic fracturing of an average well during month  $(t)$ ,  $\bar{W}$  is the monthly freshwater use constraint, and  $\phi(t)$  is the percentage of HF water that comes from freshwater resources. The BASE scenario assumes no limit on groundwater withdrawal levels ( $\bar{W} \rightarrow \infty$ ). A very large amount of  $\bar{W}$  (10 million acre-feet per month) is selected for the baseline scenario to mimic the unlimited freshwater consumption allowance. To compare the impacts of limiting withdrawal rates in scenarios BASE, W10K, W5K, and W1K, Table 2.10 summarizes the characteristics of this group of scenarios.

Table 2.10: Freshwater consumption scenarios

Scenario ID	Price scenarios	$\bar{W}$ (acre-feet per month)	$1 - \phi$	Shutdown condition (% initial oil production rate)
BASE	Reference case	$10^6$	0.2	0
W10K	Reference case	10,000	0.2	0
W5K	Reference case	5,000	0.2	0
W1K	Reference case	1,000	0.2	0

It is assumed that a freshwater constraint has a larger impact on the less productive of the four studied formations (Bone Spring, Delaware, Glorieta & Yeso, and Wolfcamp). To formulate this assumption, the number of wells in each formation is defined as shown in equation (16):

$$N_f(t) \leq \frac{\bar{W}}{\rho \times \omega_f(t)} \times \frac{Q_f(t-1)}{\sum_f Q_f(t-1)}, \quad (16)$$

where  $N_f(t)$  is the number of wells drilled in formation  $f$  at month  $t$ ,  $\omega_f(t)$  is the average HF water used per well in formation  $f$ , and  $Q_f(t-1)$  is the total oil production of the formation  $f$



during the previous month.

### Impacts on drilling

Drilling outcomes under scenarios BASE, W10K, W5K, and W1K are presented in Figure 2.34.

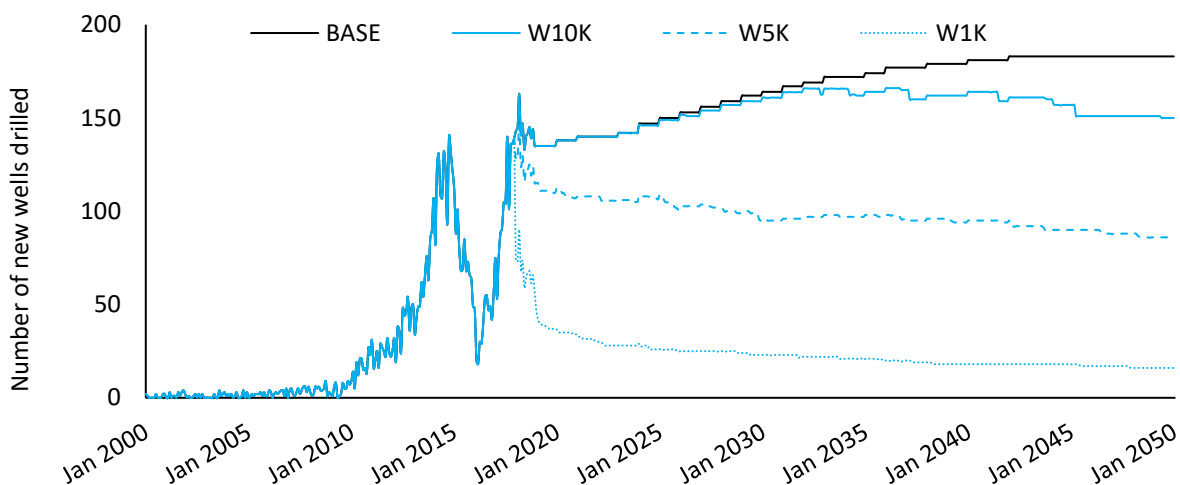


Figure 2.34: Well drilling activity under different freshwater consumption constraint scenarios

By limiting the amount of freshwater consumption to 10,000 acre-feet per month without changing the treatment volumes, drilling activity will be limited as of 2026. The decline in the number of new wells becomes larger over time, compared to the BASE scenario. This is because we are assuming HF water use per well increases over time (Figures 2.24 to 2.27). As a result, the number of new wells will be limited more by time. With 5,000 acre-feet per month and 1,000 acre-feet per month limits on freshwater consumption, drilling activity will be impacted immediately (starting in 2018). Whereas projections for the BASE scenario estimate 183 wells being drilled monthly by 2050, estimates under 10,000, 5,000, and 1,000 acre-feet/month constraints show that drilling will decline to 150, 85, and 16, respectively.

In order to show the impact of imposing a freshwater consumption on drilling activity in each

formation, the number of wells in each formation is retrieved from the simulation under the BASE scenario and W5K (BASE scenario with a 5,000 acre-feet per month freshwater consumption).

The percentage decline ( $\% \Delta(\text{decline}) = \frac{A_{BASE}^{Formation(m)} - A_{W5K}^{Formation(m)}}{A_{BASE}^{Formation(m)}} \times 100$ ) in the number of wells drilled in each formation is calculated and mapped in Figure 2.35.

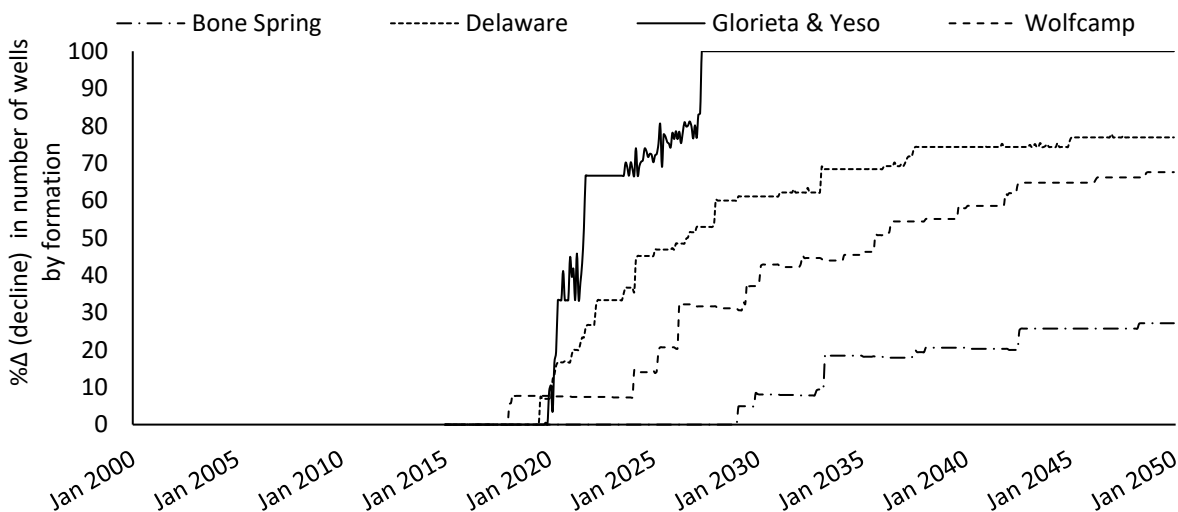


Figure 2.35: Change in the number of wells by formation as a result of posing a 5,000 acre-feet per month freshwater consumption constraint

As Figure 2.35 shows, the most efficient (high production rate and lower freshwater consumption) formation is Bone spring which had the lowest decline due to freshwater consumption constraint. Wolfcamp and Delaware lost as large as 67% and 78% of their potential new well counts, respectively. Glorieta & Yeso, with the lowest production rate amongst the studied formations would be abandoned as early as May 2027.

### Impacts on oil production

Oil production volumes under freshwater withdrawal constraints BASE, W10K, W5K, and W1K are presented in Figure 2.36. A freshwater withdrawal limit of 10,000 acre-feet per month

doesn't impact the oil production volumes until later years (2045). The oil production rate under 10,000 acre-feet per month is estimated at about 164 million barrels of oil per month by 2050. A 5,000 acre-feet per month limit on freshwater consumption results in an estimated 118.5 million barrels monthly production rate by 2050, which is more than two thirds of the 2050 oil production level under a 10,000 acre-feet per month limit. Posing a strict limitation on the freshwater withdrawal, 1,000 acre-feet per month, results in an oil production rate that is about one-sixth of the 2050 oil production level under a 10,000 acre-feet per month limit.

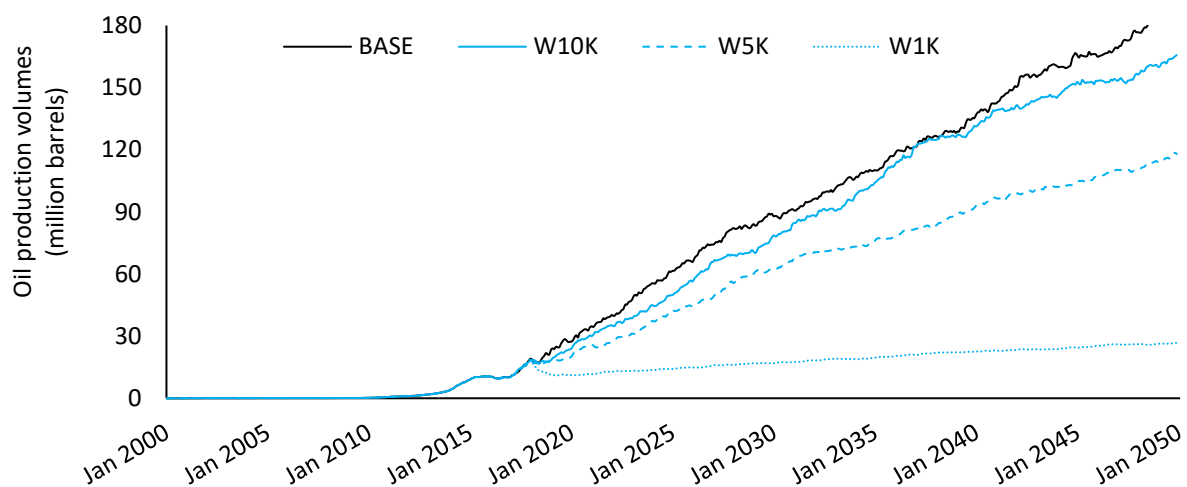


Figure 2.36: Oil production volumes under different freshwater consumption constraint scenarios

### Impact on revenue

Revenue curves are very similar to the oil production curves. The net present value of the gross oil production revenue and the state's revenue are shown in Table 2.11.

Table 2.11: Net present value (NPV) of the gross revenue and state revenue generated from oil production

Scenario ID	$\bar{W}$ (acre-feet per month)	NPV revenue (billion dollars)	NPV state revenue (billion dollars)	$\Delta R = R - R_{\text{BASE}}$ (billion dollars)
BASE	$10^6$	2,160	445	--
W10K	10,000	1,970	407	-37

W5K	5,000	1,450	299	-110
W1K	1,000	393	81	-220

### Impact on freshwater consumption

Annual freshwater consumption levels under freshwater withdrawal limit scenarios are shown in Figure 2.37.

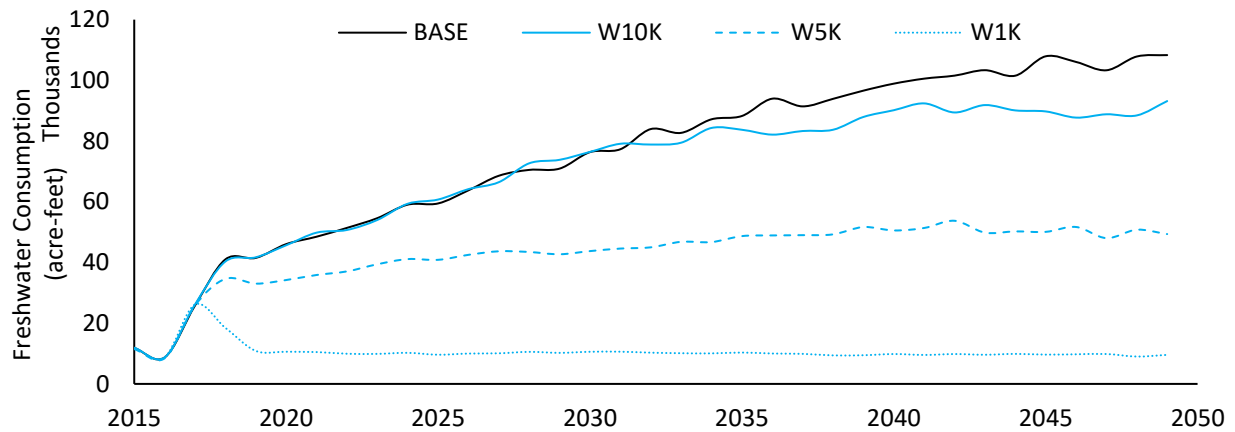


Figure 2.37: Annual freshwater consumption under different freshwater consumption constraint scenarios

Figure 2.37 verifies that the freshwater consumption limits (60,000 acre-feet per year) are being met (please note that Figure 2.37 illustrates annual levels of freshwater consumption).

### Impacts on PW generation

PW generation volumes based on BASE, W10K, W5K, and W1K scenarios are presented in Figure 2.38.

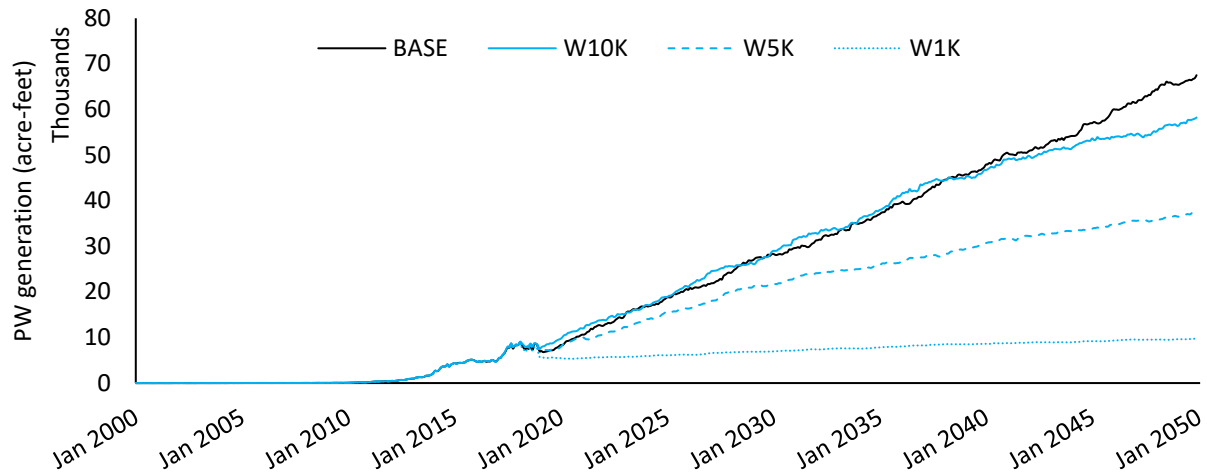


Figure 2.38: PW generation under freshwater withdrawal limit scenarios

Over time, PW volumes increase strictly in all outcomes, leading to the largest volumes in 2050.

PW generation volumes for 2050 are presented in Table 2.12.

Table 2.12: PW generation volumes (2050)

Scenario ID	$\bar{W}$ (acre-feet per month)	2050 PW generation volumes (acre-feet)
BASE	$10^6$	67,514
W10K	10,000	58,234
W5K	5,000	37,585
W1K	1,000	972

As shown in Table 2.12, limiting freshwater consumption volumes results in lower oil production, which ultimately reduces PW generation.

### 7.3. Treatment capacity scenario

Since treated PW is a substitute for fresh water in hydraulic fracturing operations, increasing the use of treated PW for HF will result in a decrease in the use of freshwater for HF. Scenarios representing different levels of treated PW consumption for HF are BASE, W5K, and TREAT, as shown in Table 2.13.

Table 2.13: Treatment capacity scenarios

Scenario ID	Price scenarios	$\bar{W}$ (acre-feet per month)	Treatment	Shutdown condition
BASE	Reference case	$10^6$	20%	0
W5K	Reference case	5,000	20%	0
TREAT	Reference case	5,000	50%	0

### Impact on drilling

Using more treated water for HF allows more wells to be drilled and completed under freshwater consumption constraints (equation (15)). Using treated PW in HF results in a later decline in the number of wells drilled, as is shown in Figure 2.39.

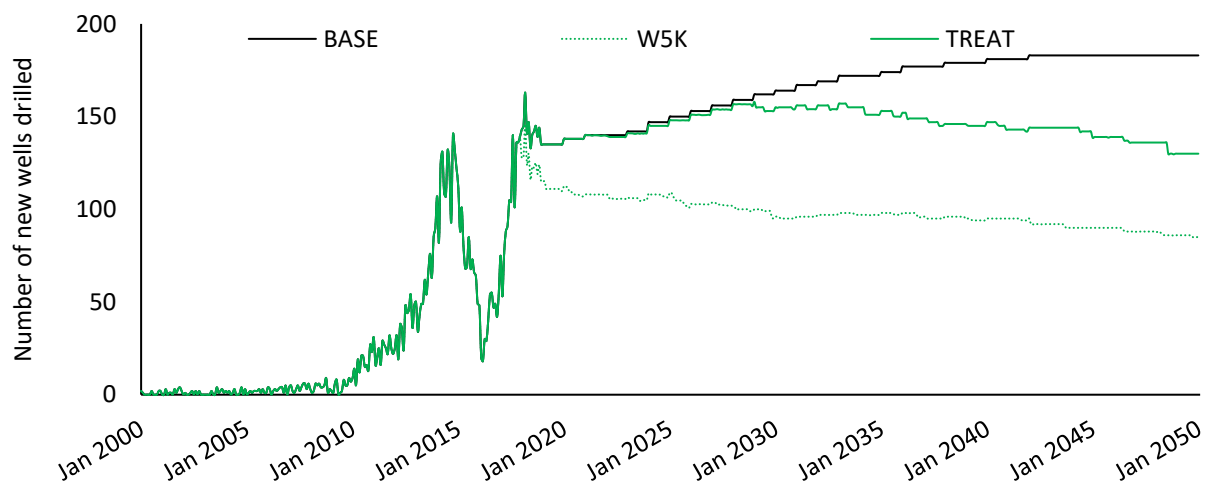


Figure 2.39: Well drilling activity under different treatment capacity scenarios

### Impacts on oil production

Like drilling activity, oil production volumes are improved by increasing treatment capacity.

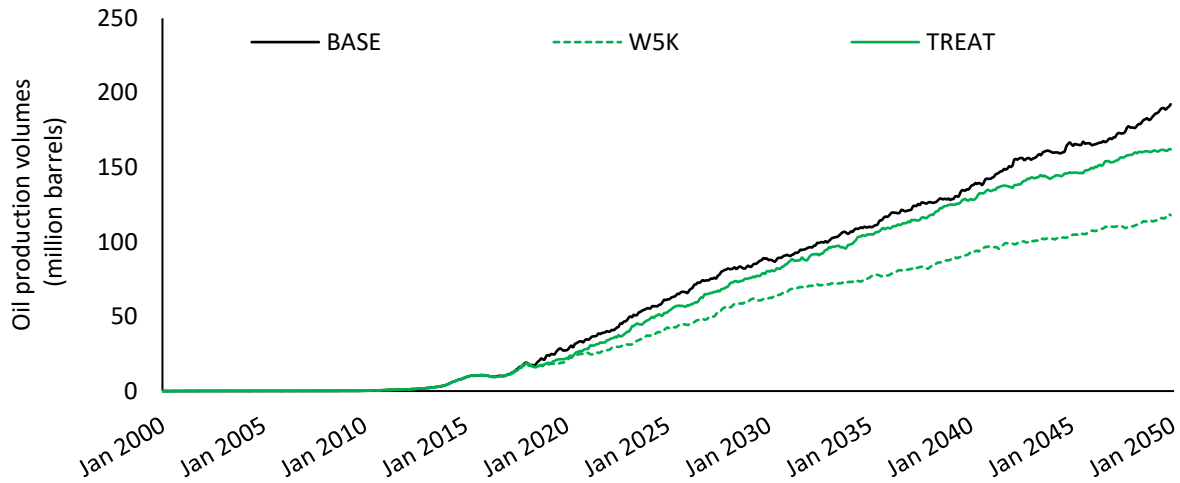


Figure 2.40: Oil production volumes under different treatment capacity scenarios

### Impact on revenue

similarly, by increasing treatment capacity, less revenue will be lost due to freshwater consumption constraints. Gross revenue and state revenue from production of oil under treatment capacity scenarios are presented in Table 2.14.

Table 2.14: Net present value (NPV) of the gross revenue and state revenue generated from oil production under treatment capacity scenarios

Scenario ID	NPV revenue (billion dollars)	NPV state revenue (billion dollars)	$\Delta R = R - R_{\text{BASE}}$ (billion dollars)
BASE	2,160	445	--
W5K	145	299	-110
TREAT	196	405	-42

Limiting the freshwater consumption to 5,000 acre-feet per month decreases state revenue by 30% of the total revenue generated under the BASE scenario. However, by improving the treatment capacity from 20% to 50%, under the TREAT scenario, about 20% of the loss is avoided.

### Impact on freshwater consumption

As Figure 2.41 confirms, the freshwater consumption constraint is met by the model design; i.e., the monthly volumes of freshwater consumption are below the constraint (5000 acre-feet per month or 60,000 acre-feet per year) for W5K and TREAT.

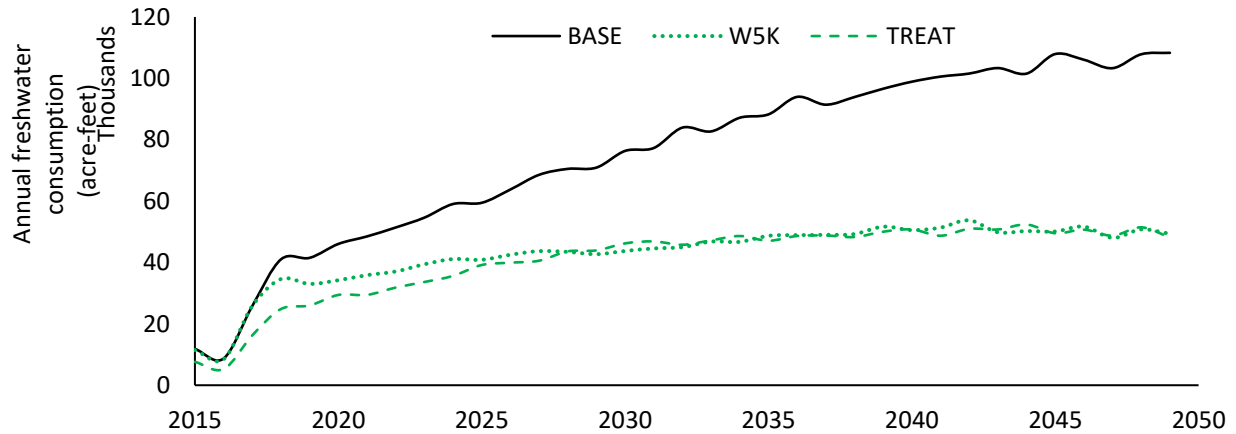


Figure 2.41: Annual freshwater consumption under different treatment capacity scenarios

### Impact on PW generation

PW generation volumes under different scenarios are presented in Figure 2.42.

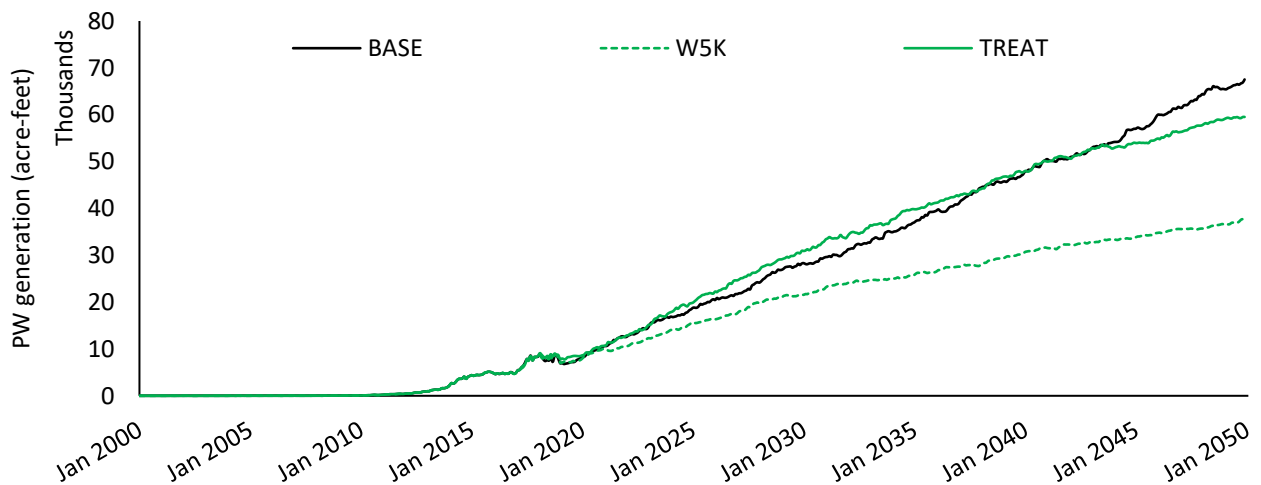


Figure 2.42: PW generation under different treatment capacity scenarios

The amounts of PW generated under the TREAT scenario is not improved compared to the W5K



scenario. The TREAT scenario is designed to reduce freshwater consumption while allowing more wells to be drilled. So, it was not expected that the PW generation would be impacted. However, the PW generation is improved compared to the BASE scenario. Figures 2.41 to 2.45 represent the estimated PW generation and disposal volumes for future years under scenarios BASE, W5K, and TREAT.

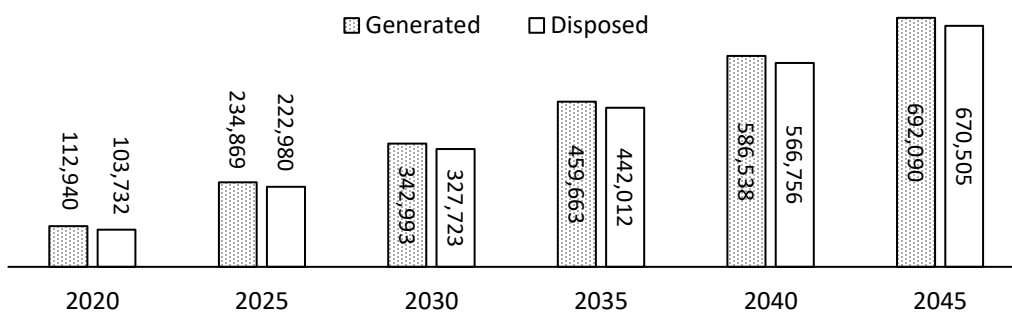


Figure 2.43: Generated and disposed PW volumes (acre-feet) under BASE scenario

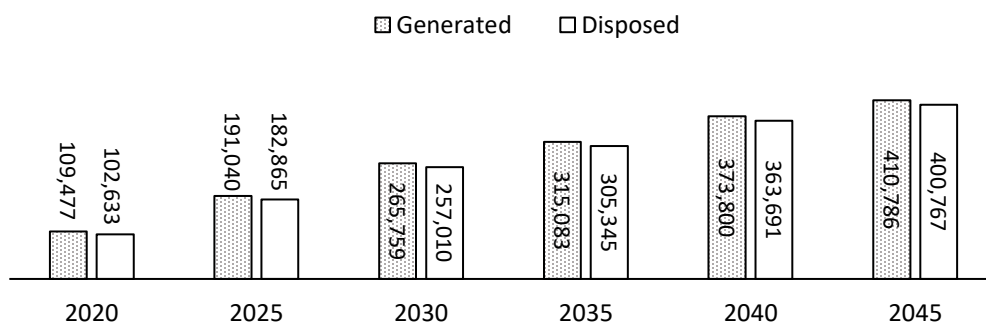


Figure 2.44: Generated and disposed PW volumes (acre-feet) under W5K scenario

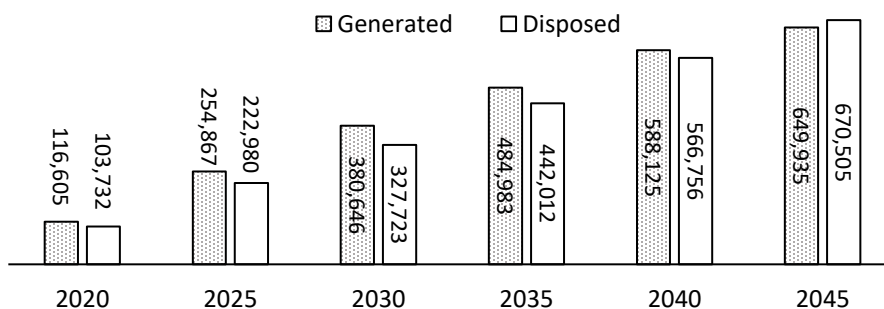


Figure 2.45: Generated and disposed PW volumes (acre-feet) under TREAT scenario

#### 7.4. Shutdown conditions

In equation (7), we showed that a well will be shut down when its production rate falls below the profit creating amounts; that is, when the revenue generated is less than the variable costs of operating the well. The policymaker does not observe variable costs incurred by the operators, but we assume that by imposing certain regulations, the policymaker can increase variable costs that result in earlier shutdown of wells. One of such regulations is raising disposal fees. However, since the total cost structure is not observed, we show the early shutdown condition in terms of higher shutdown production rates. Scenarios BASE, S10, and S25 are only different in the shutdown rates, ( $Q_s$ ). Scenario BASE assumes a well will be shut down when the production rate approaches zero, scenario S10 denotes a shutdown condition when the production rate reaches 10% of the initial production rate ( $Q_0$ ), and scenario S25 represents a shutdown condition when the production rate reaches 25% of the initial production rate. Descriptions of scenarios BASE, S10, and S25 are listed in Table 2.15.

Table 2.15: Shutdown condition scenarios

Scenario ID	Price scenarios	Freshwater consumption (acre-feet per month)	Treatment level	Shutdown condition
BASE	Reference case	$10^6$	20%	0
S10	Reference case	$10^6$	20%	$Q_s = 0.10Q_i^0 \forall i \in X$
S25	Reference case	$10^6$	20%	$Q_s = 0.25Q_i^0 \forall i \in X$

#### Impacts on drilling

Shutdown condition scenarios do not impact drilling activity. This is due to the model set up as expressed in equation (15).

### Impacts on oil production

Oil production is impacted by shutdown conditions, as is shown in Figure 2.46. A shutdown condition at 10% of initial oil production results in a slight decline in oil production, whereas shutting down wells when they reach 25% of their initial production rates could result in a large decline as large as nearly half the production without a shutdown condition.

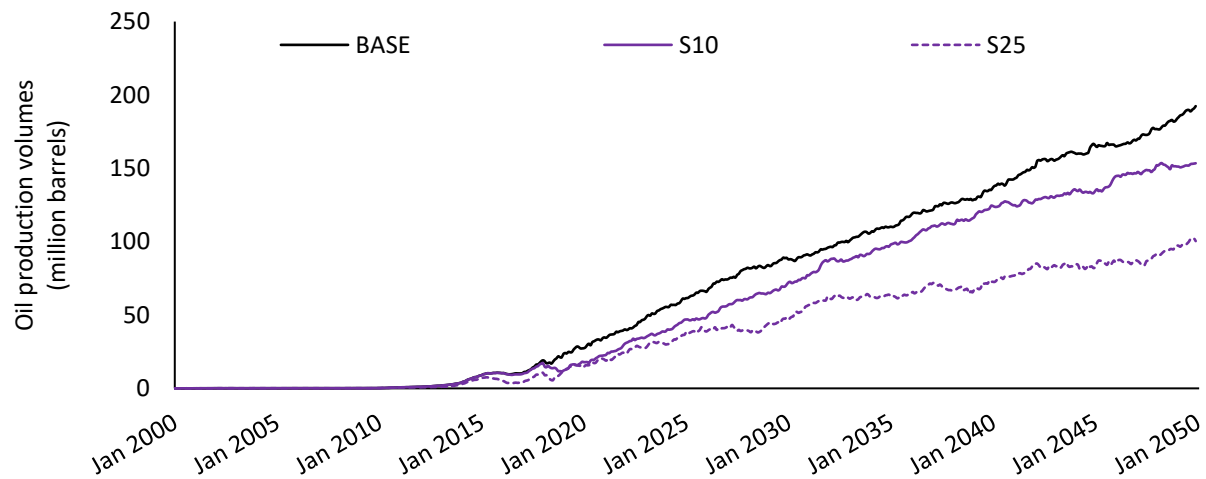


Figure 2.46: Oil production volumes under different shutdown condition scenarios

### Impacts on the economic revenue

Table 2.16 summarizes the net present values of the gross oil production revenue and the state revenue under shutdown condition scenarios.

Table 2.16: Net present value (NPV) of the gross revenue and state revenue generated from oil production under shutdown condition scenarios

Scenario ID	NPV revenue (billion dollars)	NPV state revenue (billion dollars)	$\Delta R = R - R_{\text{BASE}}$ (billion dollars)
BASE	2,160	445	--
S10	1800	373	-74
S25	1180	245	-202

### Impact on freshwater consumption

The shutdown condition does not impact freshwater consumption. Freshwater consumption is determined by the number of new wells; since the number of new wells is not changed by the shutdown condition, freshwater consumption is not impacted.

### Impact on PW generation

Since PW is a by-product of oil production, an early shutdown of the well could result in less volumes of PW generated. PW generation volumes under shutdown conditions are shown in Figure 2.47.

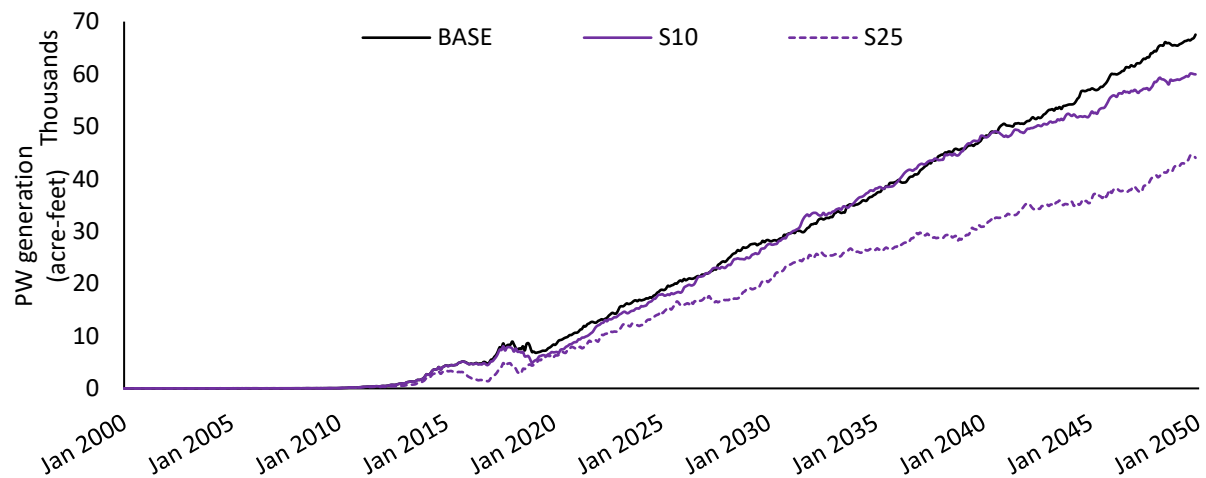


Figure 2.47: PW generation under shutdown condition scenarios

## 7.5. Summary of the results

To allow comparisons between the outcomes of different policy scenarios (W1K, W5K, W10K, S10, S25, and TREAT) and the BASE scenario, Table 2.17 lists the revenue loss, difference in the maximum monthly freshwater consumption rate, and difference in the maximum monthly PW generation rate for each. Among the policy instruments that the policymaker can select,

scenarios W10K and TREAT result in the least loss of revenue, when compared to the BASE scenario, where the policymakers takes no action. The strictest freshwater consumption constraint (1,000 acre-feet per month), and the very early shutdown condition (at 25% of initial production rate) result in highest loss of revenue.

Table 2.17: Summary of policy scenario outcomes

Scenario	Scenario ID	$\Lambda^a$ (\$ billion)	$\Delta W_{max}^b$ (thousand acre-feet)	$\Delta PW_{max}^c$ (thousand acre-feet)
Freshwater constraints	W1K	-220	-8.8	-57.8
	W5K	-110	-5.0	-20.5
	W10K	-37	-1.2	-9.3
Shutdown condition	S10	-74	0.0	-7.4
	S25	-202	0.0	-23.1
Treatment scenario	TREAT	-42	-5.0	-8.0

<sup>a</sup>  $\Lambda = \sum_t \frac{R(t) - R_{BASE}(t)}{(1+r)^t}$ : net present value of monthly revenue losses

<sup>b</sup>  $\Delta W_{max} = W_{max} - W_{max_{BASE}}$ : difference between the maximum monthly freshwater consumption under a given scenario and the BASE scenario

<sup>c</sup>  $\Delta PW_{max} = PW_{max} - PW_{max_{BASE}}$ : difference between the maximum monthly PW disposal under a given scenario and the BASE scenario

In terms of the freshwater consumption rate, the shutdown scenarios do not result in any change in freshwater consumption. In other words, as a result of imposing shutdown conditions, no improvement is made in terms of water consumption compared to no-action (the BASE scenario). Scenario W1K results in the highest conservation of freshwater, by design. And, scenarios W5K and TREAT are similar in terms of freshwater consumption conservation, also by design—both scenarios have 5,000 acre-feet per month freshwater consumption constraint.

As shown in the last column of Table 2.17, shutdown scenario S10 is not effective in reducing the PW generation volumes, as it reduces the PW generation volumes the least. Under the S25 shutdown scenario, the maximum monthly PW generation rate reduces by 3 billion acre-feet, which is a smaller reduction compared to the 4 billion acre-feet resulted from W5K scenario. Limiting freshwater consumption in the upstream under W1K and W5K scenarios results in the highest reductions in PW generation at the downstream as well.

## **8. Conclusions and policy implications**

Hydrocarbon is a major input to the economies of the southwestern states. Following the shale revolution and the economic appeal of production from unconventional O&G resources, unconventional O&G production intensified in the Southwest. Due to its proven high productivity, the Permian Basin, located in west Texas and southeast New Mexico, has attracted large O&G producers in recent years. Intense development activity resulted in the discovery of the largest ever unconventional O&G resource, reinforcing the productivity prospect of the Permian Basin.

Production of hydrocarbon from unconventional resources depends on water as an input. On the other hand, the Permian Basin region is arid. Groundwater is the main source of freshwater in the Permian Basin area and slow recharge of the groundwater has been a long-time concern for the region's economy. Exerting severe stress on groundwater levels for hydraulic fracturing could potentially lead to irreversible negative impacts on water resources, worsening the water scarcity issue for future generations.

In addition, large volumes of wastewater are generated along with O&G liquids. The current

practice for handling O&G production's wastewater is to inject it into deep disposal wells. The induced seismicity risk, as well as the unknown consequences of overloading underground geologic layers with billions of barrels of wastewater, has led some of the southwestern states, including Oklahoma and New Mexico, to adopt disposal control measures.

As described, on the one hand, oil production from unconventional resources of the Permian Basin could result in the production of economic revenue, or "good," and, on the other hand, it causes environmental degradation, or "bad." Consequently, a comprehensive and multifaceted evaluation of policies in this nexus of energy, water, and the environment is called for. This study offers a system dynamics-based policy evaluation tool that incorporates economic theory and reservoir engineering models to match the complexity of the energy, water, and environment nexus in the Permian Basin. This policy evaluation tool relies on disparate data sources, economic theory of supply, and reservoir engineering methods and models.

Revenue generation, freshwater consumption, and wastewater generation outcomes of nine policy scenarios were investigated using the proposed policy evaluation tool. Policy variables of interest were oil price regimes, freshwater consumption constraint, treatment levels, and shutdown conditions.

Using the simulation outcome, it is possible to visualize the trade-offs between revenue, water consumption, and PW generation. Scenarios can be compared from a Pareto efficiency perspective. In a multidimensional outcome space, scenario S is Pareto dominant compared to scenario S' if the outcome of S is strictly better in one dimension and is at least as good in all other dimensions. The net present value of the revenue generated between 2019 and 2050 and

the maximum monthly freshwater demand results from each scenario are compared in Figure 2.48. According to Figure 2.48, in a bidimensional outcome space (revenue and freshwater consumption), scenarios HI, TREAT, and W1K are Pareto efficient scenarios. Scenario HI corresponds to the high oil prices while treatment, shutdown condition, and freshwater consumption limits are fixed at BASE scenario levels. High oil prices result in the highest level of revenue generated while also increasing the freshwater consumption levels substantially. However, since there is no other scenario outcome that improves revenue levels resulting from high oil prices (120 billion dollars), no other scenarios are considered Pareto dominant compared to scenario HI.

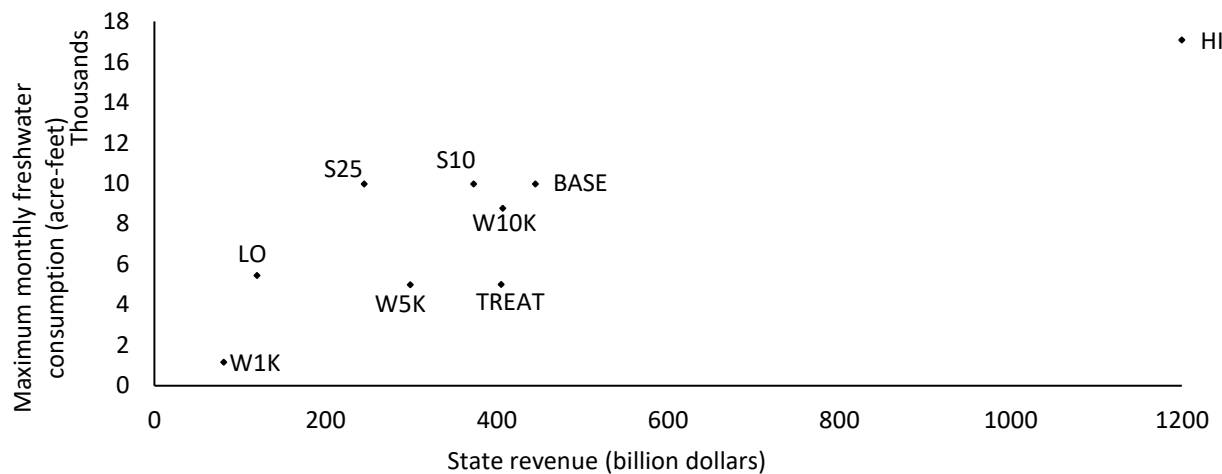


Figure 2.48: Net present value of revenue and freshwater consumption tradeoff results

Scenario TREAT presents Pareto dominance when compared to the W5K W10K, S10, S25, and LO scenarios. In other words, when compared with these six scenarios, scenario TREAT results in highest state revenue and the lowest freshwater consumption volumes. Scenario TREAT corresponds to the case of limiting freshwater consumption levels to 5,000 acre-feet per month, while increasing the share of treated PW in hydraulic fracturing operations. The combination of



a freshwater consumption limit and increasing PW treatment capacity results in the highest revenue generated and lowest freshwater consumption among both shutdown scenarios (S10 and S25), low oil price regime (LO), and larger freshwater consumption allowances (W5K and W10K). An interesting policy implication from this finding is the evaluation of the benefit of increasing treatment capacity by comparing outcomes of scenarios W5K and TREAT. All else equal; i.e., the reference case price scenario, treatment at 20% of the hydraulic fracturing (HF) demand, and 5,000 acre-feet per month freshwater withdrawal constraint; increasing treatment capacity to 50% results in roughly \$105 billion in revenue while maintaining a 5,000 acre-feet per month freshwater consumption limit. In order to maintain a 5,000 acre-feet per month freshwater consumption limit, the state of New Mexico can motivate 50% PW treatment capacity through a tax credit or investment in PW treatment infrastructure, if the investment amount does not exceed the 30-year NPV of \$106 billion.

Figure 2.49 illustrates the outcomes in the revenue-PW generation outcome space. In this space, scenarios HI, W10K, TREAT, BASE, W5K, and W1K are Pareto efficient. Scenario HI results in the highest revenue generation while also the highest disposal volumes, while scenario W1K results in the lowest revenue and lowest PW disposal volumes. Early shutdown condition scenarios S10 and S25 are shown to be inefficient as means to reduce PW generation, because they result in lower revenue generated when compared to freshwater-constrained scenarios, W5K and W10K, and the TREAT scenario. Scenario TREAT is shown to be efficient in both the revenue-freshwater consumption and revenue-PW disposal spaces.

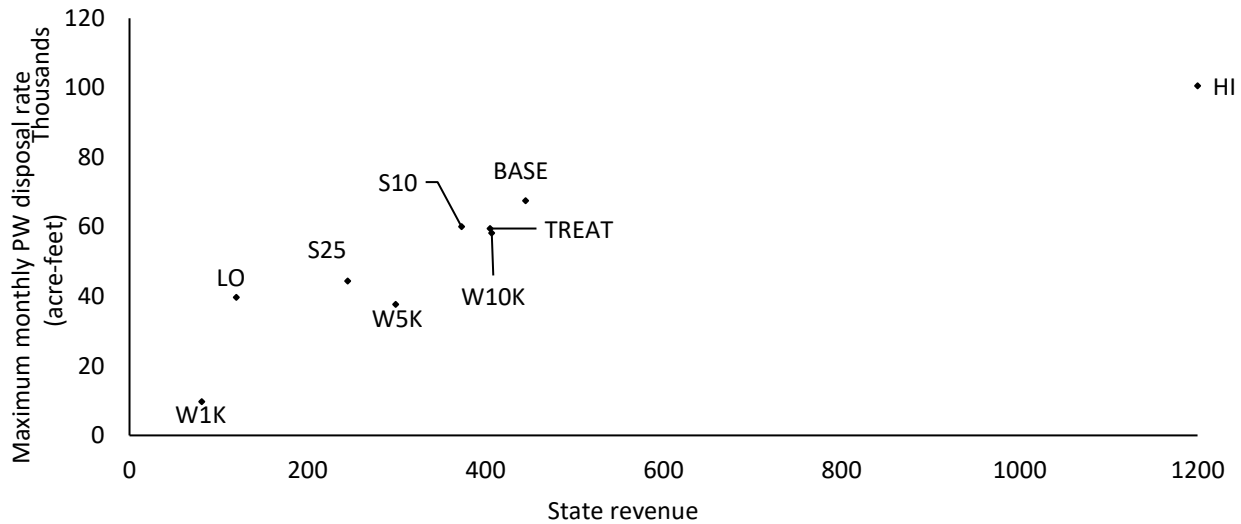


Figure 2.49: Revenue and PW generation tradeoff results

It is noteworthy that the price scenarios are not chosen by the policymaker in this study. However, the outcomes of those scenarios are presented to provide reference points. For example, Figures 2.48 and 2.49 show that with a reference case price regime, limiting freshwater consumption to 1,000 acre-feet per month results in worse outcomes than low oil price regimes. Among policy instruments available to the policy maker, i.e. W1K, W5K, W10K, S10, S25, and TREAT, the shutdown instrument is shown to be inferior. On the other hand, TREAT scenario is shown to have a relatively good performance in providing revenue to the state, while limiting freshwater consumption and PW disposal rates.

## 9. Limitations and future work

Although the objective of this study is to provide a comprehensive policy evaluation tool, there are some assumptions that limit the performance of the model. For example, it is assumed that sufficient oil resources are available for recovery under all scenarios. However, the resources are limited. Furthermore, the hydrology of the groundwater is overlooked for simplicity. In the real-

world case, when groundwater levels fall below a certain level, groundwater withdrawals should be limited more in the following months. Finally, it is assumed that there is no limit on the stock of wells, whereas, in reality, the land surface is limited and to avoid inter-well influence between new and existing wells, the distance between wells and their laterals is controlled by the New Mexico State Land Office as well as the NM-OCD.

Another significant limitation of this work is to assume a static percentage ( $\eta(t) = \eta = 20.7\%$  share of oil production revenue as the state's share. Not only could the state's share of the revenue change over time based on the tax policy adopted in certain years, but also the amount of tax deductions could increase when certain policy instruments are applied. For example, to motivate higher levels of treatment, the state could introduce a tax-credit program which is a cost to the state and impacts  $\eta(t)$ .

In addition to modifying the model to account for these limitations, the simulation will be extended to include a venting and flaring submodule. Currently, large volumes of associated gas produced in the Permian Basin's oil fields are vented or flared due to lack of natural gas capturing, storage, and transportation infrastructure. The simulation will be modified to measure the methane emissions caused by venting the associated gas, other pollutants resulted from flaring, and the natural gas sales revenue lost due to both venting and flaring

## References

- Arps, J.J. (1945). Analysis of decline curves. *Transactions of the AIME*, 160(1). SPE-945228-G.
- Bartis, J.T., LaTourrette, T., Dixon, L., Peterson, D.J. and Cecchine, G. (2005). *Oil shale development in the United States: Prospects and policy issues*. Santa Monica, CA: Rand Corporation.
- Biglarbigi, K., Killen, J.C., Mohan, H. and Carolus, M.J. (2009). SS: Unlocking the unconventional oil and gas reservoirs: Potential for oil shale development in the United States. In: *Offshore Technology Conference 2009*, pp. 2758-2769. Richardson, TX: Offshore Technology Conference.
- Budzik, P. and Perrin, J. (2014, July 9). Six formations are responsible for surge in Permian Basin crude oil production. *Today in Energy*, accessed June 16, 2019. <https://www.eia.gov/todayinenergy/detail.php?id=17031>.
- Chermak, J. and Patrick, R. (2016). Optimizing production of hydrocarbons and water: Incentives for goods and bads. Paper presented at *Implications of North American Energy Self-Sufficiency*, 34th USAEE/IAEE North American Conference, Oct. 23-26. Tulsa, OK.
- Dundon, L.A., Abkowitz, M., & Camp, J. (2015). The real value of FracFocus as a regulatory tool: A national survey of state regulators. *Energy Policy* 87, pp. 496-504.
- Energy Information Administration (EIA). (2014). *Oil and gas supply module of the National Energy Modeling System: Model documentation 2014*. Washington, DC: U.S. Department of Energy.
- Energy Information Administration (EIA). (2016). *Trends in U.S. oil and natural gas upstream costs*. Washington, DC: U.S. Department of Energy.
- Energy Information Administration (EIA) (2018a). *Crude oil proved reserves, reserves changes, and production*. Accessed May 31, 2019. [https://www.eia.gov/dnav/pet/pet\\_crd\\_pres\\_dc\\_u\\_nus\\_a.htm](https://www.eia.gov/dnav/pet/pet_crd_pres_dc_u_nus_a.htm).
- Energy Information Administration (EIA) (2018b). *Annual energy outlook 2018: With projections to 2050*. Washington, DC: U.S. Department of Energy.
- Energy Information Administration (EIA) (2019). *Drilling productivity report For key tight oil and shale gas regions* (May 2019). Accessed May 30, 2019. <https://www.eia.gov/petroleum/drilling/pdf/dpr-full.pdf>.
- Fitzgerald, T. (2015). Experiential gains with a new technology: An empirical investigation of hydraulic fracturing. *Agricultural and Resource Economics Review*, 44(2), pp. 83-105.
- Forrester, J.W. (1961). *Industrial dynamics*. Portland, OR: Productivity Press.

- Gabriel, S.A., Kydes, A.S., & Whitman, P. (2001). The national energy modeling system: a large-scale energy-economic equilibrium model. *Operations Research*, 49(1), 14-25.
- Goetze, P. (2018). Current status of the New Mexico underground injection control. Paper presented at the New Mexico Produced Water Conference: Policy, Regulations and Economics to Support Total Resource Recovery, Nov. 15-16. Santa Fe, NM. <https://nmdesal.org/nm-produced-water-conference-2018/>.
- Guo, K., Zhang, B., Aleklett, K. and Höök, M. (2016). Production patterns of Eagle Ford shale gas: Decline curve analysis using 1084 wells. *Sustainability*, 8(10), p. 973.
- International Energy Agency (IEA). (2013). *World energy outlook 2013*. Paris, France: International Energy Agency.
- James, T., Evans, A., Madly, E. and Kelly, C. (2014). *The economic importance of the Colorado River to the basin region*. Final Report. Tempe, AZ: L. William Seidman Research Institute, Arizona State University.
- Johann, L., Shapiro, S.A. and Dinske, C. (2018). The surge of earthquakes in Central Oklahoma has features of reservoir-induced seismicity. *Scientific Reports*, 8(1), article 11505.
- Johnson, H.R., Crawford, P.M. and Bunger, J.W. (2004). *Strategic significance of America's oil shale resource: Volume 2-oil shale resources technology and economics*. Washington, DC: Office of Deputy Assistant Secretary for Petroleum Reserves and Office of Naval Petroleum and Oil Shale Reserves.
- Johnson, R.H. and Bollens A.L. (1927). The loss-ratio method of extrapolating oil well decline curves. *Transactions of the AIME*, 77, p. 771.
- Kalhor, E. (2019). An empirical model of unconventional well supply in the Permian Basin, New Mexico. Unpublished.
- Kellogg, R. (2014). The effect of uncertainty on investment: Evidence from Texas oil drilling. *American Economic Review* 104(6), pp. 1698-1734.
- Keranen, K.M., Savage H.M., Abers, G.A. and Cochran, E.S. (2013). Potentially induced earthquakes in Oklahoma, USA: Links between wastewater injection and the 2011 Mw5.7 earthquake sequence. *Geology* 41 (6), pp. 699-702. <https://doi.org/10.1130/G34045.1>.
- Kondash, A.J., Lauer, N.E. and Vengosh, A. (2018). The intensification of the water footprint of hydraulic fracturing. *Science Advances*, 4(8). DOI: 10.1126/sciadv. aar5982.
- Malczynski, L.A. (2011). *Best practices for system dynamics model design and construction with Powersim studio* (SAND2011-4108). Albuquerque, NM and Livermore, CA: Sandia National Laboratories. <http://www.powersim.com/sitefiles/4053/dokumenter/WhitePaper/SANDPowersimStudioBestPracticesManual06-23-2011.Pdf>.

- Male, F. (2019). Assessing impact of uncertainties in decline curve analysis through hindcasting. *Journal of Petroleum Science and Engineering*, 172, pp. 340-348.
- Mason, C.F. and Roberts, G. (2018). Price elasticity of supply and productivity: An analysis of natural gas wells in Wyoming. *The Energy Journal*, 9(1), pp. 79-100.
- Mason, C.F. and van't Veld, K. (2013). Hotelling meets Darcy: A new model of oil extraction. Paper presented at the 20th Annual Conference of the European Association of Environmental and Resource Economists, June 26-29. Toulouse, France.
- McNally, R. (2017). *Crude volatility*. New York, NY: Columbia University Press. Kindle Edition.
- Mohr, S.H. and Evans, G.M. (2010). Long term prediction of unconventional oil production. *Energy Policy*, 38(1), pp. 265-276.
- New Mexico Office of the State Engineer (OSE). (2019). *New Mexico water use by categories 2015*. (Technical Report 55). Santa Fe: New Mexico Office of the State Engineer. [http://www.ose.state.nm.us/Pub/wucTechReports/2015/2015%20WUR%20final\\_05142019.pdf](http://www.ose.state.nm.us/Pub/wucTechReports/2015/2015%20WUR%20final_05142019.pdf).
- New Mexico Oil and Gas Association (NMOGA). (2019). New Mexico Tax Research Institute: State and local revenue impacts of the oil and gas industry. Accessed May 30, 2019. [https://www.nmoga.org/new\\_mexico\\_tax\\_research\\_institute\\_state\\_and\\_local\\_revenue\\_impacts\\_of\\_the\\_oil\\_and\\_gas\\_industry](https://www.nmoga.org/new_mexico_tax_research_institute_state_and_local_revenue_impacts_of_the_oil_and_gas_industry).
- Nicot, J.P. and Scanlon, B.R. (2012). Water use for shale-gas production in Texas, U.S. *Environmental Science & Technology*, 46(6), pp. 3580-3586.
- Paryani, M., Ahmadi, M., Awoleke, O. and Hanks, C. (2016). Using improved decline curve models for production forecasts in unconventional reservoirs. Paper presented at the SPE Eastern Regional Meeting, Sep. 13-15. Canton, OH. doi:10.2118/184070-MS.
- Ridley, M. (2011). *The shale gas shock*. London, UK: Global Warming Policy Foundation.
- Scanlon, B.R., Reedy, R.C., Male, F. and Walsh, M. (2017). Water issues related to transitioning from conventional to unconventional oil production in the Permian Basin. *Environmental Science & Technology*, 51(18), pp. 10903-10912.
- Scanlon, B.R., Reedy, R.C. and Nicot, J.P., (2014a). Will water scarcity in semiarid regions limit hydraulic fracturing of shale plays? *Environmental Research Letters*, 9(12), article 124011.
- Scanlon, B.R., Reedy, R.C. and Nicot, J.P. (2014b). Comparison of water use for hydraulic fracturing for unconventional oil and gas versus conventional oil. *Environmental Science & Technology*, 48(20), pp. 12386-12393.
- State of New Mexico and U.S. Environmental Protection Agency (EPA). (2018). *Oil and natural*

- gas produced water governance in the State of New Mexico—Draft white paper*. Accessed May 30, 2019. <http://www.emnrd.state.nm.us/wastewater/documents/Oil%20and%20Gas%20Produced%20Water%20Goverance%20in%20the%20State%20of%20New%20Mexico%20Draft%20White%20Paper.pdf>.
- Sterman, J.D. (2000). *Business dynamics: Systems thinking and modeling for a complex world*. New York, NY: McGraw Hill.
- Sterman, J.D. (2001). System dynamics modeling: tools for learning in a complex world. *California Management Review*, 43(4), pp. 8-25.
- Tidwell, V.C., Passell, H.D., Conrad, S.H. and Thomas, R.P. (2004). System dynamics modeling for community-based water planning: Application to the Middle Rio Grande. *Aquatic Sciences*, 66(4), pp. 357-372.
- Tysseling, J.C., Bjarke, J.A. and Anklam, R. (2019). *New Mexico: A comparative analysis: The oil & gas industry's fiscal contribution to state governments*. Interim Comprehensive Report to New Mexico Tax Research Institute. Accessed July 20, 2019. [https://nm4ep.com/wp-content/uploads/2019/01/18-OAG-1654-NM-Report\\_PP7-compressed.pdf](https://nm4ep.com/wp-content/uploads/2019/01/18-OAG-1654-NM-Report_PP7-compressed.pdf).
- Veil, J.A., Puder, M.G., Elcock, D. and Redweik Jr, R.J. (2004). *A white paper describing produced water from production of crude oil, natural gas, and coal bed methane* (ANL/EA/RP-112631). Argonne, IL: Argonne National Laboratory (ANL).
- Wachtmeister, H., Lund, L., Aleklett, K. and Höök, M. (2017). Production decline curves of tight oil wells in Eagle Ford shale. *Natural Resource Research*, 26(3), pp. 365-377. <https://doi.org/10.1007/s11053-016-9323-2>.
- Zemlick, K., Kalhor, E., Thomson, B.M., Chermak, J.M., Graham, E.J.S., & Tidwell, V.C. (2018). Mapping the energy footprint of produced water management in New Mexico. *Environmental Research Letters*, 13(2), 024008.





## **Chapter 3. Drilling activity in the Permian Basin: A Vector Error Correction**

### **Model**

#### **1. Introduction**

In November of 2018, the United States Geological Survey (USGS) announced the largest-ever continuous oil assessment in the Permian Basin of western Texas and Southeastern New Mexico (Demas & Gaswirth 2018). The newly added reserve is estimated to contain about 46.3 billion barrels of oil and 281 trillion cubic feet of natural gas (Gaswirth et al. 2018). Even before this substantial discovery, large United States (U.S.) oil and gas (O&G) producing firms had intensified their presence in the Permian Basin due to its high productivity. In 2017, Exxon Mobil doubled its Permian Basin holdings for up to \$6.6 billion (Scheyder 2017). In 20, Chevron Corp. and Shell acquired hundreds of thousands of acres of land in the Permian Basin. Furthermore, Conoco Phillips has signaled its plan for expansion in the Permian Basin in 2019 (Luck & Douglas 2019).

The well-placement decision, i.e., the location choice for placing a new well, is an economic

decision that involves estimations of the drilling and operational costs, the revenue prospects from a potential drilling investment, and the risks involved in the estimations (Guyaguler & Horne 2001). Of all these variables, actual cost information is known the least, due to different practices adopted by the operators and to the ownership rights associated with the cost data. The Energy Information Administration (EIA) lists rig and drilling fluid costs, casing and cement costs, completion costs, operation and maintenance costs, and site operations costs, among others, as the costs involved in the upstream of O&G production (Energy Information Administration 2016). However, the role of regulatory costs in placement decision is not accounted for by the EIA or in other studies. The objective of this study is to investigate the potential impact of the regulatory system on the drilling location choice. In other words, all else equal, does a difference in the regulatory environment surrounding potential drilling locations result in different degrees of competitiveness for different locations?

The Permian Basin is one of a few instances of a shared basin between two separate regulatory systems in the United States. The Permian Basin's O&G production is the source of substantial state income for both Texas (TX) and New Mexico (NM) (Tysseling, Bjarke & Anklam 2019). More specifically, the scheme of land ownership (private, state, and federal) is different between the two states. During 2018, only 8.7% of the total oil production in Texas took place on state lands (no production on federally owned lands); whereas, in New Mexico, 53% of crude oil production occurred on federal lands, 34% on state-owned lands, and only 13% on private lands. This difference in landownership creates different economic and regulatory environments, especially different tax policies. Furthermore, the environmental regulations that impact O&G operations are different in Texas and New Mexico and could result in different cost structures for producers.

We test the impact of different regulatory environments by investigating the drilling activity in the New Mexico and Texas portions of the Permian Basin. In the absence of actual costs, we associate differences in drilling choices between those portions of the Permian Basin to variations in costs derived from the regulatory environment by assuming that the petrophysical characteristics of the Permian Basin are not significantly different between the two states. We utilize a vector error correction model (VECM) to measure the impacts of price shock on drilling in the Texas and New Mexico portions of the Permian Basin. We further investigate the interaction between drilling activity in those states using the VECM. We do so to understand the dynamics of drilling activity in those portions of the Permian Basin and their relationship to changes in oil prices. We are especially interested in answering three questions: (1) Do New Mexico and Texas drilling activities (in the Permian Basin) react differently to price shocks? (2) Does Texas drilling impact New Mexico drilling, and vice versa? and 3) Does drilling activity in the Permian Basin impact oil prices?

## **2. Background**

### **2.1. U.S. oil prices**

Some studies are built based on the assumption that the United States is considered a price taker in the crude oil market (Kellogg 2014; Newell, Prest & Vissing 2016; Ringlund, Rosendahl & Skjerpen 2008, among others) and as a result, the US oil price is affected by global crises, wars, and sanctions as well as the boom-bust cycles of large economies like Europe, Japan, and China. Between 2000 and 2018, West Texas Intermediate (WTI) crude oil prices witnessed two major collapses (Figure 3.1):

- from an average monthly \$134 per barrel in June 2008 to an average monthly \$39 per barrel in February 2009, which was attributed to the global financial crisis (Baumeister & Kilian 2016), and
- from an average monthly \$112 per barrel in June 2014 to an average monthly \$47 per barrel in January 2015; which was attributed to a series of global events including Organization of the Petroleum Exporting Countries (OPEC) policies and to a decline in oil demand in China, Japan, and the United States (McNally 2017).

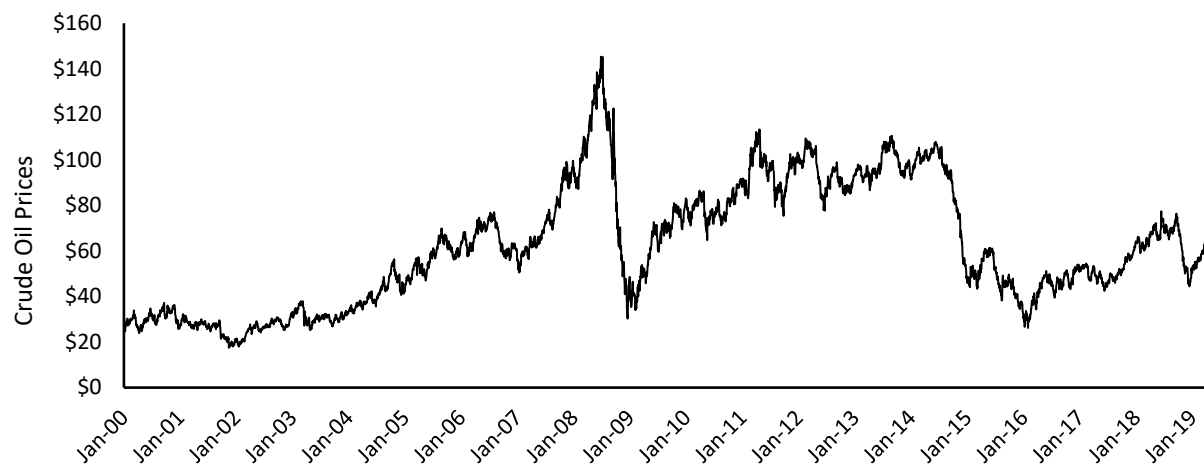


Figure 3.1: The U.S. West Texas Intermediate crude oil price

Baumeister and Kilian (2014) applied a simple vector autoregressive (VAR) model to explain the oil price decline between June and December of 2014. Their model accounted for past oil prices, global oil production, the global level of proved reserves, and global economic activity; it showed that more than half of the price decline in 2014 was predictable by those variables. They also concluded that the price decline of 2014, was mainly due to global economic activity and the decline in the demand for oil, rather than to OPEC policy.

## 2.2. The relationship between oil price and drilling activity in the United States

A natural economic question with regards to shocks to oil prices is the extent of the impact on U.S. oil production. However, that the production of oil from a drilled well is an economic decision purely affected by prices is debatable (Mason & Roberts 2018). Based on empirical evidence, oil production does not respond to prices directly, as is shown in Figure 3.2.

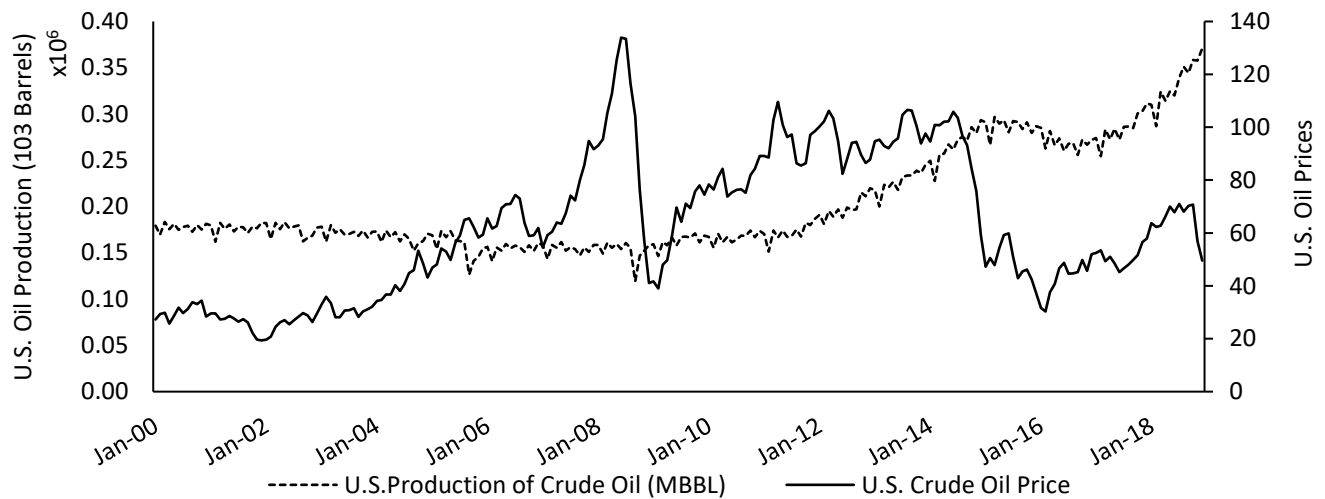


Figure 3.2: Changes in oil prices and U.S. oil production

Despite the U.S. oil price collapse in 2008-2009, U.S. oil production increased slightly. It increased at a higher rate during the 2009-2014 period, irrespective of the oil price fluctuations in the same period. Oil production decreased slightly between 2014 and 2017 and resumed growing in 2018.

Petroleum engineering principles suggest that production from a well is a physical process that is mainly governed by the pressure difference between the formation and well, among other petrophysical characteristics (Mason & Roberts 2018). In addition, since the operation costs are small compared to the drilling and completion costs of a well, an operator tends to produce as much oil as possible in order to break even with the capital costs (Newell, Prest & Vissing 2016).

It is possible that the oil industry responds to oil prices through changes in drilling activity intensity. This hypothesis is supported by the empirical evidence as is shown in Figure 3.3. Both oil price crashes, discussed earlier, are reflected in the number of wells drilled monthly between 2000 and 2018.

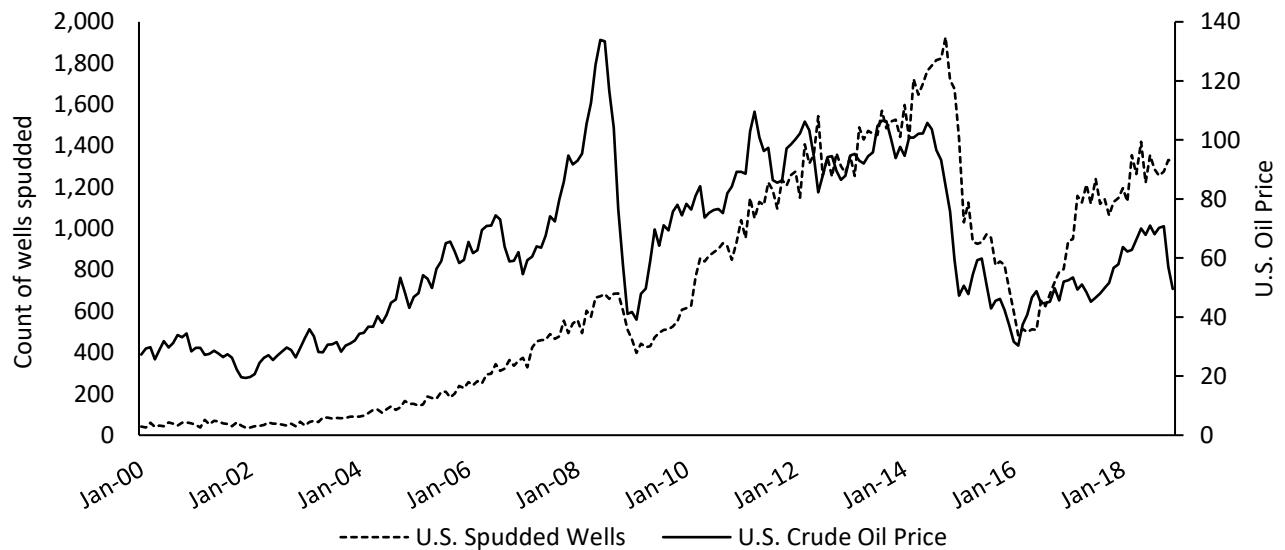


Figure 3.3: Relationship between oil price and drilling activity in the U.S.

The relationship between drilling activity and oil prices is even more evident after 2009, when the “shale revolution” took place. Shale formations are a form of unconventional O&G resources that need to be stimulated by hydraulic fracturing in order to yield oil and gas. A successful combination of horizontal drilling and hydraulic fracturing technologies in the 1990s lent itself to the economic recovery of O&G from shale formations (Ridley 2011). However, the mass adoption of this technology was due to the success of its application in exploratory operations in 2009-2010 which resulted in the record-breaking additions to the US proved reserve stocks (Energy Information Administration 2017) (Figure 3.4).

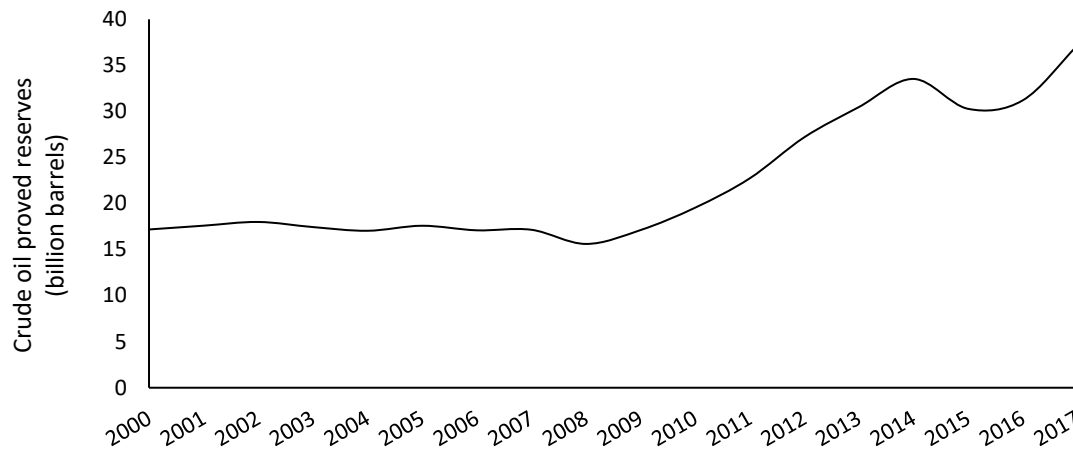


Figure 3.4: The U.S. onshore proved reserves stocks (Source Energy Information Administration [EIA] 2017)

A resource is added to the stock of proved reserves if it is estimated to contain crude oil (and natural gas) liquids at a high confidence and that the existing technology allows for the economic recovery of the hydrocarbon from it<sup>18</sup>. By adding the shale reserves to the stock of proved reserves, EIA essentially recognized the economic feasibility of production from shale formations in 2009.

The close relationship between oil prices and drilling activity after the shale revolution (Figure 3.3) could be due to the profile of production from shale formations. Rates of production (volume per day) from wells drilled in both conventional and unconventional formations decline over time. This decline is due to the decline in the formation's pressure which is the result of extraction (Chermak, Crafton & Patrick 2012). However, the decline rate of production from shale resources is much higher than that from conventional formations (International Energy 2013).

Due to the sharp and early decline in production from the unconventional wells, more wells need

---

<sup>18</sup> Based on the EIA's Energy Glossary (Energy Information Administration [EIA] 2019b)

to be drilled in order to maintain the unconventional production level or to increase it (IEA 2013).

To better understand the economics of the drilling activity and its response to the oil prices, Newell, Prest and Vissing (2016) developed an oil and gas new well supply model by accounting for the quarterly O&G revenue from shale wells in Texas, as well as the total vertical depth and lateral length of the wells as drilling cost factors. Kellogg (2014) modeled the drilling investment decision in Texas, accounting for oil price volatility and the firm's discount rate. Ringlund, Rosendahl, and Skjerpen (2008) modeled the relationship between oil prices and oil rig activity in the United States and non-OPEC regions through multivariate time series analyses.

We expand the analysis of price responsiveness of drilling activity to include the regulatory differences within a shared basin. Using VECM, we investigate the differences and similarities of the drilling response in the Texas and New Mexico portions of the Permian Basin to price changes. Furthermore, we search for proof of a relationship (unilateral or bilateral) between drilling activity in the Texas and New Mexico portions of Permian Basin irrespective of prices to see if producers prefer one regulatory environment over the other.

### **3. Study area and data**

#### **3.1. Study area**

The study area is the Permian Basin located in the western Texas and southeastern New Mexico (Figure 3.5). About 50% of the total rigs in the U.S. were attracted by the Permian Basin during 2017 and 2018 (Energy Information Administration 2019a). Furthermore, during the same period, the Permian Basin produced 45% of the U.S. oil production and 15% of the United States



natural gas production. More than 25% of crude oil proved reserves<sup>19</sup> in the Permian Basin are in New Mexico<sup>20</sup>. However, New Mexico's potential has not been realized compared to the Texas portion of the Permian Basin. Between 2000 and 2018, out of the total annual production in the Permian Basin, about 13% was in the New Mexico portion. This low share of production can be attributed to the lower level of drilling activity in the state; between 2000 and 2018, during an average year, 16% of drilling activity took place in New Mexico.<sup>21</sup>

In November 2018, the largest unconventional resource was discovered within the Delaware Basin, a sub-basin of the Permian Basin. New Mexico owns roughly 26% of the oil resources and 37% of the gas resources of the Delaware Basin.

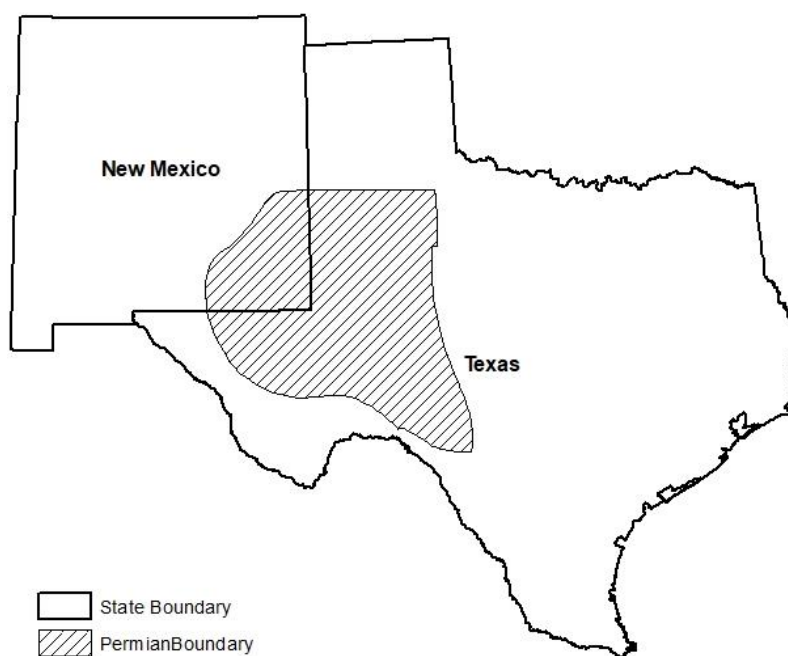


Figure 3.5: Location map for the study area

---

<sup>19</sup> High-confidence estimations of available crude oil that is recoverable in an economically feasible manner. (EIA Energy Glossary)

<sup>20</sup> Author's calculation based on EIA's annual proved reserves reports.

<sup>21</sup> Author's calculations based on data from Rystad Energy's Shale Well Cube dataset

The composition of land ownership in the Texas and New Mexico portions of the Permian Basin is quite different. Figures 3.6 and 3.7<sup>22</sup> present the distribution of land ownership types within the NM and TX portions, respectively; as shown in these figures, federal and state lands constitute the majority of producing areas in the NM portion. In comparison, the majority of producing areas in the TX portion are privately owned.

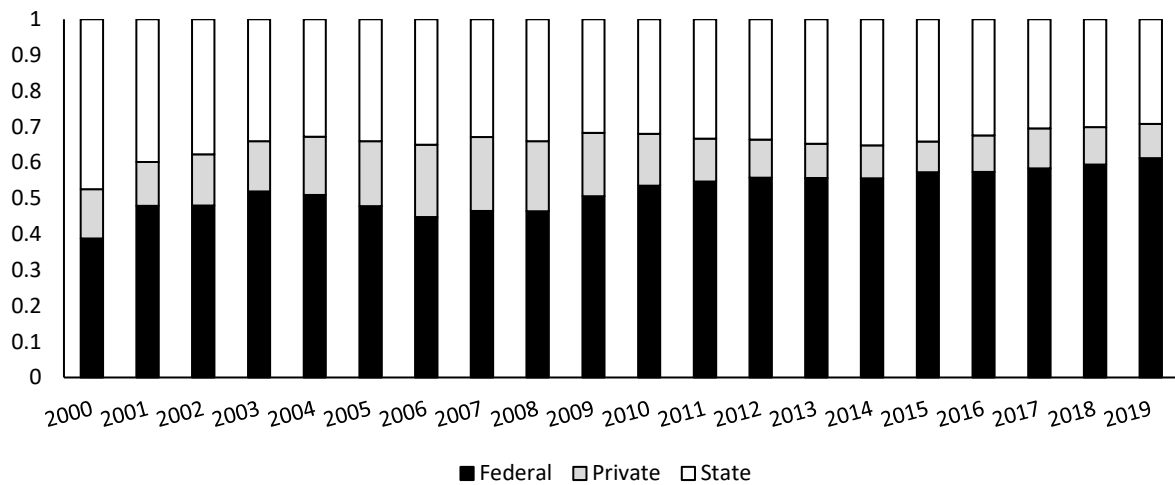
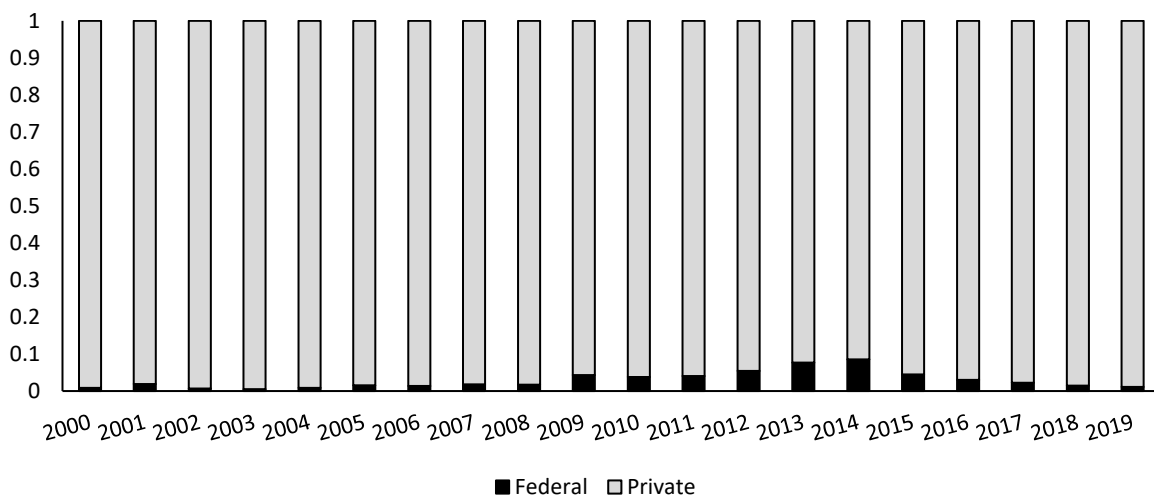


Figure 3.6: Percentage of oil production by land ownership in NM



<sup>22</sup> Authors' calculations based on data from Rystad Energy's ShaleWellCube dataset.

Figure 3.7: Percentage of oil production by land ownership in TX

Due to the difference in land ownership, the New Mexico and Texas economies are impacted differently by oil production in the Permian Basin. A recent study by Tysseling, Bjarke, and Anklam (2019) showed that in 2017, New Mexico collected an equivalent of 9.2% of statewide O&G production revenue as the state's land income. Texas collected the equivalent of 2% of the statewide O&G production revenue as its land income. In terms of production taxes (including severance tax, school tax, conservation tax, property tax, etc.), Texas collected an equivalent of 12.8% of production revenue, only 1.3 percentage points higher than that of New Mexico.

In addition to the difference in tax policies, the two states take different stands in terms of environmental regulations in O&G production areas, which could be attributed to their different political profiles. In 2019, New Mexico House Bill 398 was introduced; if passed it would have increased New Mexico's royalty rates on oil, gas, and vented gas from 20% to 25%. New Mexico Senate Bill 186 was also introduced; if passed it would have allowed the New Mexico Oil Conservation Division (NM-OCD) to penalize O&G operators for violating environmental regulations. Such regulations could ultimately add to the operational costs of O&G production in New Mexico as compared to Texas.

### 3.2. Data

Data for this study comes from two sources. The number of new wells drilled in Texas and New Mexico is available from the Railroad Commission (RRC) of Texas and from NM-OCD, respectively. For the number of well counts we use the Rystad Energy's ShaleWellCube dataset, which collects data from RRC and NM-OCD. This is especially beneficial considering that the two districts may have different data reporting systems whereas ShaleWellCube provides a homogenous database.

Our study period is 2000-2018 and since it includes the years prior to the shale revolution we account for wells that are drilled in both conventional and unconventional formations. Oil price data used in this study are for West Texas Intermediate (WTI). WTI refers to a certain grade of oil that is extracted in TX and Oklahoma (OK) and is a benchmark grade for oil pricing. We use the spot prices, which are the one-time transaction for immediate delivery of a commodity (crude oil in this case). WTI prices are collected from the Energy Information Administration (EIA).

The timeseries variables utilized in this study include new wells counts in the Texas and New Mexico portions of the Permian Basin and the WTI price. All three of the time series are log-transformed to remove potential skewness in the data. Table 3.1 shows the variable names and descriptions used in this analysis.

Table 3.1: Time series variables' description

Variable	Description
$NMW_t$	Logged count of wells drilled in NM during month $t$ (seasonally adjusted)
$TXW_t$	Logged count of wells drilled in TX during month $t$
$WTI_t$	Logged WTI spot price in month $t$

Since data are in timeseries format, the need for seasonal adjustment for all the variables is investigated. The X-13ARIMA model proposed by the U.S. Census is used to test the need for seasonal adjustment and to seasonally adjust the timeseries if applicable. Among the three variables, only the New Mexico drilling time series underwent seasonal adjustment.

#### 4. Econometric modeling

The econometric model used in this study is a vector timeseries analysis and is explained step-by-step in the following paragraphs.

#### 4.1. Vector autoregressive models and Granger causality

In its generic form, a vector autoregressive (VAR) model is written as follows:

$$\mathbf{Y}_t = \boldsymbol{\alpha} + \sum_{l=1}^p \boldsymbol{\phi}_l \mathbf{Y}_{t-l} + \mathbf{U}_t, \quad (1)$$

where  $\mathbf{Y}_t$  is a vector of timeseries components:

$$\mathbf{Y}_t = \begin{bmatrix} \mathbf{y}_{1t} = (y_{1t}, y_{1t+1}, \dots, y_{1T}) \\ \mathbf{y}_{2t} = (y_{2t}, y_{2t+1}, \dots, y_{2T}) \\ \dots \\ \mathbf{y}_{nt} = (y_{nt}, y_{nt+1}, \dots, y_{nT}) \end{bmatrix}. \quad (2)$$

Similarly,  $\mathbf{U}_t$  is a vector of error terms,  $\boldsymbol{\alpha}$  is a vector of constant terms,  $\boldsymbol{\phi}_l$  is a vector of coefficients for lagged vectors of the endogenous variables, and  $l$  is the lag index.  $\mathbf{y}_{it}$ 's in equation (2) denote timeseries processes. Equation (2) is explicitly written as follows:

$$\begin{bmatrix} \mathbf{y}_{1t} \\ \dots \\ \mathbf{y}_{nt} \end{bmatrix} = \begin{bmatrix} \alpha_{10} \\ \dots \\ \alpha_{n0} \end{bmatrix} + \sum_{l=1}^p \begin{bmatrix} \phi_{l11} & \dots & \phi_{l1n} \\ \vdots & \ddots & \vdots \\ \phi_{ln1} & \dots & \phi_{lnn} \end{bmatrix} \begin{bmatrix} \mathbf{y}_{1t-l} \\ \dots \\ \mathbf{y}_{nt-l} \end{bmatrix} + \begin{bmatrix} \mathbf{u}_{1t} \\ \dots \\ \mathbf{u}_{nt} \end{bmatrix}. \quad (3)$$

As shown in equation (3), VAR models are systems of autoregressive (AR) equations. In order to test the impact of the variable  $y_i$  on  $y_j$ , Granger (1969) proposes a framework:

In the  $n$  – variate model shown in equation (3), suppose  $F_t$  includes all the available information; i.e.  $F_t = \{ \mathbf{y}_{1t}, \dots, \mathbf{y}_{it}, \dots, \mathbf{y}_{nt} \}$ . By subtracting information associated with one variable,  $\mathbf{y}_{it}$ , Granger derives  $F_{-i,t} = \{ \mathbf{y}_{1t}, \dots, \mathbf{y}_{i-1,t}, \mathbf{y}_{i+1,t}, \dots, \mathbf{y}_{nt} \}$ . Granger then suggests using  $F_t$  and  $F_{-i,t}$ , separately, to forecast  $\mathbf{y}_{jt}$ , where  $j \neq i$ . Let  $\mathbf{e}_t$  be the error vector associated with the forecasts of  $\mathbf{y}_{it}$  based on  $F_t$ , and  $\mathbf{e}_{i,j,t}$  be the error term of forecasting  $\mathbf{y}_{jt}$  based on  $F_{-i,t}$ . It is said the  $\mathbf{y}_i$  Granger causes  $\mathbf{y}_j$  if:

$$Var(\mathbf{e}_{i,jt}) < Var(\mathbf{e}_{it}). \quad (4)$$

In other words,  $y_i$  Granger causes  $y_j$  if by incorporating  $y_i$  the efficiency of forecasting  $y_j$  is improved (Tsay 2013).

#### 4.2. Impulse-response functions

More often than not, in multivariate time series analysis, it is of interest to measure the impact of a change in one variable on other variables. Through a number of assumptions, Hamilton (1994) rewrites the equation (1) in an infinite moving average form ( $MA(\infty)$ ):

$$\mathbf{Y}_t = \boldsymbol{\mu} + \mathbf{U}_t + \boldsymbol{\Psi}_1 \mathbf{U}_{t-1} + \boldsymbol{\Psi}_2 \mathbf{U}_{t-2} + \dots, \quad (5)$$

where the matrix  $\boldsymbol{\Psi}_s$  can be interpreted as:

$$\boldsymbol{\Psi}_s = \frac{\partial \mathbf{Y}_{t+s}}{\partial \mathbf{U}'_t}. \quad (6)$$

In other words,  $\Psi_s(i, j)$ , the element on row  $i$  and column  $j$  of the  $\boldsymbol{\Psi}_s$ , measures the impact of a change in variable  $j$ ,  $y_j$ , on variable  $i$ ,  $y_i$ , at time  $t + s$ :

$$\Psi_s(i, j) = \frac{\partial y_{i,t+s}}{\partial u_{j,t}}. \quad (7)$$

The plot of  $\Psi_s(i, j)$  is called the impulse-response function (IRF). A difficulty with the impulse-response function calculated by equation (7) is that the variance-covariance of the vector of residuals,  $\Sigma_U$ , is not a diagonal matrix (Tsay 2013); in other words, a change in  $y_j$ , cause other variables  $y_{z \neq j}$  to change as well. Variable  $y_i$  also responds to the changes in  $y_{z \neq j}$  and ultimately the response obtained from equation (7) does not reflect the isolated impact of  $y_j$  on  $y_i$ . This issue is addressed by the Cholesky decomposition approach. The Cholesky method involves

decomposition of  $\Sigma_U$  into a diagonal matrix  $D$  and a lower triangular matrix  $A$ :

$$\Sigma_U = ADA'. \quad (8)$$

Equation (8) can be rearranged as follows:

$$\Sigma_U = AD^{\frac{1}{2}}D^{\frac{1}{2}}A' = PP'. \quad (9)$$

And the orthogonalized IRF parameter can be calculated as follows:

$$\frac{\partial y_{i,t+s}}{\partial v_{j,t}} = \Psi_s P_j, \quad (10)$$

where  $\partial v_{j,t}$  is  $u_{j,t}$  divided by  $\sqrt{d_{jj}}$ , and  $d_{jj}$  is the diagonal element on row and column  $j$  of the matrix  $D$ .  $P_j$  is the  $j^{th}$  column of the matrix  $P$ . For more details on the derivation of equations (5) to (14), the readers are referred to Hamilton (1994 pp. 318-323). The orthogonalized impulse size is one standard deviation (SD) of the impulse variable,  $y_j$ .

#### 4.3. Stationarity and unit root test

For a generic time series  $\mathbf{y}_t = (y_t, y_{t+1}, \dots, y_T)$ , strict stationarity requires that the joint distribution of a subset  $(y_{t_1}, y_{t_1+1}, \dots, y_{t_k})$  of  $\mathbf{y}_t$  be identical to that of  $(y_{t_1+\tau}, y_{t_1+k+\tau}, \dots, y_{t_k+\tau})$ , where  $\tau$  is a positive integer. In other words, statistical properties of a strictly stationary process are time invariant. A weak version of stationarity is the case where the timeseries' mean and the covariance between any two observations are time invariant (Tsay 1951). A stationary process is also called integrated of order zero, or  $I(0)$ . In real life, stationary timeseries are rare (Thomson 1994). The stationarity of a process is determined by estimating the coefficient  $\rho$  of an autoregressive (AR) model. The following equation shows an AR model with one lag of the endogenous variable on the right-hand side which is referred to as an AR (1) equation:

$$y_t = \rho y_{t-1} + \varepsilon_t. \quad (11)$$

Timeseries  $y_t$  is considered stationary if  $|\rho| < 1$  and nonstationary otherwise. When  $|\rho| = 1$ , the variance of  $y_t$  is  $t\sigma^2$ , and when  $|\rho| > 1$  the variance increases exponentially with time (Dickey & Fuller 1979). The case where  $|\rho| = 1$  is called difference-stationary, in that, the time series of first difference of  $y_t$ ,  $\Delta y_t = (y_{t_1+1} - y_{t_1}, y_{t_1+2} - y_{t_1+1}, \dots, y_{t_k} - y_{t_k-1})$ , is stationary. A difference-stationary process is also said to be integrated of order 1, or  $I(1)$ .

The unit-root test investigates the null hypothesis that  $\rho < 1$  against the alternative hypothesis that  $\rho = 1$ . There are various ways for conducting unit root. The unit-root test adopted in this study is the test proposed by Dickey and Fuller (1979). The Dickey-Fuller test suggests utilizing an ordinary least square (OLS) model to estimate  $y_t$  as a function of the  $y_{t-1}$  and a trend variable  $t$ :

$$y_t = \alpha + \rho y_{t-1} + \delta t + u_t^{23}, \quad (12)$$

and to test the null hypothesis  $H_0: \rho = 1$  against the alternative  $H_a: \rho \neq 1$ . A difficulty with the Dickey-Fuller test is that it is based on the assumption that the error term,  $u_t$ , is an independently and identically distributed zero mean error term; in other words, the Dickey-Fuller test is based on the assumption that the error term in equation (12) is a white noise. However, If post-estimation diagnostics suggest that the estimated residuals,  $\hat{u}_t$ , are not white noise, the augmented Dickey-Fuller test should be conducted:

$$\Delta y_t = \alpha + \rho y_{t-1} + \delta t + \gamma_1 \Delta y_{t-1} + \gamma_2 \Delta y_{t-2} + \dots + \gamma_k \Delta y_{t-k} + u_t \quad (13)$$

The number of delays in equation (13),  $k$ , is based on the goodness of fit of the estimation and is

---

<sup>23</sup> Setting  $\alpha = 0$  and/or  $\delta = 0$  is arbitrary.



chosen by iterating the analysis over different values of  $k$  and choosing the on lag associated with the model that shows the best fit. In the augmented Dickey Fuller test, the null hypothesis changes to  $H_0: \rho = 0$  and similarly, the alternative hypothesis has to be altered to  $H_a: \rho \neq 0$ . It is noteworthy that the t-statistic used for testing Dickey-Fuller and augment Dickey-Fuller tests are different from the t-statistics for OLS hypothesis testing and can be found in Dickey (1976, p. 53).

An important assumption made by Granger (1969) in defining this causality is that series  $\mathbf{y}_{it}$  are all stationary. In case of non-stationarity,  $Var(\mathbf{e}_{it})$  changes over time and so does the causality.

If it is shown that a VAR model's time-series are nonstationary there is a risk of spurious regression. The result of spurious regression can only indicate correlation between economic variables and not causation. However, if the nonstationary timeseries share a common trend, instead of evolving independently through time, the spuriousness can be averted by using an error correction model that is explained in section 4.5. Whether or not two or more time-series share a common trend is estimated by cointegration analysis.

#### 4.4. Cointegration

In case of nonstationary  $\mathbf{Y}_t$  we test for a common trend between  $\mathbf{y}_{it}$ 's which is referred to as cointegration (Granger 1986). The vector process  $\mathbf{Y}_t$  is considered cointegrated when there is a linear combination of  $\mathbf{y}_{it}$ 's that is stationary:

$$\sum_{i=1}^n \beta_i \mathbf{y}_{it} \sim I(0) \left| \left( \sum_{i=1}^n \beta_i \right) \neq 0. \quad (14)$$

To test the cointegration between time series  $\mathbf{y}_{it}$  and  $\mathbf{y}_{jt}$ , Engle and Granger (1987) suggest

testing the stationarity of the residual that results from regressing  $y_{it}$  on  $y_{jt}$ :

$$e_t = y_{it} - \beta y_{jt}. \quad (15)$$

The augment Dickey-Fuller test, explained in section 4.3, can determine whether or not the estimated residuals in equation (15),  $\hat{e}_t$ , is a stationary process.

#### 4.5. Vector error correction models

Engle and Granger (1987) propose a vector error correction model (VECM) for assessing causality in nonstationary and cointegrated vectors. In its generic matrix form, VECM is presented as follows:

$$\Delta Y_t = \alpha + \sum_{l=1}^p \phi_l \Delta Y_{t-l} + \delta EC_t + U_t, \quad (16)$$

where  $EC_t$  is the error correction vector, the estimated (and stationary) residuals from the cointegration regression, equation (15). In the VECM context, Granger causality can be identified by testing the significance of the coefficients ( $\phi_l$ 's) (Oh and Lee 2004).

## 5. Estimation results

### 5.1. Descriptive statistics

The descriptive statistics of the variables are presented in Table 3.2.

Table 3.2: Descriptive statistics

Variable	Min	Mean	Max	SD
<i>NMW</i>	2.97	4.25	4.90	0.47
<i>TXW</i>	5.07	5.93	6.70	0.42
<i>WTI</i>	2.98	4.03	4.67	0.32

Number of observations: 250

## 5.2. Stationarity test results

To test stationarity, first, the Dickey-Fuller test, equation (12), is tested. Subsequently, the white noise characteristics of the estimated error term determines whether or not the augmented Dickey-Fuller test should be used instead. For all time-series in this study, post-estimation diagnostics led to the use of the augmented Dickey-Fuller test, equation (13). The number of lags in the augmented Dickey-Fuller test,  $k$  in equation (13), is selected based on different goodness-of-fit measures, but in case of inconsistency with the goodness-of-fit results, the Akaike information criterion ( $AIC^{24}$ ) (Akaike 1974) is used as the lag selection criterion. Accordingly, we test if the level and the first difference of the variables are stationary. The null hypothesis is that the coefficient of the lagged dependent variable,  $\rho$  in equation (13) is equal to zero ( $H_0: \rho = 0$ ), in which case, the time series is nonstationary. The alternative hypothesis is that the time series is stationary or  $H_a: \rho \neq 0$ . A significance test is used to determine if the estimated  $\rho$  is significantly different from zero. The 1% critical value of the z-statistics for the augmented Dickey Fuller test with 250 observations is  $-3.46$  and the null hypothesis is rejected when the test statistic is greater than the given critical value.

Table 3.3: Unit-root test results

Level/Difference	Variable	z-statistic	Stationarity remarks
Level	<i>NMW</i>	-2.58	Nonstationary
	<i>TXW</i>	-2.27	Nonstationary
	<i>WTI</i>	-2.22	Nonstationary
First difference	<i>NMW</i>	-9.95	Stationary
	<i>TXW</i>	-5.97	Stationary

---

<sup>24</sup>  $AIC = \log\left(\frac{SSR(p)}{n}\right) + \frac{2(p+1)}{n}$ , where  $SSR(p)$  is the sum of squared residuals that resulted from the model with  $p$  lags, and  $n$  is the number of observations.

According to the unit-root test results presented in Table 3.3, all of the time series are nonstationary but become stationary after first differencing.

### 5.3. Cointegration test results

Since the time series are not stationary in variable levels, in order to avoid spurious regression, we need to test for cointegration. To test for cointegration, the stationarity of the residuals of regressing one variable on other variables is tested, as is shown in the following:

$$NMW_t = \beta_0 + \beta_1 TXW_t + \beta_3 WTI_t + e_t. \quad (17)$$

The estimated residual,  $\hat{e}_t$ , is subject to the stationarity test. The common wisdom is to suppress the constant term when conducting a unit-root test on  $\hat{e}_t$ <sup>25</sup>. Hence, the 1% critical value for the unit-root test on  $\hat{e}_t$  drops to -2.583. The test statistic is estimated at -2.673 and the existence of the unit root can be rejected. In other words, there is a linear combination of the variables that is stationary and the existence of cointegration is verified.

### 5.4. VECM model, lag selection and estimated coefficients

Due to non-stationarity and the existence of cointegration, the appropriate mode is the VECM. Equations (18) to(20) together represent the VECM model.

$$\Delta WTI_t = \phi_1 + \sum_i^p \alpha_{11,i} \Delta WTI_{t-i} + \sum_i^p \beta_{12,i} \Delta TXW_{t-i} + \sum_i^p \gamma_{13,i} \Delta NMW_{t-i} + \delta_1 EC_{t-1} + \varepsilon_{1t} \quad (18)$$

---

<sup>25</sup> That is, in equation (12),  $\alpha = 0$ .

$$\Delta TXW_t = \phi_2 + \sum_{i=1}^p \alpha_{21,i} \Delta WTI_{t-i} + \sum_{i=1}^p \beta_{22,i} \Delta TXW_{t-i} + \sum_{i=1}^p \gamma_{23,i} \Delta NMW_{t-i} + \delta_2 EC_{t-1} + \varepsilon_{2t} \quad (19)$$

$$\Delta NMW_t = \phi_3 + \sum_{i=1}^p \alpha_{31,i} \Delta WTI_{t-i} + \sum_{i=1}^p \beta_{32,i} \Delta TXW_{t-i} + \sum_{i=1}^p \gamma_{33,i} \Delta NMW_{t-i} + \delta_3 EC_{t-1} + \varepsilon_{3t} \quad (20)$$

In order to select the appropriate lags for the VECM model, the number of lags is selected based on the order selection criteria that resulted from the AIC. The order,  $p$  in equation 10, and equations (18) to (20) is selected by iterating VAR models of different orders on the timeseries, and choosing the order that results in the least AIC value. The graph of AIC values based on different choices of lags is shown in Figure 3.8. According to the AIC-lag graph, the optimal AIC occurs when 3 lags are selected.

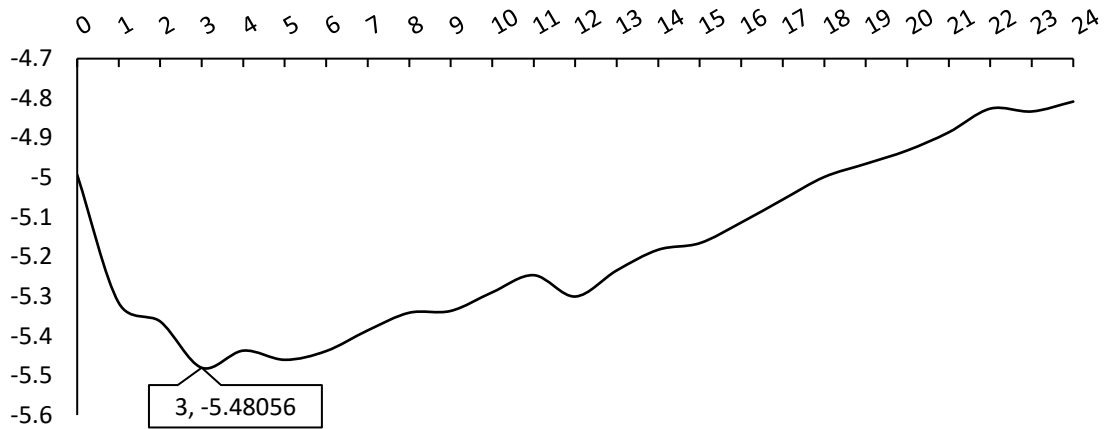


Figure 3.8: AIC for lag selection; an order of 3 results in the minimum AIC and is selected as the optimal order

The coefficients estimated from the VECM are presented in Tables 3.4 to 3.6.

Table 3.4: VECM coefficient estimates

Dep. Var.	$\phi$	$\Delta WTI_{t-1}$	$\Delta WTI_{t-2}$	$\Delta WTI_{t-3}$	$\Delta TXW_{t-1}$	$\Delta TXW_{t-2}$	$\Delta TXW_{t-3}$	$\Delta NMW_{t-1}$	$\Delta NMW_{t-2}$	$\Delta NMW_{t-3}$	$EC_{t-1}$
$\Delta WTI_t$	0.001 (0.022)	0.256*** (0.071)	0.095 (0.077)	-0.062 (0.078)	0.015 (0.060)	0.046 (0.062)	0.055 (0.056)	-0.073 (0.056)	-0.090 (0.056)	-0.024 (0.053)	0.006 (0.022)
$\Delta TXW_t$	-0.001 (0.007)	0.229*** (0.083)	0.204** (0.090)	0.179** (0.090)	-0.386*** (0.070)	-0.008 (0.072)	0.145** (0.065)	0.050 (0.065)	0.075 (0.065)	0.086 (0.062)	0.070** (0.025)
$\Delta NMW_t$	-0.012 (0.026)	0.392*** (0.085)	0.011 (0.092)	0.284*** (0.092)	0.107 (0.072)	0.209*** (0.073)	0.196*** (0.066)	-0.189*** (0.066)	-0.080 (0.066)	-0.127** (0.063)	-0.012 (0.026)

Note: Numbers in parentheses are standard errors. \*\*\*, \*\*, and \* indicate statistical significance at the 0.01, 0.05, and 0.10 levels,

Table 3.5: Coefficients of the error correction term

Dep. Var.	$\phi$	$WTI_{t-1}$	$TXW_{t-1}$	$NMW_{t-1}$
$EC_t$	3.731 (---)	1 (---)	-1.475*** (0.294)	0.244 (0.395)

Table 3.6: Model measures

Equation	$N$	AIC	$R^2$
$\Delta WTI_t$			0.1068
$\Delta TXW_t$	224	-5.535	0.3003
$\Delta NMW_t$			0.2547

### 5.5. Granger causality

In order to test the Granger causality between variables, and to test if there is a bi-directional relationship between variables, the joint significance of the estimated coefficients in each equation is tested. The null hypothesis, test statistics and test results are presented in Table 3.7.

Table 3.7: Granger causality results

Dep. Var.	$H_0$	$\chi^2$	$pr > \chi^2$	Remarks
$\Delta WTI$	$\beta_{12,1}, \beta_{12,2}, \beta_{12,3} = 0$	3.76	0.288	TX drilling doesn't Granger cause oil price
	$\gamma_{13,1}, \gamma_{13,2}, \gamma_{13,3} = 0$	1.12	0.772	NM drilling doesn't Granger cause oil price
$\Delta TXW$	$\alpha_{21,1}, \alpha_{21,2}, \alpha_{21,3} = 0$	19.65	0.000	Oil price does Granger cause TX drilling
	$\gamma_{23,1}, \gamma_{23,2}, \gamma_{23,3} = 0$	3.24	0.356	NM drilling doesn't Granger cause TX drilling
$\Delta NMW$	$\alpha_{31,1}, \alpha_{31,2}, \alpha_{31,3} = 0$	31.76	0.000	Oil price does Granger cause NM drilling
	$\beta_{32,1}, \beta_{32,2}, \beta_{32,3} = 0$	12.29	0.007	TX drilling does Granger causes NM drilling

An important diagnostic test for the VECM, similar to almost all other empirical models, is to test if the residuals are white noise. The null hypothesis of the Lagrange Multiplier (LM) test is that there is no autocorrelation in the residuals. In other words, the null hypothesis states that the residuals exhibit white noise behavior. To test white noise condition on a vector of residuals,  $\hat{U}$  resulting from estimation (16), the LM test used. The test statistics for the LM test is shown in the following equation:

$$LM_s = (N - d - 0.5) \ln\left(\frac{|\hat{\Sigma}|}{|\hat{\Sigma}_s|}\right), \quad (21)$$

where  $N$  is the number of observations in the VECM,  $d$  is the number of coefficients estimated in the VECM,  $\hat{\Sigma}$  is the maximum likelihood of the variance-covariance matrix of residuals,  $\Sigma$ , and  $\hat{\Sigma}_s$  is the maximum likelihood of  $\Sigma$  resulting from the estimation. The large sample distribution

of the LM test converges to a  $\chi^2$  distribution, which is used to determine the intervals where the null hypothesis is rejected. The LM test statistics are calculated for the number of optimal lags,  $p = 3$ , and the results are presented in Table 3.8.

Table 3.8: LM test results for testing VECM residuals' white noise characteristics

Lag	$\chi^2$	$pr > \chi^2$	Remarks
1	11.703	0.231	The residuals are white noise
2	15.934	0.068	The residuals are white noise
3	16.285	0.061	The residuals are white noise

The degrees of freedom for the test statistics, denoted by  $d$  in

According to LM results shown in Table 3.8, the residuals pass the white noise diagnostics test (at 95% confidence).

## 5.6. Impulse response functions

The orthogonalized impulse-response functions resulting from the VECM (equations (18) to (20)) are presented in Figures 3.9 to 3.11 to. In each Figure, the impact that a unit increase in one variable has on the other two variables is presented. The size of the shock is one SD of the impulse variable and the response size is the percentage of the response variable.

Figure 3.9 shows that a positive shock in the oil price, results in a permanent increase in drilling activity in both Texas and New Mexico. However, Texas drilling activity shows an immediate positive response to price changes whereas New Mexico's immediate response to an oil price shock is negligible. An oil price shock has a larger impact on Texas drilling than on New Mexico drilling at all times, with the exception of the very first month after the oil price shock when the impacts are almost the same.



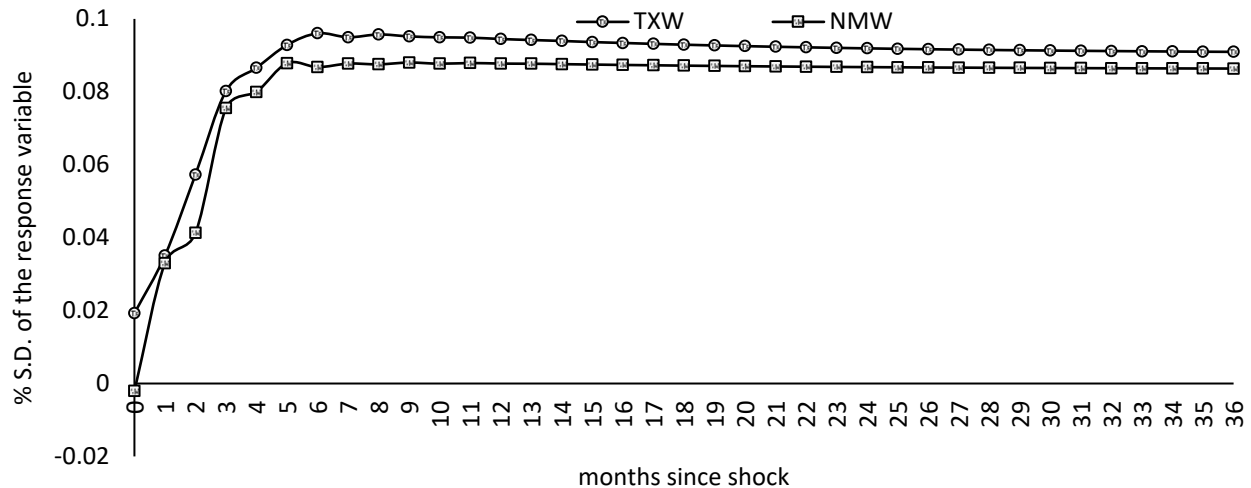


Figure 3.9: Response of TX and NM drilling to one SD unit shock to oil price

Figure 3.10 illustrates the effects of one SD change in Texas drilling on drilling in New Mexico and on oil prices. An increase in Texas drilling increased drilling activity in New Mexico immediately at about 1.5 percent. The impact increases throughout the first quarter after the shock and reaches a maximum of 4.5% at the third month. The New Mexico response to Texas drilling shock decreases after three months but, stabilizes at about 1.5 percent in the long run. According to Figure 3.10, an increase in Texas drilling results in a negligible change in oil prices and a negative 1.5% impact in the long run. The insignificant short-run impact of TX drilling on oil prices was validated by the Granger causality results. In the long run, it is possible that the higher drilling activity in Texas translates to higher oil production and ultimately lowers oil prices.

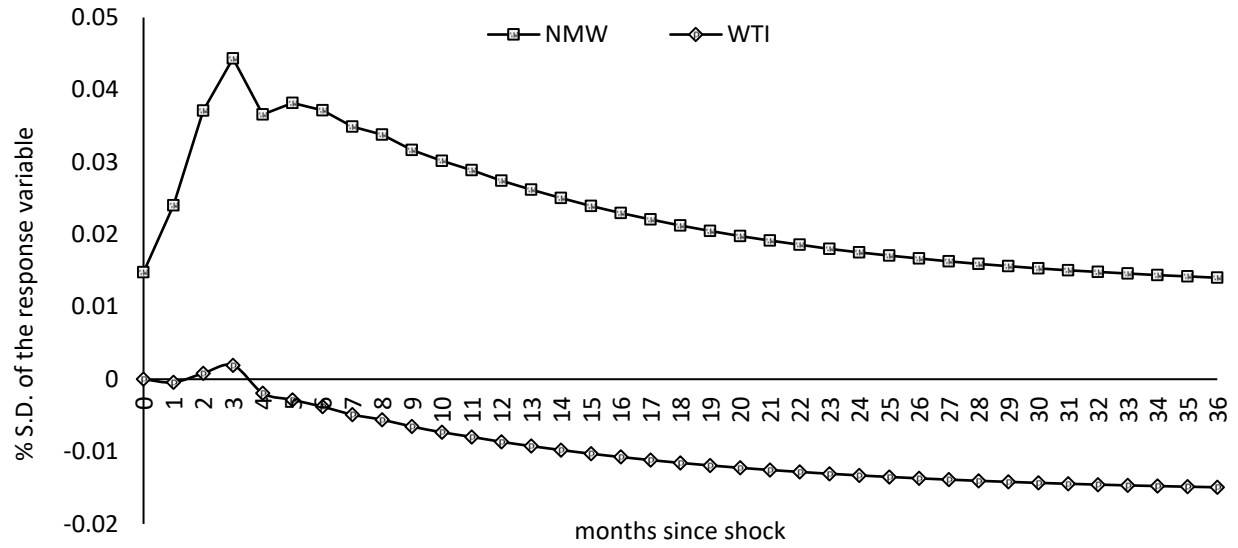


Figure 3.10: Response of oil price and NM drilling to one SD unit shock to TX drilling

Figure 3.11 shows changes in Texas drilling and in U.S. oil prices as a result of a one SD increase in New Mexico drilling activity.

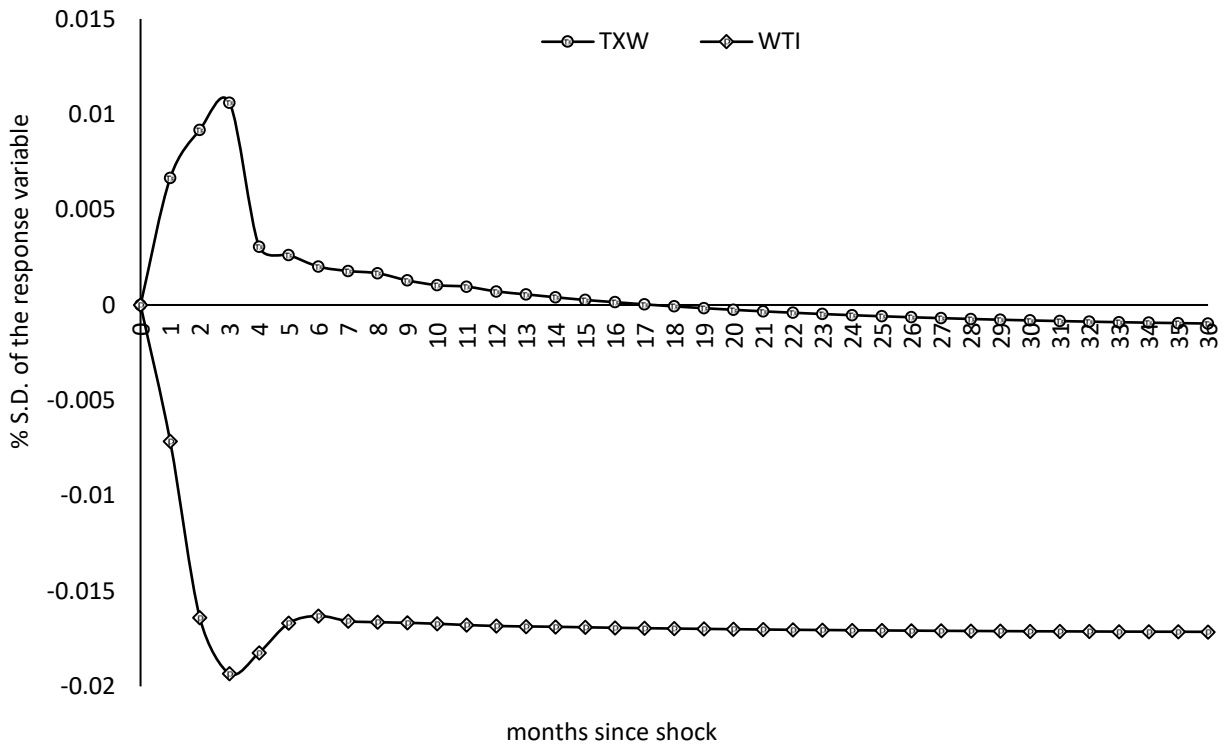


Figure 3.11: Response of oil price and TX drilling to one SD unit shock to NM drilling

According to Figure 3.11, there are small (less than 1%) changes in Texas drilling activity due to an increase in New Mexico drilling, but the Granger causality test results shows that this impact is not statistically significant. The impact of New Mexico drilling on Texas drilling is quite insignificant in the long run. Similar to the impulse-response function for a change in Texas drilling, (Figure 3.10), there is a long-run effect on oil prices as a result of a change in New Mexico drilling.

## **6. Conclusion**

A vector error correction model is utilized to estimate the interaction between three timeseries oil price, drilling activity in the Texas portion of the Permian Basin, and drilling activity in the New Mexico portion of the Permian Basin. It is shown that in both the short and the long run, an increase in the price of oil increases drilling activity in both Texas and New Mexico. However, the benefit to Texas from an oil price increase is shown to be larger than the benefit to New Mexico, in both the short and the long run. The relationship between Texas drilling and New Mexico drilling has one direction, in that, only Texas drilling impacts New Mexico drilling and not the other way around. Our results show that an increase in Texas drilling results in a boost in New Mexico drilling, and that the two portions of the Permian Basin do not necessarily act like substitutes.

In the short run, neither Texas nor New Mexico drilling impacts oil prices, but the impulse-response functions show that in the long-run, an increase in drilling in the Permian Basin could potentially negatively impact oil prices, which shows that the WTI is not entirely exogenous, at least in the long run.

An interesting finding is that the increase in prices impacted Texas drilling slightly higher than New Mexico drilling, which could be attributed to the higher drilling costs in New Mexico. Although the characteristics of the wells (total vertical depth and lateral length, among others) are similar in Texas and New Mexico, the regulatory environment surrounding state and federal lands in New Mexico could add to the drilling cost or result in delays in drilling. A future improvement would be to investigate the impact of land ownership on the drilling location choice by operator. This could be accomplished by further disaggregating New Mexico drilling into drilling on the private lands, and on public lands (state and federal).

## References

- Akaike, H. (1974). A new look at the statistical model identification. *IEEE Transactions on Automatic Control*, 19, pp. 716-723.
- Baumeister, C. and Kilian, L. (2014). Real-time analysis of oil price risks using forecast scenarios. *IMF Economic Review*, 62(1), pp. 119-145.
- Baumeister, C. and Kilian, L. (2016). Understanding the decline in the price of oil since June 2014. *Journal of the Association of Environmental and Resource Economists*, 3(1), pp. 131-158.
- Chermak, J.M., Crafton, J.W. and Patrick, R.H. (2012). Impacts of hydraulic fracturing and completion decisions on shale gas well productivity, SSRN Working Paper 2162486. Rochester, NY: Social Science Research Network. Accessed June 24, 2019. [https://papers.ssrn.com/sol3/papers.cfm?abstract\\_id=2162486](https://papers.ssrn.com/sol3/papers.cfm?abstract_id=2162486).
- Demas, A. and Gaswirth, S. (2018). USGS announces largest continuous oil assessment in Texas and New Mexico. Accessed January 30, 2019. <https://www.usgs.gov/news/usgs-announces-largest-continuous-oil-assessment-texas-and-new-mexico>.
- Dickey, D.A. (1976). Estimation and hypothesis testing for nonstationary time series., PhD. diss, Iowa State University, Ames.
- Dickey, D.A. and Fuller, W.A. (1979). Distribution of the estimators for autoregressive time series with a unit root. *Journal of the American Statistical Association*, 74(366a), pp. 427-431.
- Energy Information Administration (EIA). (2016). *Trends in U.S. oil and natural gas upstream costs*. Washington, DC: U.S. Department of Energy. Accessed May 30, 2019. <https://www.eia.gov/analysis/studies/drilling/pdf/upstream.pdf>
- Energy Information Administration (EIA). (2019, May). *Drilling productivity report For key tight oil and shale gas regions*. Accessed May 30, 2019. <https://www.eia.gov/petroleum/drilling/pdf/dpr-full.pdf>.
- Engle, R.F. and Granger, C.W.J. (1987). Co-integration and error correction: Representation, estimation, and testing. *Econometrica*, 55(2), pp. 251-276.
- Gaswirth, S.B., French, K.L., Pitman, J.K., Marra, K.R., Mercier, T.J., Leathers-Miller, H.M., Schenk, C.J., Tennyson, M.E., Woodall, C.A., Brownfield, M.E., Finn, T.M. and Le, P.A. (2018). *Assessment of undiscovered continuous oil and gas resources in the Wolfcamp Shale and Bone Spring Formation of the Delaware Basin, Permian Basin Province, New Mexico and Texas, 2018*, U.S. Geological Survey Fact Sheet 2018–3073. <https://doi.org/10.3133/fST10%0183073>.
- Guyaguler, B. and Horne, R.N. (2001). Uncertainty assessment of well placement optimization. Paper presented at the SPE Annual Technical Conference and Exhibition, Sep. 30-Oct. 3, 2001.

- New Orleans, LA. doi:10.2118/71625-MS.
- Granger, C. (1969). Investigating causal relations by econometric models and cross-spectral methods. *Econometrica*, 37(3), pp. 424-438. doi:10.2307/1912791.
- Hamilton, J.D. (1994). *Time series analysis. Economic Theory*. II, Princeton University Press, 625-630.
- Kellogg, R. (2014). The effect of uncertainty on investment: Evidence from Texas oil drilling. *American Economic Review*, 104(6), pp. 1698-1734.
- Luck, M. and Douglas, E. (2019). Big oil's investments in Permian pay off as earnings soar. *Houston Chronicle*, February 1. Accessed June 16, 2019. <https://www.houstonchronicle.com/business/article/Big-oil-s-investments-in-Permian-pay-off-as-13582121.php>.
- Mason, C.F. and Roberts, G. (2018). Price elasticity of supply and productivity: An analysis of natural gas wells in Wyoming. *The Energy Journal*, 9(1), pp. 79-100.
- McNally, R. (2017). *Crude volatility*. New York, NY: Columbia University Press. Kindle Edition.
- Newell, R.G., Prest, B.C. and Vissing, A. (2016). *Trophy hunting vs. manufacturing energy: The price-responsiveness of shale gas* (NBER Working Paper 22532). Cambridge, MA: National Bureau of Economic Research.
- Oh, W. and Lee, K. (2004). Causal relationship between energy consumption and GDP revisited: The case of Korea 1970–1999. *Energy Economics*, 26(1), pp. 51-59.
- Ridley, M. (2011). *The shale gas shock*. London, UK: Global Warming Policy Foundation.
- Ringlund, G.B., Rosendahl, K.E. and Skjerpen, T. (2008). Does oilrig activity react to oil price changes? An empirical investigation. *Energy Economics*, 30(2), pp. 371-396.
- Scheyder, E. (2017). Exxon doubling Permian Basin holdings in U.S. for up to \$6.6 billion. *Reuters*, January 17. Accessed May 30, 2019. <https://de.reuters.com/article/us-exxon-mobil-deals-permian-idUKKBN15120F>.
- Thomson, D.J. (1994). Jackknifing multiple-window spectra. In: *Proceedings of the IEEE International Conference on Acoustics, Speech and Signal Processing*, VI, pp. 73-76. New York, NY: Institute of Electrical and Electronics Engineers.
- Tysseling, J.C., Bjarke, J.A. and Anklam, R. (2019). *New Mexico: A comparative analysis: The oil &*

*gas industry's fiscal contribution to state governments*. Interim Comprehensive Report to New Mexico Tax Research Institute. Accessed July 20, 2019. [https://nm4ep.com/wp-content/uploads/2019/01/18-OAG-1654-NM-Report\\_PP7-compressed.pdf](https://nm4ep.com/wp-content/uploads/2019/01/18-OAG-1654-NM-Report_PP7-compressed.pdf).

Tsay, R.S. (2013). *Multivariate time series analysis: With R and financial applications*. Hoboken, NJ: John Wiley & Sons.





## **Chapter 4. A Dynamic and Integrated Simulation for Measuring Economic and Environmental Outcomes of a Long-Range Regional Transportation Plan with a Congestion Reduction Goal**

### **1. Introduction**

To test the impacts of urban policy, it is essential to capture externalities that arise from the fact that transportation and land-use systems are interconnected (Coppola et al. 2013). Accessibility is considered a normal good in the location choices made by households and firms (Waddell et al. 2003). On the other hand, utilization of the links in the transportation network depends on the land-use characteristics, namely population and the level of economic activity. Integrated land-use and travel demand models are analytical tools that account for the interoperation between the two urban subsystems.

Integrated land-use and travel demand models are utilized for forecasting the outcomes of the

long-range regional transportation plans (LRTPs). An LRTP, put together by a metropolitan planning organization (MPO), is a set of policies and projects designed to improve the quality of life for the urban residents. A comparative analysis by Nadafianshahamabadi and Rowangould (2017) showed that the majority of MPOs have congestion reduction goals in designing LRTPs. Mobility, defined as the ability of individuals to move freely from one location to another (Epple & Romer 1991), is a service provided by the transportation network that contributes to the household utility (Stanley et al. 2011) as well as to firms' productivity. As a result, road congestion, which is the main hindrance to mobility, is costly. For example, Schrank, Eisele, and Lomax (2012) estimated the cost of congestion in 498 urban areas in the U.S. at \$121 billion (2011' dollars), which included extra hours spent on traveling, more fuel consumed, longer delays in delivery of goods and services, and additional greenhouse gas (GHG) emissions, among others. Road capacity expansion (through investing in new lanes) is a natural solution adopted by many MPOs to reduce road congestion and enhance mobility. A difficulty with increasing the number of lanes, however, is the induced travel demand, also known as the fundamental law of road congestion (Duranton & Turner 2011). In other words, increasing the number of road lanes ("lane kilometers") brings about new and latent travel demand and could ultimately result in new congestion, defeating the original purpose of the capacity expansion.

The question of whether or not induced and latent travel demand takes place as a result of road capacity expansion is empirically studied in many cities and regions (e.g., Goodwin 1996; Fulton et al. 2000; Prakash, Oliver, & Balcombe 2001; Cervero 2003; Duranton & Turner 2011). However, less attention is paid to the source and mechanisms of the induced travel demand formation. One noteworthy exception is Cervero (2003) who used path analysis to decompose the

mechanisms of induced demand formation. Cervero (2003) showed that the short-term travel behavior changes and the long-term land-use changes induced by an increase in road lanes are the main sources of congestion rebound effect. He called for long-range, robust, and sophisticated forecasting models that allow evaluation of these unintended consequences of the LRTPs.

This study is especially focused on the dynamic integration of land-use and travel demand models in evaluating the long-term outcomes and externalities of urban policies; in particular, road capacity expansion policies. We argue that to capture the dynamically related location and movement choices made by individuals and firms, the interaction of land-use and travel demand models has to be at an appropriate frequency. We test this hypothesis by forecasting the outcomes of adding new lanes to parts of the transportation network under two integration frequencies: annual integration and first-and-last year (of the planning horizon) integration. In doing this, we pursue two objectives:

- to measure the impacts of a road expansion policy in the long run, using an analytical, integrated land-use and travel demand model, and
- to compare the results of the high-frequency integration with the results from a conventional first-and-last year analysis and to highlight the risk of bias associated with the latter approach.

## **2. Background**

### **2.1. Long Range Regional Transportation plan (LRTP)**

The Federal-Aid Highway Act of 1962 designated metropolitan area organizations (MPOs) for

planning urban areas with population of 50,000 and higher. In 2012, Moving Ahead for Progress in the 21st Century (MAP21) further expanded the responsibilities of MPOs by adding a requirement for a long-range transportation plan (LRTP) that spans 20 years or more. The Fixing America's Surface Transportation Act (FAST Act) of 2015, required MPOs to pursue eight planning goals in their LRTPs:

- Supporting economic vitality,
- Increasing the safety of the transportation system,
- Increasing the security of the transportation system,
- Increasing accessibility and mobility,
- Protecting and enhancing the environment,
- Enhancing the connectivity of the transportation system, and
- Preserving the existing transportation system

Due to the long-term scope of the LRTPs, forecast models are required to evaluate the LRTPs and to compare different scenarios (Handy 2008). Evaluation of an LRTP is based on the goals and performance metrics set by the proposing MPO. MPOs carry out these long-term goals through a transportation improvement program (TIP), a list of projects prioritized by implementation year through the LRTP's planning horizon. The success of an LRTP depends on the forecasting of the future implications of present decisions (Meyer & Miller, 2001).

## 2.2. Congestion relief and induced demand

Road congestion relief has been a high-priority goal for many MPOs (Nadafianshahamabadi & Rowangould 2017). According to a 2017 U.S. Department of Transportation travel survey, an

average American traveled 56.62 minutes per day in a passenger car, which is 6.7 minutes less than in 2001 (U.S. Department of Transportation 2017); this reduction in travel time could be partly due to the MPOs efforts to increase mobility and accessibility.

In order to relieve traffic congestion on a road, it is a natural solution for many MPOs to expand road capacity by increasing the number of lanes. However, a long-standing debate in this regard is about whether or not increasing the supply of lanes leads to sustainably resolving the congestion problem. A seminal study by Hansen (1995) posed the question “*Do new highways generate traffic?*”. The market clearance condition, shown in Figure , suggests that in the long-run adding to the supply of lanes, a right-side shift in the supply curve (from  $S$  to  $S'$ ), results in an increase in the number of vehicle miles traveled (VMT),  $m$  in Figure 4.1.

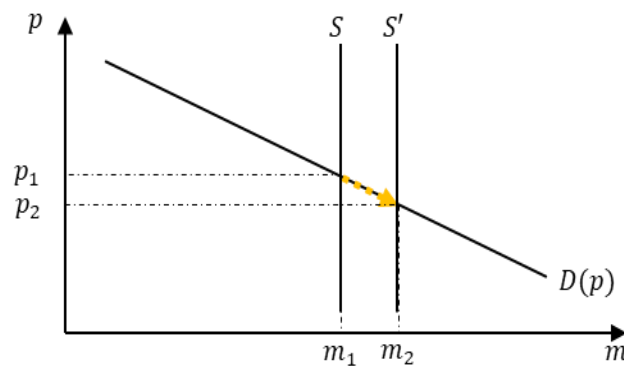


Figure 4.1: Market for vehicle miles traveled (VMT)

In other words, by expanding a road’s capacity by adding more lanes, the quantity demanded, VMT, will increase over time to the point that new congestion could emerge. This dynamic behavior, also referred to as the fundamental law of road congestion, is empirically studied in the literature. Duranton and Turner (2011) estimated the relationship between the lane kilometers of the road provided and VMT across the United States; they showed that increasing

the number of highway lanes results in a rapid increase in the VMT on highways and a less immediate increase in the VMT on other road types. They suggested that the increase in VMT comes from current residents, in addition to the VMT for commercial purposes as well as migration.

Cervero and Hansen (2002) tested a reciprocal relationship between road investment and VMT in urban areas of California. Through a simultaneous three stage least squares (3SLS) estimation model, Cervero and Hansen showed that road investment results in an increase in travel demand while an increase in travel demand calls for more road investment. They estimated the immediate investment elasticity of VMT at 0.59 and an intermediate (5-year) elasticity of 0.79. Hymel, Small, and Van Dender (2010) used cross-sectional time series data at the level of U.S. states for the 1966-2004 period. They found much smaller elasticity measure, 0.019 short-run elasticity, and 0.094 long-run elasticity of VMT to the road-miles per state.

Cervero (2003) adopted a systems-based approach for evaluating the relationship between the supply of road lanes and the VMT on selected freeways of California. Through a path analysis, Cervero (2003) decomposed the causal effect of road enhancement on VMT into immediate and long-run impacts. The results suggested that an increase in the number of road lanes almost immediately result in an increase in road speed, which subsequently induces changes in travel behavior such as latent trips and route diversion. Furthermore, the study showed that within a five to six-year period, the provision of additional road lanes results in land-use changes that ultimately attract new travel demand. Cervero (2003) also emphasized that the immediate travel behavior and the long-term land-use changes induced by increasing the supply of road lanes should be incorporated into the evaluation of LRTPs.

### 2.3. Interactive land-use and travel demand modeling

The transportation network serves households' and firms by providing mobility. Mobility is also an input to the households and firms' location choice function. Failing to account for the feedback between the land-use and travel demand models could result in potential misspecification of the outcomes of urban policy scenarios. Coppola et al. (2013) discussed the evolution of the models that account for the simultaneous modeling of land-use and travel scenarios.

The spatial scope and the socioeconomic activities in the integrated land-use and travel demand modeling can be disaggregated at various scales. In recent years, activity-based travel demand models that study travel decisions at the individual level have become increasingly popular (e.g. Katoshevski et al. 2015; Childress et al. 2015; Yasmin, Morency and Roorda 2017; Tayarani & Rowangould 2019, to name a few). In contrast, the temporal resolution of the interaction between land-use and travel demand models has received less attention in the literature. Both land-use and transportation systems change over time. For example, adding a faster lane between two locations could attract new households and/or businesses to either location. On the other hand, when the population increases in an area, there is higher travel demand, which could result in higher utilization of the lanes and consequently reduce the speed of traffic.

Similar to the performance analysis of other complex systems, different temporal resolution adopted in the forecasting procedure result in a trade-off between the accuracy of the results and the complexity and run-time of the model. The conventional LRTP evaluation adopted by MPOs is to measure the performance outcome of the LRTP at a low temporal resolution. This approach, referred to as "endpoint" simulation allows the exchange between the land-use and

travel demand model outcomes only at the beginning and the final years of the planning horizon (Tayarani et al. 2018). This low temporal resolution (endpoint modeling) approach could fail to capture the dynamics of the integrated system of land-use and travel demand models. It is also prone to generating biased results in estimating the outcomes of the TIP, and consequently the LRTP.

In comparison, a high temporal resolution approach allows the exchange between the inputs and outputs of the land-use and travel demand models during each year of the LRTP horizon. Tayarani et al. (2018) showed that compared to the high-resolution modeling procedure, the endpoint model overestimated the GHG outcomes of Albuquerque, New Mexico's LRTP. We propose the annually integrated land-use travel demand (ALT) approach for evaluating the outcomes of a road capacity expansion policy. To tease out the economic and environmental impacts resulting from a road capacity expansion project, we compare two LRTPs an actual LRTP proposed for Albuquerque with a TIP spanning 2012 to 2040 and a modified LRTP that includes the original LRTP as well as a hypothetical road capacity expansion project on one of the Rio Grande river overpasses. In addition to evaluating the impacts of this road capacity expansion using the proposed ALT approach, we evaluate the impacts using the conventional endpoint approach and compare the path of outcomes generated by the two approaches.

### **3. Theoretical model**

An annually integrated land-use travel demand (ALT) model is proposed. The underlying theory is that to evaluate the outcomes of an LRTP, land-use induced travel demand changes and travel-time induced land-use changes should be accounted for simultaneously:



$$\begin{cases} x_t = f_1(y_{t-1}, x_{t-1}, E_t) \\ y_t = f_2(y_{t-1}, x_{t-1}, E_t) \end{cases} \quad (1)$$

where  $x_t$  is the travel scheme assigned to the transportation network,  $y_t$  is the land-use assignment across the planning landscape during year ( $t$ ),  $E_t$  is a vector of exogenous variables (such as population, income, auto ownership, etc.), and  $f_1$  and  $f_2$  are complex nonlinear functions. In order to evaluate the performance of a given LRTP, the performance metrics are calculated for each year:

$$Z_t = g(x_t, y_t, E_t). \quad (2)$$

$Z(t)$  is a vector of economic and environmental variables including vehicle miles traveled (VMT), traffic speed, percentage of the congested roads in the transportation network, fuel consumption for transportation, and greenhouse gas (GHG) emissions.

The travel demand model ( $f_1$ ) is determined through network analyses described in section 3.1 and the land-use model ( $f_2$ ) is an agent-based model described in section 3.2.

### 3.1. Travel demand model

The travel demand model explained in the following sections is a four-step travel demand model adopted from Systra Mobility (2010).

#### Trip generation

A trip generation model estimates the number of person-trips generated from and to a traffic analysis zone (TAZ). The number of trips generated by households is categorized by trip purpose (home-based work, home-based shopping, non-home-based work, etc.). For each trip purpose, the trip production rate, from a TAZ, is estimated based on household size, household income,

and number of workers in a household as well as the households' automobile ownership. Truck trip production rates are assigned based on the TAZ's employment composition (basic, retail, and service). Similarly, trip attraction rates are assigned to TAZs based on the trip purpose, number of households, employment type, and school enrollment.

### Trip distribution

Trip distribution connects trips that are produced at a TAZ to TAZs that attract trips. The gravity-based<sup>26</sup> trip distribution model is adopted in this study. Trip distribution between zones  $i$  and  $j$  is formulated as follows:

$$\text{Trip}_{ij} = \frac{Pr_i \times At_j \times f_{ij} \times k_{ij}}{\sum_i Pr_i \times At_j \times f_{ij} \times k_{ij}}, \quad (3)$$

where  $\text{Trip}_{ij}$  is the number of trips exchanged between source zone  $i$  and destination zone  $j$  (including  $i$  itself),  $Pr_i$  is the number of trips produced at zone  $i$ ,  $At_j$  is the number of trips attracted by zone  $j$ ,  $f_{ij}$  is the friction factor between zones  $i$  and  $j$ , and  $k_{ij}$  is an adjustment factor.  $f_{ij}$  is the utility (or log-sum) of the trip between zones  $i$  and  $j$ , which is a function of the travel impedance defined by travel time and travel cost, for each travel mode, between the two zones.

### Mode choice

The mode choice model determines the travel mode for each trip from zone  $i$  to zone  $j$ . Eight

---

<sup>26</sup> Gravitational force between masses  $m_1$  and  $m_2$  is related to the magnitude of the masses and the inverse of the distance between the two.

modes of travel are of interest in this study, including transit with drive access (kiss-and-ride and park and ride), transit with walk access (to the premium transit route, and to the local route), Automobile (drive-alone, 2-person share-ride, and share-ride between three people and more), and non-motorized travel. The mode of travel for each trip is assigned based on a random utility model that is calibrated for the study area based on independent variables including travel time, operating cost, parking cost, walk time, wait time, drive access time, etc.

#### *Time of day model*

To estimate the hourly volume of traffic, trips are assigned to a time of the day, based on the trip purpose.

#### *Highway and public transport assignment*

The highway assignment model allocates vehicle trips to the highway network, whereas transit trips are allocated to the public transit network.

### 3.2. Land-use model

The land-use model adopted in this study is an agent-based microsimulation model provided in a simulation software called UrbanSim (Waddell et al. 2003). UrbanSim is a high-resolution simulation of land development and has been successfully utilized to analyze different policy scenarios in Austin, Texas; Eugene Oregon; Detroit, Michigan; Salt Lake City, Utah; San Francisco, California; and Seattle, Washington (Kakaraparthi & Kockelman 2010). Three types of agents and their decisions are explained, namely households, businesses, and developers. The following formula and model setting are adapted from Waddell et al. (2003).

### Accessibility

In an urban economics context, accessibility is considered a normal good; households and developers prefer locations with high accessibility. Accessibility of location  $i$ ,  $A_i$  is defined in equation (4).

$$A_i = \sum_{j=1}^J D_j e^{L_{aij}}, \quad (4)$$

where  $D_j$  is the activity level in location  $j$ , and  $L_{aij}$  is the composite utility to households with vehicle ownership level  $a$  from location  $i$  to location  $j$ . Accessibility index is an input to the household and business location choice sub-models which will be explained in this section.

### Economic transition

Economic transition is defined at the sector level, changes in the number of employments  $J$ , in sector  $s$  in year  $t$  are defined exogenously:

$$\Delta J_{st} = C_{st} - |J_{s(t-1)}|, \quad (5)$$

where  $C_{st}$  is the exogenous total employment in sector  $s$  during year  $t$ .

### Demographic transition

Similar to equation (5); changes in the household population are defined based on an exogenous predictor.

### Mobility

Employment mobility is defined as the number of jobs in sector  $s$  that move during year  $t$ , and is denoted by  $M_{st}$ :

$$M_{st} = \{j \in J_{st} | P(j, t)\}, \quad (6)$$

where  $P(j, t)$  is the probability of  $j$  jobs moving during year  $t$ , generated by a Monte Carlo simulation process. Household mobility is modeled similar to equation (6).

### Location choice

Employers choose a location for reloacted jobs or new jobs from the available job locations. Selection of a location as an employment relocation/allocation spot is based on a log-sum or expected utility model<sup>27</sup> that uses real estate prices, land-use mix, business and housing density, access to population, travel time to business centers and central infrastructure like airports, proximity to highways, and local agglomeration within and between sectors. Similar to employment location choice, the probability that a household chooses a location, is based on an expected utility model where utility is a function of independent variables including housing prices, housing density, land-use mix, housing age, job accessibility, and travel time to business centers and critical infrastructure, as well as neighborhood characteristics.

### Real estate development

Real estate developers choose to implement new construction or to intensify or convert existing buildings. The rate of new construction, intensification, or conversion projects can be defined using historical data (year built) or by the modeler.

### Land price

---

<sup>27</sup>  $P(y_{it}) = \frac{e^{\beta_i' X_t}}{\sum_j e^{\beta_j' X_t}}$ , where  $X$  is the vector of independent variables determining utility.

Land prices are determined using a hedonic price method (Waddell et al. 2003). To estimate the property value in a competitive market, the hedonic price method in UrbanSim uses independent variables such as land-use mix, the density of development, proximity to highways and other infrastructure, zoning constraints, and neighborhood characteristics. The value of the constant in the hedonic regression model is adjusted based on the position of the current and structural vacancy rate, as shown in the following:

$$P_{ilt} = \alpha + \delta \left( \frac{V_i^s - V_{it}^c}{V_i^s} \right) + \beta X_{ilt}, \quad (7)$$

where  $P_{ilt}$  is the price of land type  $i$ , at location  $l$ , and year  $t$ ;  $V_{it}^c$  is the current vacancy rate in year  $t$ ,  $V_i^s$  is the long-term structural vacancy rate; and  $X_{ilt}$  is a vector of independent variables enumerated in this section.

#### 4. The study area

The study area for this chapter is Albuquerque, New Mexico. Albuquerque is the largest metropolitan area in the state of New Mexico. The University of New Mexico (UNM), the largest academic institution in the state is located in Albuquerque. Furthermore, Sandia National Laboratories, UNM hospitals, and Kirtland Air Force Base, among others, are Albuquerque-based large employers in the state. Albuquerque's MPO is the Mid-Region Council of Governments (MRCOG). Albuquerque LRTP, *Futures 2040 Metropolitan Transportation Plan*, was developed in 2015 by MRCOG (2015), with 2012 set as the baseline year. The goals of the Albuquerque LRTP are to increase mobility, economic vitality, environmental resilience and place activity. The total cost of the proposed projects in the Albuquerque LRTP-related transportation improvement program (TIP) for the 2012-2040 period is estimated at \$6.29 billion, and the total cost of capacity

expansion projects is estimated at \$2.19 billion.

Interstates 25 (north/ south) and 40(east/west) divide Albuquerque into four quarters. On the northwest quarter of Albuquerque, three river overpass roads, namely Alameda Blvd., Paseo del Norte, and Montañó Blvd., connect the relatively recently developed west side of Albuquerque and the city of Rio Rancho to the businesses and residential areas of the rest of Albuquerque. Among the three river overpasses, we focus on the Paseo del Norte, as shown in Figure 4.2. Paseo del Norte was ranked the 13<sup>th</sup> most congested road in Albuquerque's LRTP, after Alameda Blvd. (1<sup>st</sup>) and Montañó Blvd. (6<sup>th</sup>). Because of its low congestion ranking, the Albuquerque LRTP does not propose any capacity expansion projects for the highlighted area in the LRTP.

To test the changes in performance metrics that might be caused by adding additional lanes to the transportation networks, we derive a new LRTP from the original LRTP proposed for Albuquerque. The only difference between the derived LRTP and the original LRTP is a hypothetical capacity expansion on a portion of the Paseo del Norte, as shown in Figure 4.2. The hypothetical policy proposal is to double the number of lanes on the selected section of the road.

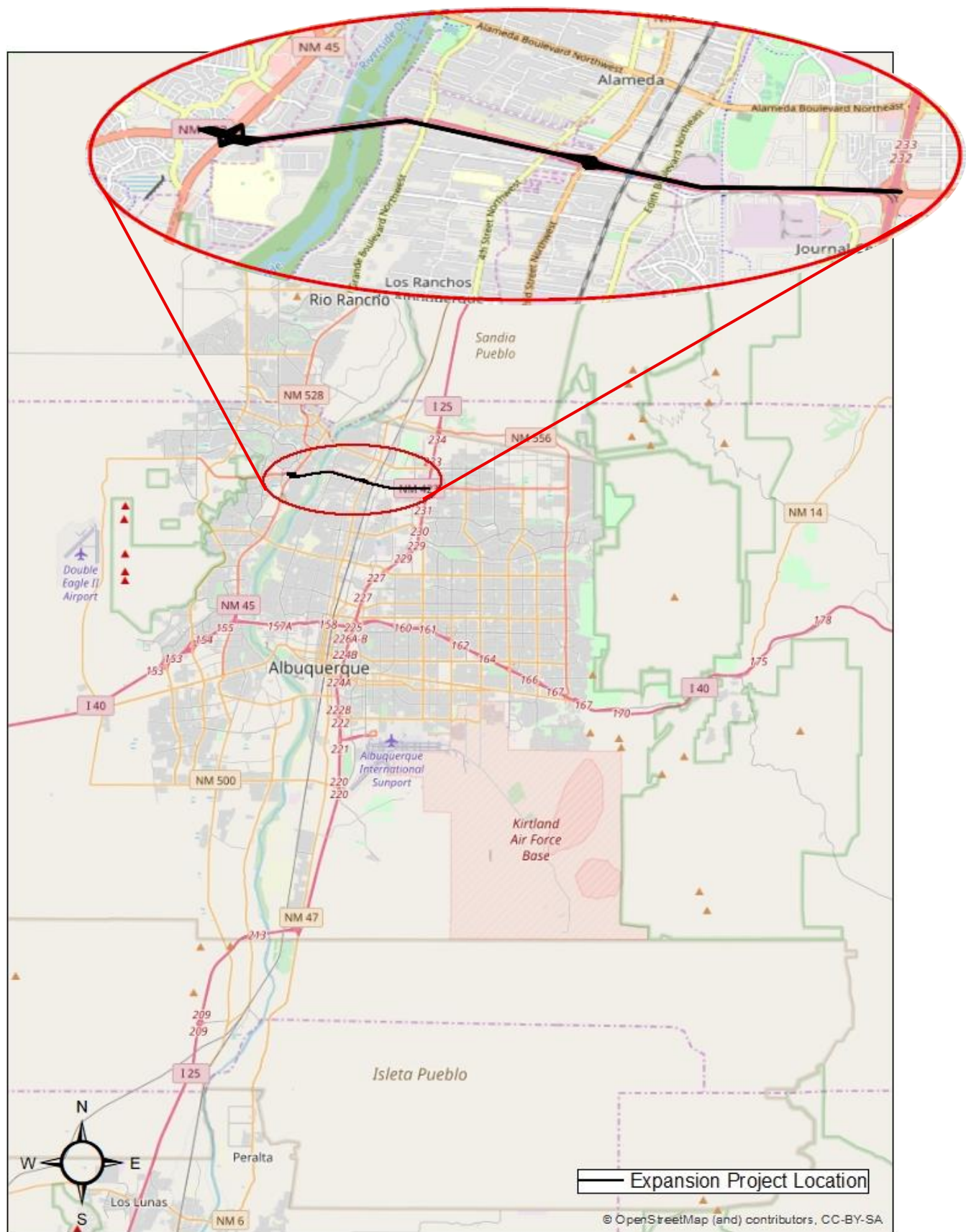


Figure 4.2: Location map of the capacity expansion project



## 5. Model architecture and data

The proposed ALT approach was originally developed at the transportation laboratory at the department of civil, construction and environmental engineering, University of New Mexico. This model has been used to test the impact of the adoption of autonomous vehicles on transportation network congestion and air quality (Nadafianshahamabadi & Rowangould 2017), and on the cumulative multi-criteria impacts of an LRTP in the Albuquerque metropolitan area (Tayarani et al. 2018). The model architecture for measuring the performance of an LRTP using ALT is presented in Figure 4.3. Travel demand and land-use modules are explained in sections 3.1, and 3.2, respectively. External values that impact both land-use and travel demand are the exogenous demographic variables and the urban policy instruments, as listed in Figure 4.3. The policy investigated in this study is the addition of new lanes to part of the transportation network.

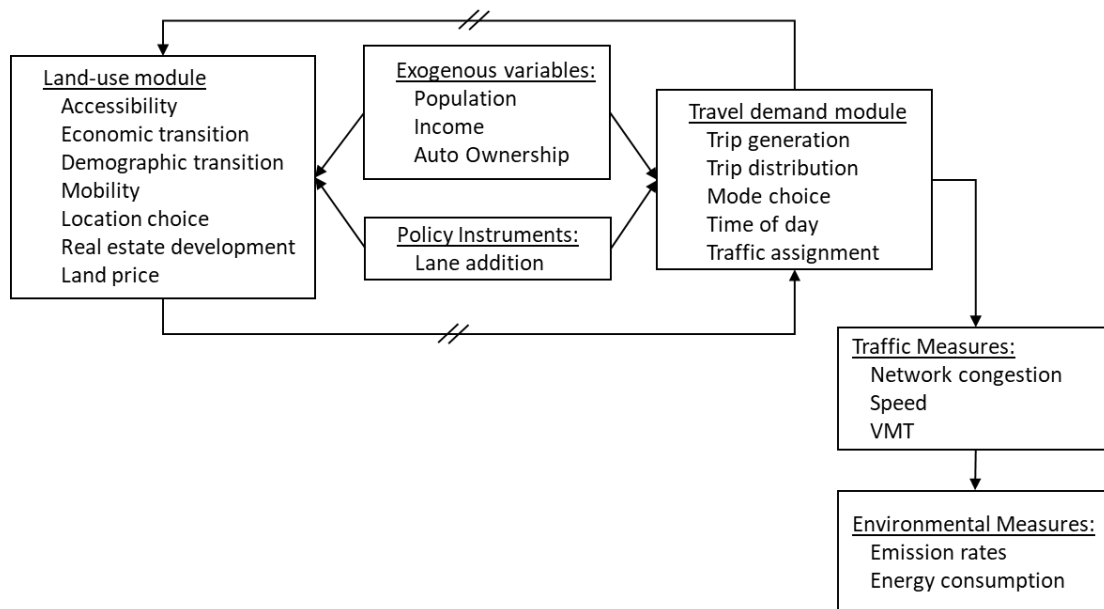


Figure 4.3: Proposed model architecture

For each year in the planning period of the LRTP (2012-2040), the two modules, travel demand,

and land-use exchange information. The reciprocation starts from the land-use module. The levels of socioeconomic activity (population, number of workers, automobile ownership, etc.) taking place in each traffic analysis zone (TAZ) are derived from the land-use module for the year 2012, and the results serve as input to the travel demand module. The travel demand module uses these socioeconomic inputs from the land-use module to update the transportation network's traffic data for 2012. Based on the given socioeconomic data, the travel demand module estimates trip generation, trip distribution, time of the day and highway and public transport trip assignment and it determines the traffic load, traffic speed, and other traffic variables for each link in the transportation network. Travel times and costs generated by the travel demand module for 2012 are then used in the land-use module to generate the results for 2013, and so on. The “//” symbol on the links between the travel demand and land-use modules presents the serial relationship between the two.

The land-use module is simulated in UrbanSim software developed by Waddell et al. (2003). For Albuquerque, MRCOG has calibrated and adjusted coefficients and rates used in UrbanSim. The travel demand module is simulated in Cube software, a product of Citilabs Inc. The travel demand model is also adjusted and calibrated for Albuquerque by MRCOG. Census data and traffic counts for 2012 are utilized for model calibration. Detailed information about the calibration and validation of the model components can be found in the Systra Mobility report(2010).

In addition to traffic performance metrics (traffic load, speed, etc.), environmental outcomes including energy consumption and GHG emissions are also estimated using the motor vehicle emission simulator (MOVES) developed by the Environmental Protection Agency (EPA) along with

the traffic speed resulted from the travel demand model. MOVES' inputs are the geographic location, year, month, day, and time of the day. MOVES outputs are lookup tables that list the energy consumption rate, and pollutant emission rates for each road type, traffic speed, and time of the day. The estimated traffic speed and the given road type are matched with the MOVES database to retrieve the pollutants' emission rates and fuel consumption under different policy scenarios.

## **6. Simulation results and discussion**

The ALT approach was utilized to evaluate Albuquerque's original and derived LRTPs and the results are compared in section 6.1. In order to compare and contrast the outcomes of the proposed ALT with the static endpoint model, the performance metrics of the original and derived LRTPs are illustrated and compared in section 6.2.

### **6.1. Road expansion outcomes**

Figures 4.4 to 4.9 illustrate the changes in the morning peak-hour traffic load that result from the addition of the hypothetical road expansion project. Maps showing the spatial distribution of the changes were developed for every year from 2012 to 2040, but the six maps associated with years 2015, 2020, 2025, 2030, 2035, and 2040 (Figures 4.4 to 4.9) provide a time series of these changes. An increase in the traffic load is shown in red and a decrease in the traffic load is shown in blue. According to Figures 4.4 to 4.9, a change in the capacity of a section of a road changes the traffic load throughout the network. Except for the year 2025, when the scheme of changes seems chaotic, the pattern is quite consistent throughout other years, with similar signs of change but higher intensities towards 2040.

One of the important changes shown in all the Figures, except for Figure 4.6, is that both the Alameda and the Montañito river overpasses experience a decrease in the morning peak volume, but the traffic load on the Paseo del Norte river overpass increases. It is possible that the river crossings are substitutes for one another, and due to a higher supply of lanes and consequently lower travel costs created by the hypothetical capacity expansion on Paseo del Norte, a route diversion takes place.

Furthermore, the traffic volume on the roads in the city of Rio Rancho, located in the far northwest of Albuquerque, increases overall and there is a similar increase in the traffic volume on the east side of Interstate 25. Since the increase in the volume intensifies over time, one possible explanation is that long-term land-use changes resulting from the hypothetical expansion project create new travel demand.

Figures 4.10 to 4.15 illustrate the changes in the morning peak-hour traffic speed for every fifth year starting with 2015 and ending with 2040. Unlike the changes in traffic load, which are realized throughout the transportation network, changes in traffic speed are specific to certain links in the network. Particularly, speed is shown as increasing in all the river overpasses, including north and south of Interstate 40. This increase in speed is consistent with the changes in the traffic load. While a decrease in traffic load on river overpasses other than Paseo del Norte results in the higher traffic speed, the increased traffic load on Paseo del Norte does not result in lower speeds due to the additional capacity.

Figures 4.16 to 4.21 show the absolute changes in population per TAZ. It is noteworthy that total population is an exogenous variable and doesn't depend on the network characteristics.

Population growth rate comes from Census estimates and the largest difference between annual populations for the two scenarios (trend and modified network) is 263 persons in 2029. In other words, changes in the zonal populations shown in Figures 4.16 to 4.21 are, almost completely, due to movements and different migration rates resulted from changes in the network.

According to the time series of changes in zonal populations, land-use changes are not significant in the first 10 years, but changes become stronger towards the last decade of the planning horizon. The proposed capacity expansion on the Paseo del Norte river overpass results in changes in land-use across the study area. Some of these changes could be attributed to the random variables in the model, but some patterns are consistent through time, which is unlikely to be random. For example, the net population change in the west of the Rio Grande is positive in all figures. This could be the result of a higher mobility provided to the west side residents, making westside a desirable choice for relocation. Another interesting observation is that on the east side of the river, the population is showing a slight inward movement; that is, on the east side of Interstate 20, and across the far east of the city boundary population has reduced whereas the inner east area experiences an increase in population.



Figure 4.4: Percentage change in morning peak-hour traffic load between the original and derived LRTPs for year 2015

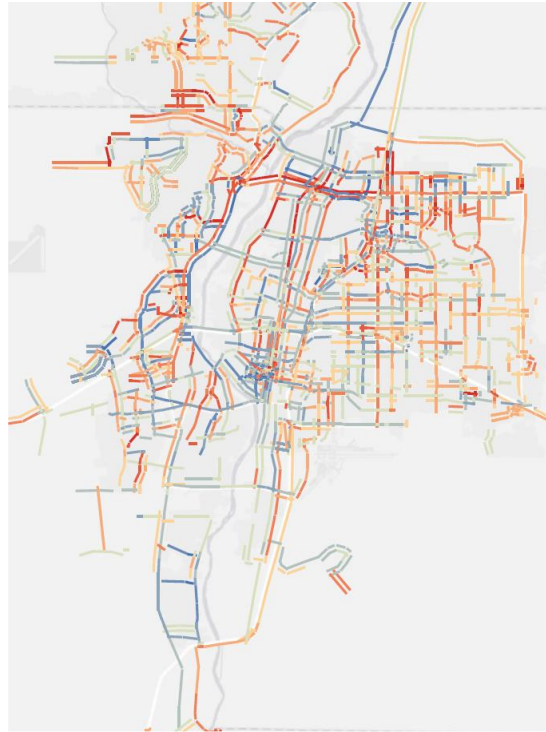
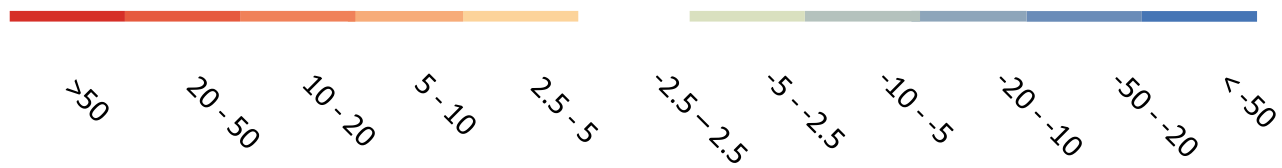


Figure 4.5: Percentage change in morning peak-hour traffic load between the original and derived LRTPs for year 2020



Figure 4.6: Percentage change in morning peak-hour traffic load between the original and derived LRTPs for year 2025



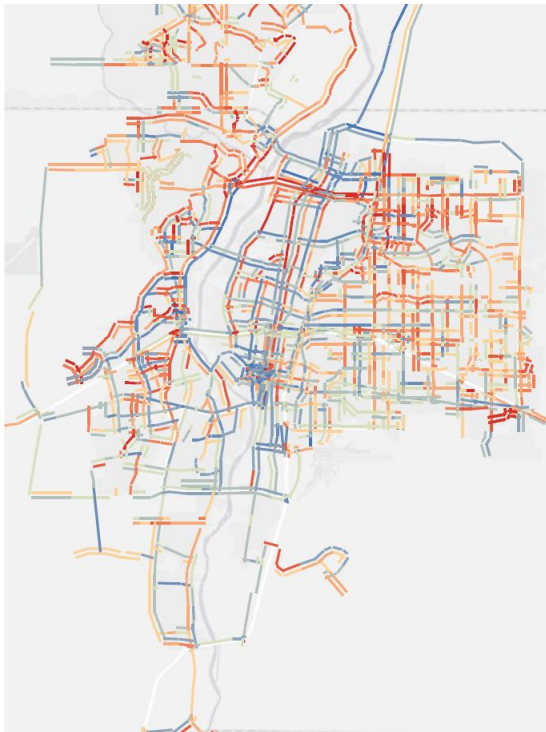


Figure 4.7: Percentage change in morning peak-hour traffic load between the original and derived LRTPs for year 2030

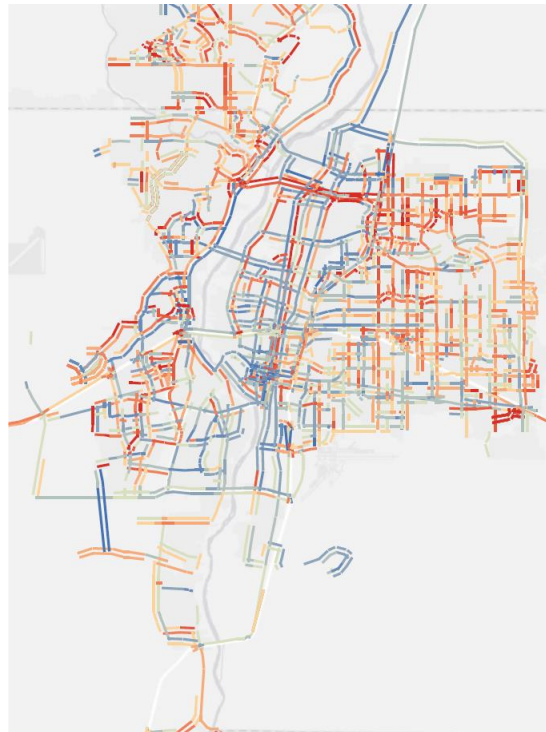


Figure 4.8: Percentage change in morning peak-hour traffic load between the original and derived LRTPs for year 2035

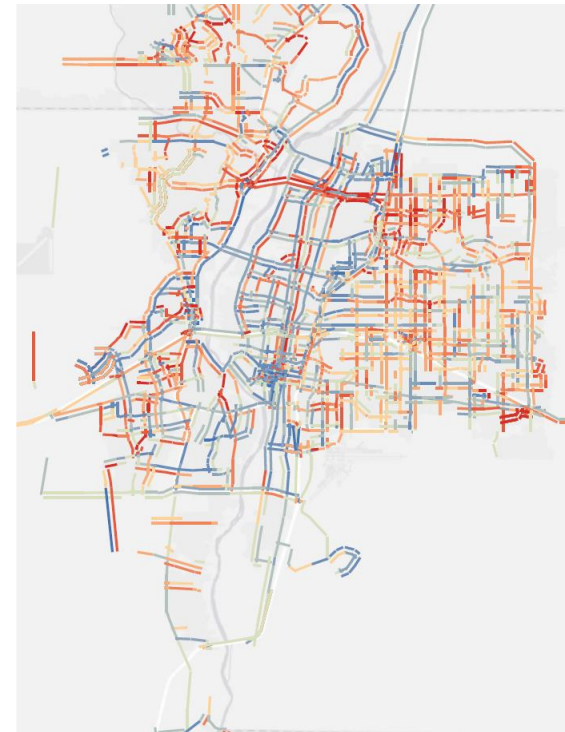
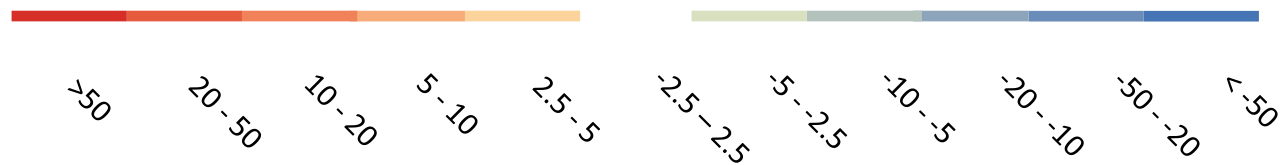


Figure 4.9: Percentage change in morning peak-hour traffic load between the original and derived LRTPs for year 2040



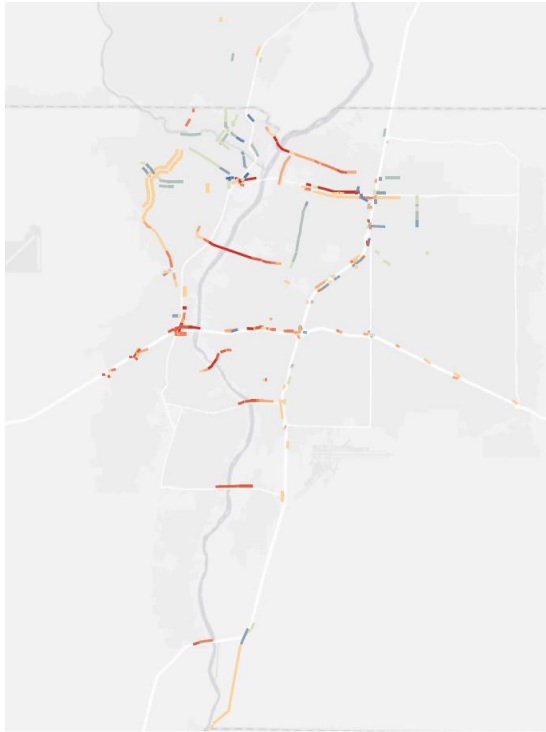


Figure 4.10: Percentage change in morning peak-hour traffic speed between the original and derived LRTPs for year 2015



Figure 4.11: Percentage change in morning peak-hour traffic speed between the original and derived LRTPs for year 2020



Figure 4.12: Percentage change in morning peak-hour traffic speed between the original and derived LRTPs for year 2025

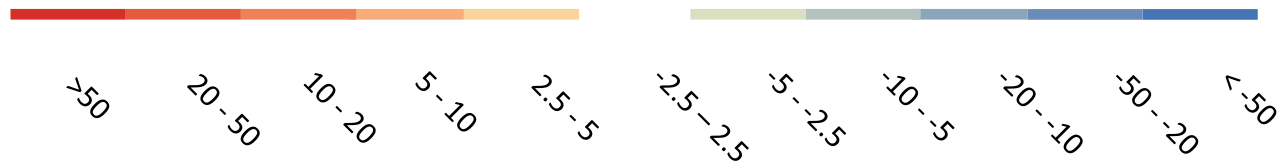






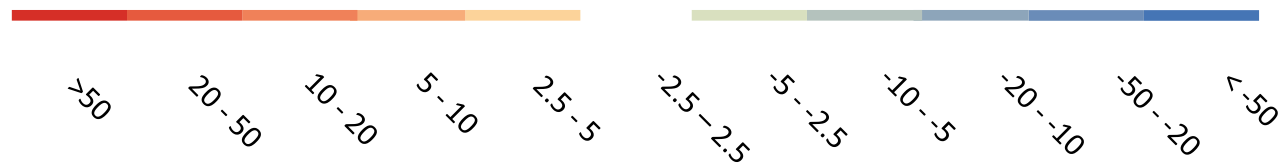
Figure 4.13: Percentage change in morning peak-hour traffic speed between the original and derived L RTPs for year 2030



Figure 4.14: Percentage change in morning peak-hour traffic speed between the original and derived L RTPs for year 2035



Figure 4.15: Percentage change in morning peak-hour traffic speed between the original and derived L RTPs for year 2040



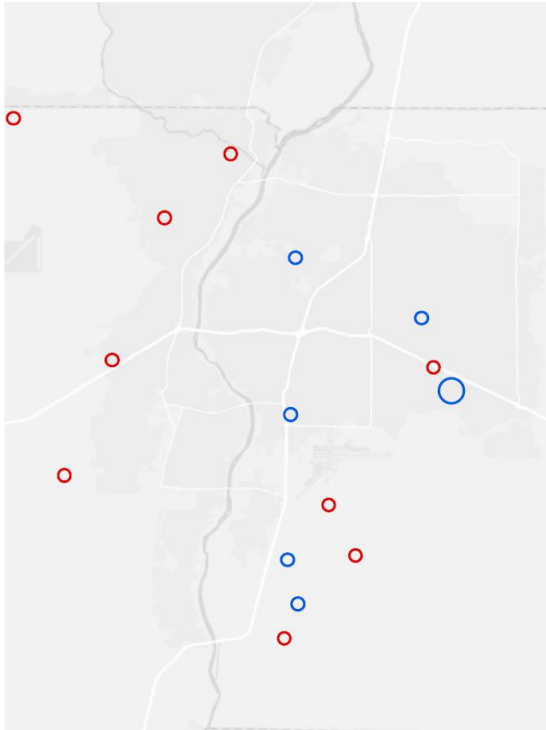


Figure 4.16: Absolute change in population between the original and derived LRTPs for year 2015

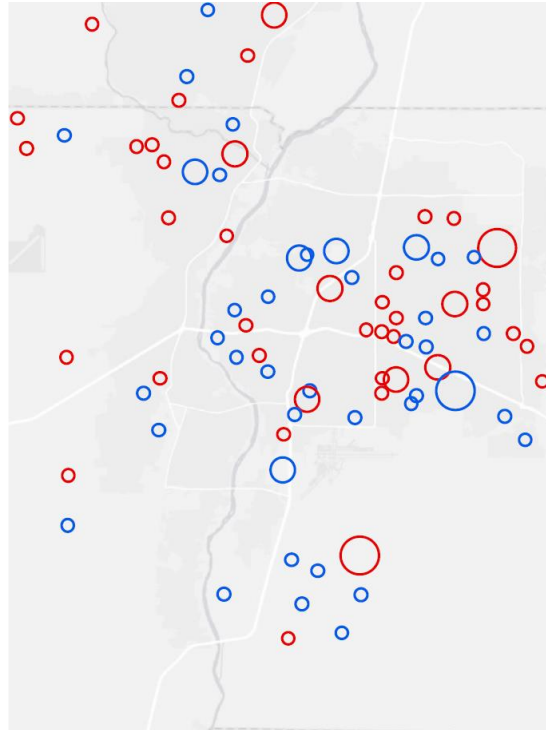


Figure 4.17: Absolute change in population between the original and derived LRTPs for year 2020

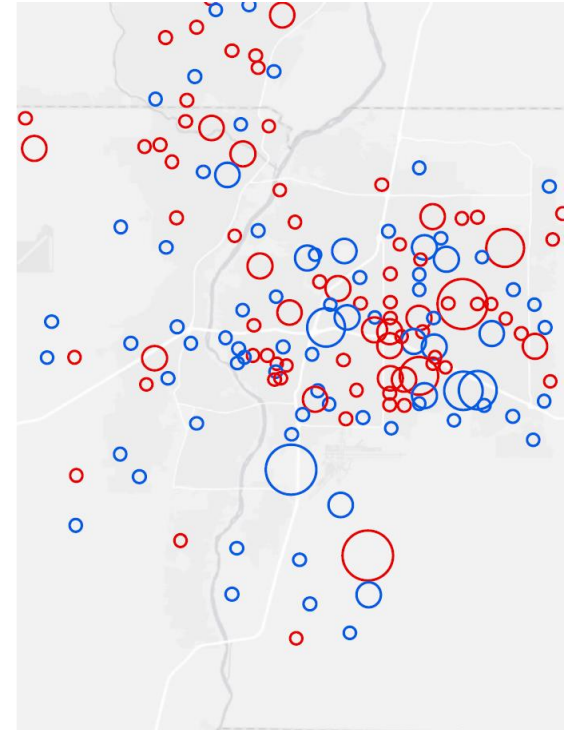
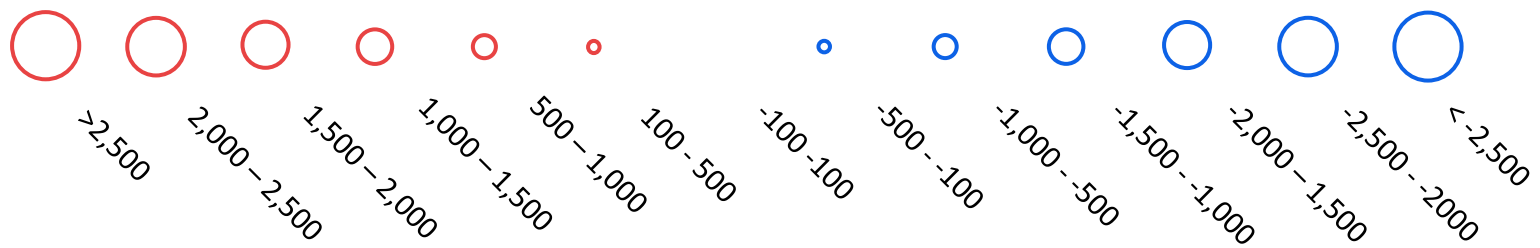


Figure 4.18: Absolute change in population between the original and derived LRTPs for year 2025



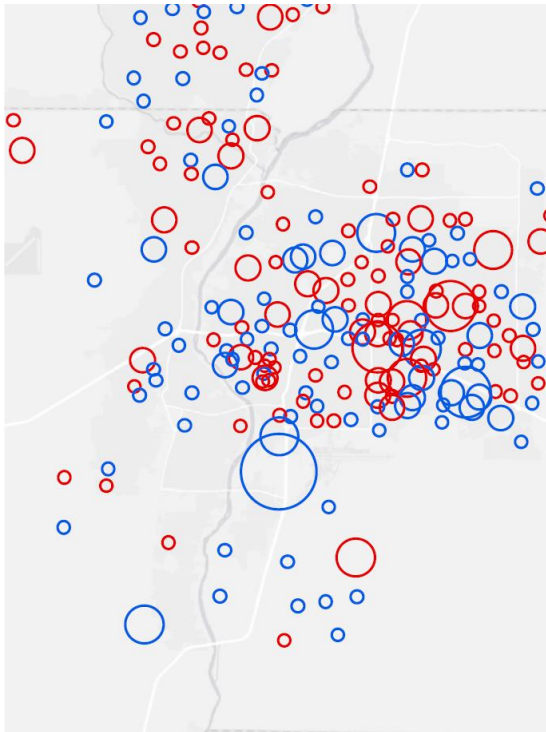


Figure 4.19: Absolute change in population between the original and derived LRTPs for year 2030

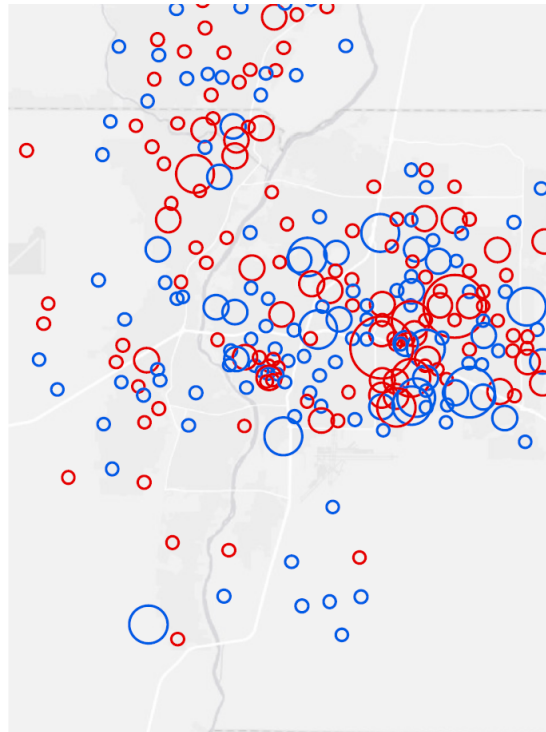


Figure 4.20: Absolute change in population between the original and derived LRTPs for year 2035

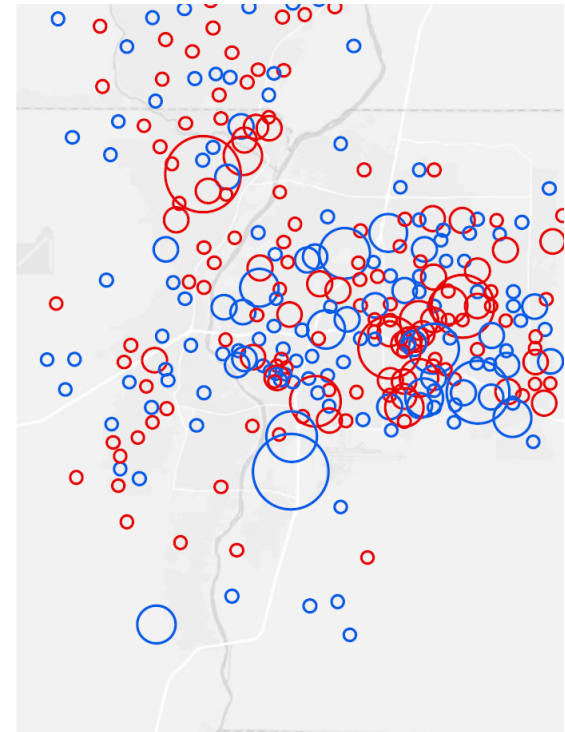
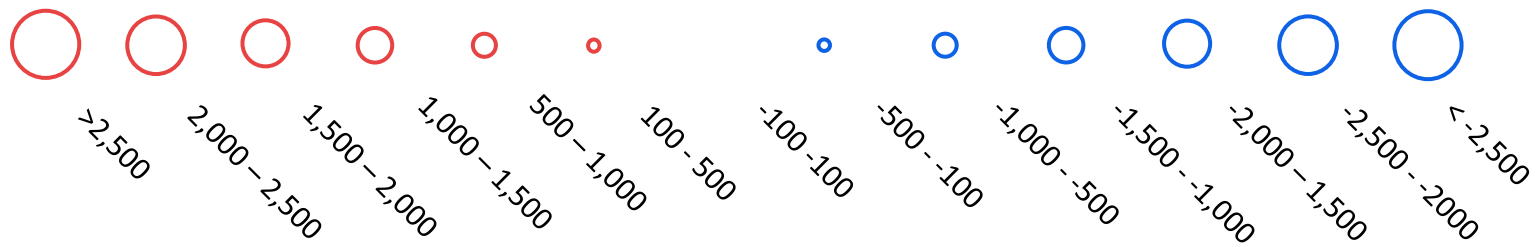


Figure 4.21: Absolute change in population between the original and derived LRTPs for year 2040



In addition to spatial changes in the land-use and traffic patterns, we are interested in the changes in road congestion across the network. There are different congestion measures; the one used in this study is the ratio of traffic load to road capacity:

$$CG_i(t) = \frac{L_i(t)}{C_i}, \quad (8)$$

where  $L_i(t)$  is the traffic load on link  $i$  during time  $t$ ,  $C_i$  is link  $i$ 's capacity, and  $CG_i(t)$  is the congestion index. A congested road has a  $CG$  greater than unit. In order to measure the overall congestion on the transportation network, the percentage of the congested links are graphed in Figure 4.22.

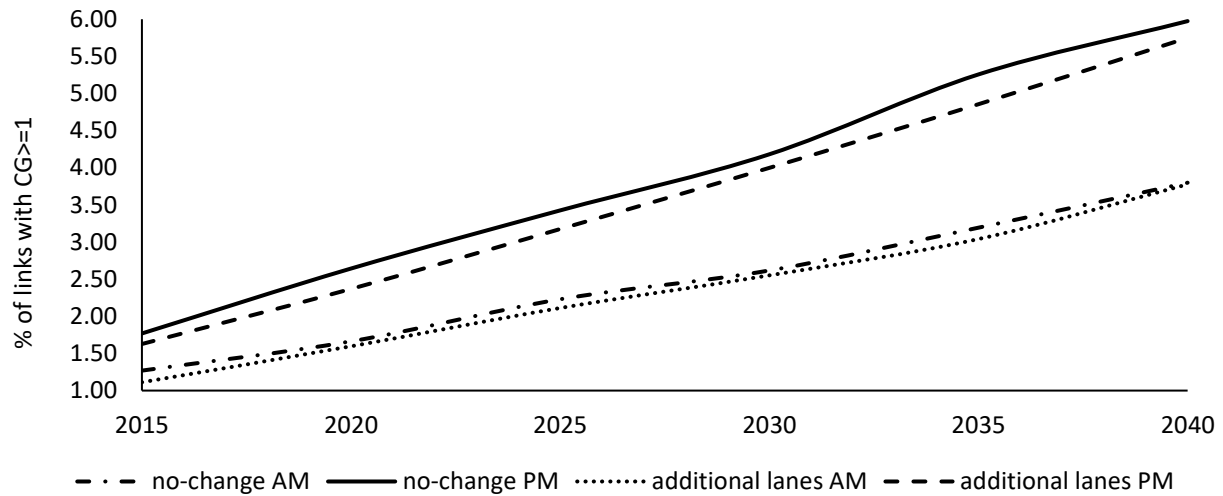


Figure 4.22: Percentage of congested links during the morning and afternoon peak hours for the original and new L RTPs

According to Figure 4.22, in all cases, congestion increases over time. However, by adding lanes to the Paseo del Norte overpass, congestion is reduced slightly throughout the planning horizon. In both cases, afternoon congestion is higher than morning congestion. Furthermore, improvements in congestion due to the proposed project are more pronounced for the afternoon

peak hours.

As shown in Figures 4.10 to 4.15, adding new lanes to a part of the network, results in an increase in the traffic speed. Higher traffic speed demands higher energy consumption and consequently results in higher CO<sub>2</sub> emissions. Figures 4.23 and 4.24 compare the energy consumption and CO<sub>2</sub> emissions between the two networks. Both energy consumption and CO<sub>2</sub> emissions increase for the first five years but then decrease throughout the rest of the planning horizon. The decrease in energy consumption and CO<sub>2</sub> emissions could be attributed to an increase in vehicular energy efficiency.

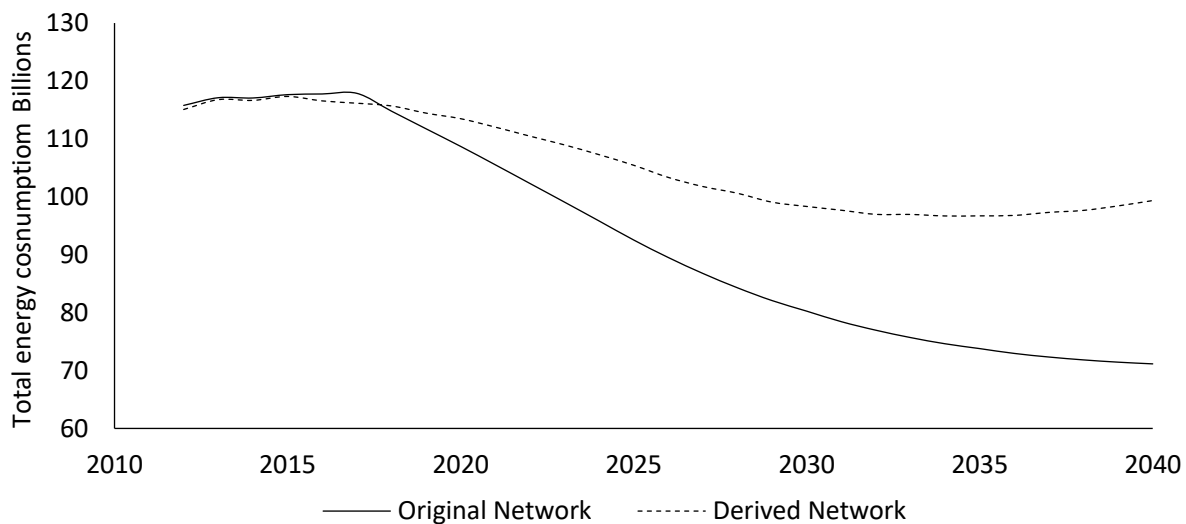


Figure 4.23: Annual energy consumption on the original and derived networks

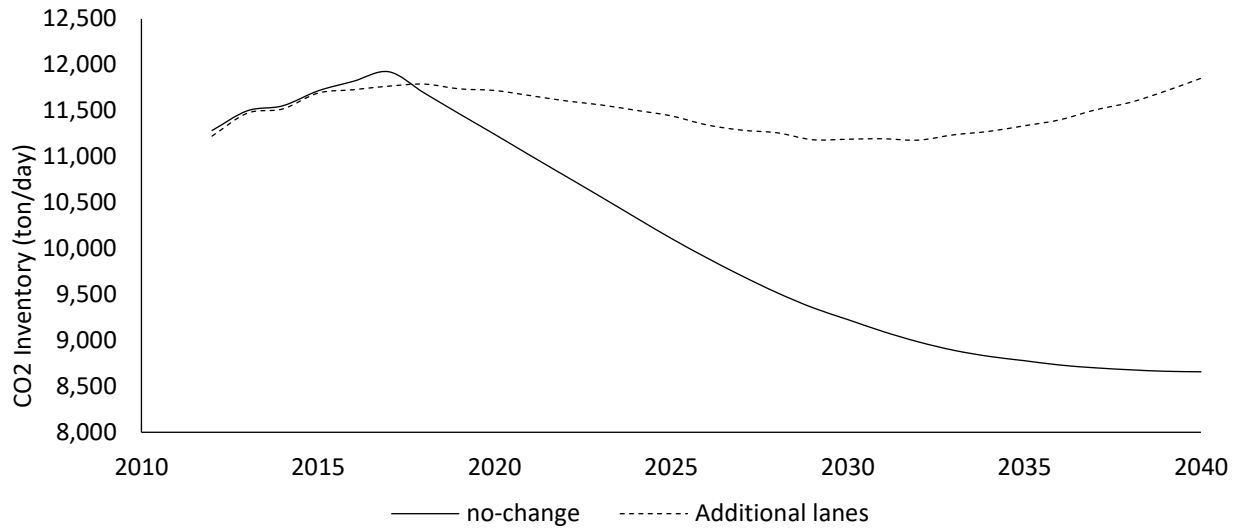


Figure 4.24: Annual CO<sub>2</sub> emission on the original and derived networks

## 6.2. Comparison between the results of the ALT and endpoint approaches

The second objective of this chapter is to compare the conventional endpoint analysis with the proposed ALT approach. Figure 4.25 shows the changes in demand, (vehicle miles traveled, or VMT) over time resulting from the two approaches. When analyzed by the proposed dynamic integration approach, it is observed that demand drops sharply during the first 2-3 years, remains more or less the same until about 2030, and decreases again towards the end of the planning horizon. The endpoint approach estimates a slightly higher demand for the end year (2040) in both trend and modified scenarios. In addition, by assuming a linear pattern for the interim years throughout the 2012-2040 period, the endpoint procedure estimates much higher VMTs.

Figure 4.26 shows the average traffic speed during morning peak hours estimated by both ALT and endpoint approaches. In the case of traffic speed, the endpoint procedure finds lower traffic speed for both LRTPs for 2040. Furthermore, the endpoint model underestimates the traffic speed throughout the planning horizon.

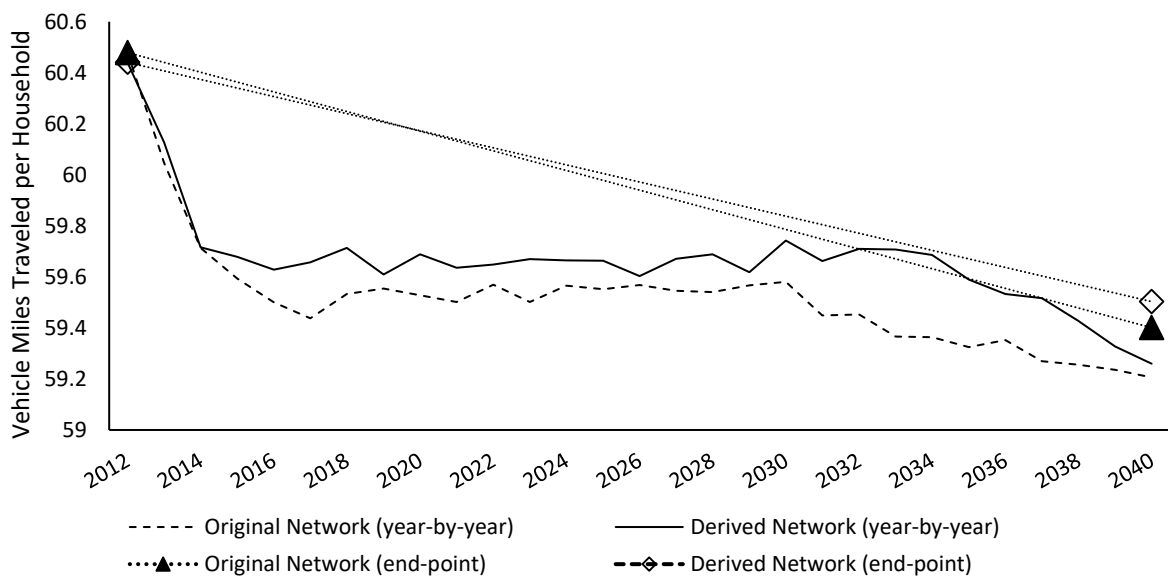


Figure 4.25: Vehicle miles traveled per household

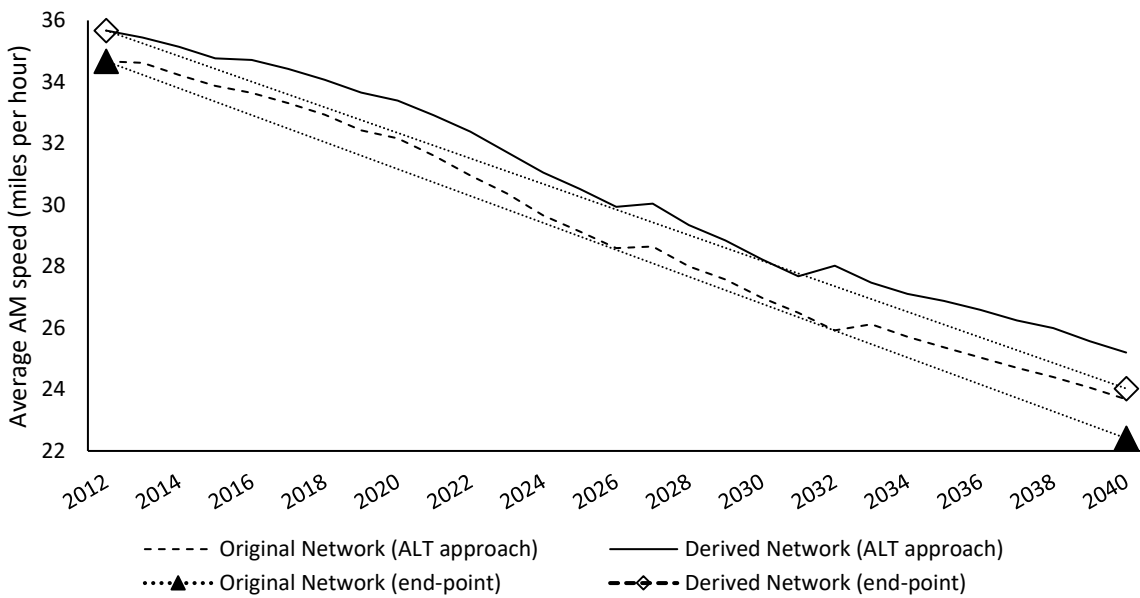


Figure 4.26: Average traffic speed on the network

We are also interested in measuring the environmental outcomes of transportation planning.

Using EPA's MOVES database, we estimate the fuel consumption rate (in Btu) and CO<sub>2</sub> emissions (tons per day). Figure 4.27 presents fuel consumption results based on the proposed ALT approach and the endpoint approach. According to the results of the proposed simulation procedure, energy consumption increases during the first decade of the planning horizon then declines until 2035. After 2035, fuel consumption slightly increases. The endpoint approach assumes a linear pattern between the first and last year, and consequently underestimates fuel consumption during the early years of the planning horizon and overestimate it during the second part of the planning horizon.

Figure 4.28 illustrates the CO<sub>2</sub> emission outputs estimated by the proposed approach as well as the endpoint approach. Similar to the energy consumption pattern, CO<sub>2</sub> emissions results of the year-by-year approach show two turning points. At first, CO<sub>2</sub> emissions increases sharply between 2012 and 2018, then the emission rates decrease until 2032, and during the last eight years in the planning horizon emission rates increase sharply. Throughout the same period, the endpoint approach estimates an upward linear pattern which results in a biased estimation for the interim years.



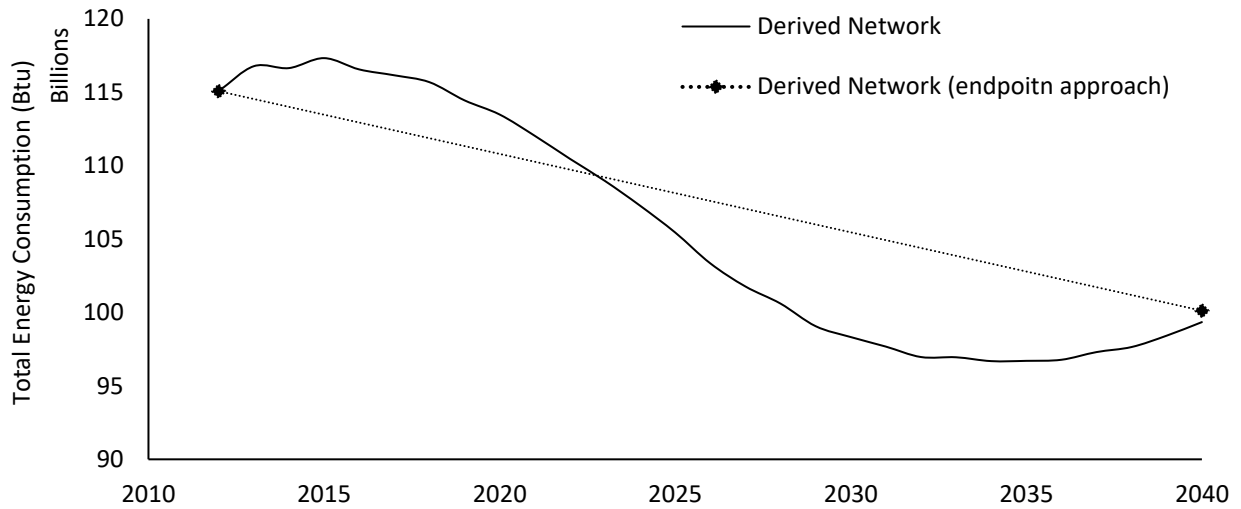


Figure 4.27: Fuel energy consumption on modified network

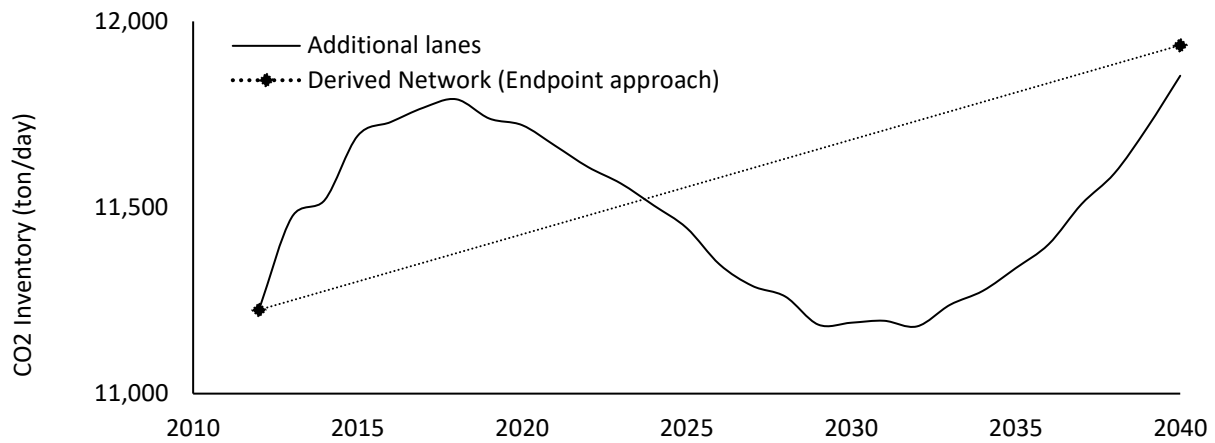


Figure 4.28: CO<sub>2</sub> accumulation on the modified network

## 7. Conclusions

An annually integrated land-use travel demand model (ALT) is proposed to investigate the impacts of an additional road capacity expansion project in an LRTP with a congestion reduction goal. To simulate the interactive relationship between land-use and travel demand decisions made by households and businesses, the proposed approach requires that the exchange of inputs and outputs between the travel demand and land-use models take place every year throughout

the planning horizon. Compared to the conventional endpoint approach adopted by MPOs, where the exchange takes place only at the start and end years, the proposed approach has a higher temporal resolution. The ALT approach can help identify nonlinear patterns in the performance metrics of LRTPs. We utilize the ALT model to map the performance metrics of two LRTPs, namely an original LRTP, which was actually proposed for the city of Albuquerque and a derived LRTP that includes an additional road capacity expansion project. Comparing the performance of the two LRTPs with the same ALT approach allows us to tease out the particular impacts of the additional road capacity expansion proposal. Furthermore, by presenting the nonlinearities in the performance metrics obtained from the proposed ALT approach, we show that the linearity assumption implied in the endpoint approach leads to biased results during the interim years.

Comparison between the original and derived LRTPs did not show a congestion rebound effect, as the number of congested roads was slightly smaller for the derived LRTP than the original LRTP throughout the planning horizon, and the average traffic speed was shown to be higher for the modified LRTP compared to the original LRTP. However, by mapping the network and zonal changes it is shown that the proposed model could successfully capture the changes in travel behavior and land-use choices resulted from a single road capacity expansion project. Consistent with the findings of Cervero (2003) it is shown that the travel behavior changes quite early and then land-use changes are more visible after a few years. The road segment chosen for the capacity expansion is an overpass of the Rio Grande in Albuquerque. Since the very first year of the planning scope (i.e. 2012), the traffic load reduced on other river overpasses and increased on the expanded overpass. The speed of traffic increased on all overpasses, which could be

attributed to the reduction of traffic load on other overpasses and the expanded capacity on the overpass of interest. Land-use changes are shown in terms of changes in the household population per each traffic analysis zone. It is shown that better mobility provided by the expansion, the population was increased on one side of the river, which is mostly residential.

We also compared the path of the network metrics over the planning horizon with that resulted from the endpoint approach. VMT, traffic speed, energy consumption and CO<sub>2</sub> emission are the metrics of interest. It is shown that the endpoint approach results in an overestimation of the VMT. The biasedness of the endpoint approach in estimating the traffic speed during interim years is not quite insignificant. However, the endpoint approach results in a large bias when estimating the environmental metrics (energy consumption and CO<sub>2</sub> emission) for the interim years during the planning period. We conclude that the computation intensity of the proposed ALT approach is justified by higher accuracy of the LRTP's performance metrics estimations.

## References

- Cervero, R. and Hansen, M. (2002). Induced travel demand and induced road investment: a simultaneous equation analysis. *Journal of Transport Economics and Policy*, 36(3), pp. 469-490.
- Cervero, R. (2003). Road expansion, urban growth, and induced travel: A path analysis. *Journal of the American Planning Association*, 69(2), pp. 145-163.
- Childress, S., Nichols, B., Charlton, B. and Coe, S. (2015). Using an activity-based model to explore the potential impacts of automated vehicles. *Transportation Research Record*, 2493(1), pp. 99-106.
- Coppola, P., Ibeas, A., dell'Olio, L. and Cordera, R. (2013). LUTI model for the metropolitan area of Santander. *Journal of Urban Planning and Development*, 130(3), pp. 153-165.
- Duranton, G. and Turner, M.A. (2011). The fundamental law of road congestion: Evidence from US cities. *American Economic Review*, 101(6), pp. 2616-2652.
- Epple, D. and Romer, T. (1991). Mobility and redistribution. *Journal of Political Economy*, 99(4).
- Fulton, L.M., Noland, R.B., Meszler, D.J. and Thomas, J. (2000). A statistical analysis of induced travel effects in the U.S. mid-Atlantic region. *Journal of Transportation and Statistics*, 3(1), pp. 1-14. Accessed June 19, 2019. [https://www.bts.gov/archive/publications/journal\\_of\\_transportation\\_and\\_statistics/volume\\_03\\_number\\_01/index](https://www.bts.gov/archive/publications/journal_of_transportation_and_statistics/volume_03_number_01/index).
- Goodwin, P.B. (1996). Empirical evidence on induced traffic. *Transportation*, 23(1), pp. 35-54.
- Hansen, M. (1995). Do new highways generate traffic? *ACCESS Magazine*, 1(7), pp. 16-23. Accessed <https://escholarship.org/uc/item/3ri612zh>
- Handy, S. (2008). Regional transportation planning in the US: An examination of changes in technical aspects of the planning process in response to changing goals. *Transport Policy*, 15(2), pp. 113-126. <https://doi.org/10.1016/j.tranpol.2007.10.006>.
- Hymel, K.M., Small, K.A. and Van Dender, K. (2010). Induced demand and rebound effects in road transport. *Transportation Research Part B: Methodological*, 44(10), pp. 1220-1241.
- Kakraparthi, S.K. and Kockelman K.M. (2010). Application of UrbanSim to the Austin, Texas, region: Integrated-model forecasts for the year 2030. *Journal of Urban Planning and Development* 137(3), pp. 238-247.
- Katoshevski, R., Glickman, I., Ishaq, R. and Shiftan, Y. (2015). Integrating activity-based travel-demand models with land-use and other long-term lifestyle decisions. *Journal of Transport and Land Use*, 8(3), pp. 71-93.

- Meyer, M.D. and Miller, E.J. (2001). *Urban transportation planning: A decision-oriented approach*, second ed. New York, NY: McGraw-Hill.
- Mid Region Council of Governments (MRCOG). 2015. *Futures 2040 metropolitan transportation plan*. Mid-Region Metropolitan Planning Organization. Accessed June 19, 2019. <https://issuu.com/mrcog/docs/mrmpo-futures-2040-mtp-no-appendice>.
- Nadafianshahamabadi, R. and Rowangould, G. (2017). Evaluating sustainability in transportation plans: Review of long-range transportation plans in the United States. Paper presented at the 2017 Transportation Research Board Annual Meeting, Jan. 8-12. Washington, DC. [http://amonline.trb.org/63532-trb-1.3393340/t027-1.3402384/694-1.3402925/17-05402-1.3402218/17-05402-1.3402928?login\\_formerror=auth&q=1](http://amonline.trb.org/63532-trb-1.3393340/t027-1.3402384/694-1.3402925/17-05402-1.3402218/17-05402-1.3402928?login_formerror=auth&q=1).
- Prakash, A.B., Oliver, E.H.D'A., IV and Balcombe, K. (2001). Does building new roads really create extra traffic? Some new evidence. *Applied Economics*, 33(12), pp. 1579-1585.
- Schrank, D. Eisele, B. and Lomax, T. (2012). *TTI's 2012 urban mobility report*. College Station: Texas A&M Transportation Institute. Accessed June 17, 2019. <https://www.pagregion.com/Portals/0/documents/HumanServices/2012MobilityReport.pdf>
- Stanley, J., Hensher, D.A., Stanley, J., Currie, G., Greene, W.H. and Vella-Brodrick, D. (2011). Social exclusion and the value of mobility. *Journal of Transport Economics and Policy*, 45(2), pp. 197-222.
- Systra Mobility. (2010). *Middle Rio Grande regional travel model recalibration and validation report*. Prepared by Systra Mobility for the Mid Region Council of Governments.
- Tayarani, M., Nadafianshahamabadi, R., Poorfakhraei, A. and Rowangould, G. (2018). Evaluating the cumulative impacts of a long-range regional transportation plan: Particulate matter exposure, greenhouse gas emissions, and transportation system performance. *Transportation Research Part D: Transport and Environment*, 63, pp. 261-275.
- Tayarani, M. and Rowangould, G. (2019). Differences in exposure to vehicle emissions: Comparing dynamic analysis to conventional static exposure analysis at the home address. Paper presented at the 98th Transportation Research Board Annual Meeting, Jan. 13-17. Washington, D.C.
- U.S. Department of Transportation, Federal Highway Administration. *2017 National Household Travel Survey*. URL: <http://nhts.ornl.gov>.
- Waddell, P., Borning, A., Noth, M., Freier, N., Becke, M. and Ulfarsson, G. (2003). Microsimulation of urban development and location choices: Design and implementation of UrbanSim. *Networks and Spatial Economics*, 3(1), pp. 43-67.
- Yasmin, F., Morency, C. and Roorda, M.J. (2017). Macro-, meso-, and micro-level validation of an

activity-based travel demand model. *Transportmetrica A: Transport Science*, 13(3), pp. 222-249.

## **Chapter 5. Conclusion and Summary**

This work focuses on analyzing the economic and environmental outcomes of policy instruments applied to complex systems. Complex systems consist of economic agents who make decisions to maximize their utilities and profits. To fulfill their utility/profit maximization objectives, agents rely on natural resources and the environment (natural or man-made). The collective actions of individuals result in significant changes to the environmental conditions and natural resources. As a result, the social planner has to use policy instruments to balance between maximizing profit and minimizing the potential negative impacts on natural resources and the environment.

More often than not, the impacts of a policy on such integrated and complex systems are realized over time and because the economic agents are making decisions at all times, variables that determine the performance of a policy proposal are dynamic. We developed three integrated and dynamic models to investigate the outcomes of potential policy scenarios in real-life situations which will be discussed in the following paragraphs.

Chapter 2 presents the complex process of oil production in the New Mexico portion of the Permian Basin. Several (large and small) oil producers are already active in the study area and a recent discovery of the largest unconventional reserve has improved its growth prospect even more. Oil is an important income source in the state of New Mexico. However, production of oil from unconventional resources consumes large amounts of water and generates large volumes of wastewater. There are several oil producing geologic formations in the study area; the levels of oil production, water consumption and wastewater generation are different among these formations.

We proposed and evaluate six policy instruments to search for an optimal policy that ensures revenue maximization while minimizing freshwater consumption and waste disposal volumes. The proposed policies include severe (1,000 acre-feet per month), moderate (5,000 acre-feet per month) and mild (10,000 acre-feet per month) freshwater consumption constraints; 10% and 25% (of the initial oil production rate) shutdown conditions; and a combination of the moderate freshwater consumption constraint and improved (from 20% of water consumption volume to 50%) treatment capacity.

We showed that shortening the production lifetime of wells by imposing early shutdown conditions resulted in inferior outcomes compared to other policies. The amount of revenue lost due to early shutdown of wells could not be justified by the reductions in the produced water generation when compared with the moderate and mild freshwater consumption constraints. Compared to the sole freshwater consumption constraint scenarios, the combination of moderate freshwater consumption levels and high treatment levels was shown to result in



relatively high revenues while limiting freshwater consumption. Since produced water is generated at significantly larger volumes compared to the amount of freshwater consumed in hydraulic fracturing processes, reusing lightly treated water in oil and gas operation does not seem to reduce the disposal volumes significantly.

Furthermore, we were able to estimate the net profit of improving treatment capacity by comparing the revenue outcomes of the sole freshwater consumption constraint with that of the combination of freshwater consumption constraint and improved treatment capacity. We estimated that by imposing 5,000 acre-feet per month freshwater consumption constraint, the net present (2018) value of all the revenue streams generated in the planning interval (2019-2050) will be roughly \$299 billion; whereas by increasing the treatment capacity and reusing the produced water for 50% of hydraulic fracturing demand instead of 20%, the state revenue will increase to roughly \$405 billion. In other words, for a policymaker who is interested in reducing freshwater consumption levels to below 5,000 acre-feet per month, it is of significant economic interest to invest in policy scenarios that result in an increase in the treatment levels from 20% to 50% of the hydraulic fracturing water demand.

This dynamic analysis also highlights the importance of frequent water consumption data collection by state officials. Water consumption for mining purposes in the Permian Basin is almost completely for hydraulic fracturing purposes. Wells that are newly drilled have to be hydraulically fractured to be able to produce oil and gas liquids from unconventional shale resources. The number of new wells is directly related to oil prices. High oil prices in a year can drive high intensity drilling activity in the Permian Basin, which consumes large amounts of

freshwater. Currently, The New Mexico Office of the State Engineer collects water consumption data every five year. The most update version of the water consumption by category, pertaining to 2015, was published in 2019. This low frequency of water budgeting poses a risk to freshwater water resource as it may fail to capture irreversible instances of large water withdrawals.

Chapter 3 explores the possibility that the regulatory environment is factored into firms' location decision. Shared between two different regulatory boundaries, the Permian Basin presents a natural assignment of well drilling location options. We used the Granger causality concept to understand the relationship between drilling activity in the New Mexico and Texas portions of the Permian Basin and to compare how an increase in oil prices impacts the drilling activity within these two regulatory environments.

Since the timeseries of oil prices, and drilling activities are cointegrated, we carried out a vector error correction model (VECM). The results of the Granger causality tests showed that oil prices drive drilling activity in both parts of the Permian Basin. Furthermore, we showed that an increase in drilling activity in the Texas portion drives a slight increase in the New Mexico portion's drilling activity. However, there is no evidence that drilling activity in the New Mexico Permian spills over into the Texas portion.

Furthermore, the long-term effects of an increase in one variable on other variables was investigated by mapping the impulse-response functions. A shock in the price of oil had a permanent impact on drilling activities on either side of the Permian Basin. Results showed that the impact of a shock in Texas drilling activity on New Mexico drilling is also permanent although the impact becomes quite small after a year. Drilling activity in the New Mexico portion does not

impact drilling activity in the Texas portion in the long-term. An interesting observation was that a shock in drilling activity in the Permian Basin, either New Mexico or Texas portions, caused a slight decline in oil prices in the long run. Based on this observation, it is possible that U.S. oil prices are not completely exogenous.

Chapter 4 is about integration of the land-use and travel demand models to assess the performance of a long-range transportation plan (LRTP). We are specifically interested in measuring short- and long-term outcomes of adding to the road capacity by supplying more lanes. The fundamental law of road congestion suggests that by adding to the number of lanes of a transportation network to alleviate road congestion, induced and latent travel demand will emerge over time and the congestion problem will reappear. We compared two LRTPs, one is an original LRTP designed for the Albuquerque metropolitan area, and the other a modified version of the same LRTP, with an additional lane on the Paseo del Norte river overpass. We compare the two LRTPs to measure changes in traffic speed, vehicle miles traveled, total number of the congested links on the transportation network, and changes in zonal population, among others, resulting from the addition of the new lanes.

The uniqueness of the proposed land-use travel demand model is the frequency of the input/output exchange between the two modules. Although the integration of land-use and travel demand models is not a new approach, there is no prescription about the frequency of the interaction. The metropolitan area planning organizations (MPOs) estimated the performance of LRTPs by allowing the interaction between land-use travel demand models only the beginning and end years of the planning horizon which is more than 20 years; this approach referred to as

the endpoint approach assumes that land use and travel demand change in isolation in the interim years of the planning horizon. The proposed approach, on the other hand, links the two modules during each year of the planning horizon. That is, the travel times resulting from the travel demand module are utilized to update the zonal population and economic activity for the same year, and the zonal population and economic activity data are input to the travel demand module to update the travel times of the next year. We compared the performance outcomes of resulting from the proposed approach of the LRTP with additional lanes with the endpoint method and mapped the outcomes over the planning horizon.

Comparisons between the two LRTPs, Albuquerque's original LRTP and the same LRTP with additional lanes, did not indicate the congestion rebound, since the number of congested roads throughout the network was reduced for the LRTP with additional lanes. By comparing the performance metrics of the two networks (with and without additional lanes) we showed that speed increase over the majority of links on the network. Our results also showed route diversion which is a travel behavior change. We could also show that households and businesses relocate as a result of adding new lanes although such land-use changes take place at lower pace as compared to network measures. Whereas the congestion rebound didn't take place for the afternoon traffic, our results showed that in the long run the level of congestion on the network during morning hours returns to the levels without adding the new lanes. Last but not least, our proposed approach could show that by adding new lanes, the energy consumption and CO<sub>2</sub> emission increased over the entire network.

Comparisons between the endpoint approach and the proposed approach (with annual

interaction between the land-use and travel demand modules) revealed that the endpoint approach showed significant biased results when estimating the outcomes of an LRTP. The endpoint approach showed significant bias in estimating the energy and environmental outcomes of the LRTP. When estimated via the proposed methods, the timeseries of CO<sub>2</sub> generated on the network and the transportation energy consumption were shown as nonlinear functional forms, which could not be captured by the endpoint approach.